MycoKeys 41: 1–15 (2018)
doi: 10.3897/mycokeys.41.27536
http://mycokeys.pensoft.net

RESEARCH ARTICLE

A peer-reviewed open-access journal
MycoKeys
Launched to accelerate biodiversity research

Beta-tubulin and Actin gene phylogeny supports *Phaeoacremonium ovale* as a new species from freshwater habitats in China

Shi-Ke Huang[1,2,3,7], Rajesh Jeewon[4], Kevin D. Hyde[2], D. Jayarama Bhat[5,6], Putarak Chomnunti[2,7], Ting-Chi Wen[1]

1 *Engineering and Research Center of Southwest Bio-Pharmaceutical Resources, Ministry of Education, Guizhou University, Guiyang 550025, China* **2** *Center of Excellence in Fungal Research, Mae Fah Luang University, Chiang Rai 57100, Thailand* **3** *Key Laboratory for Plant Biodiversity and Biogeography of East Asia (KLPB), Kunming Institute of Botany, Chinese Academy of Sciences, Kunming, 650201, Yunnan, China* **4** *Department of Health Sciences, Faculty of Science, University of Mauritius, Reduit, Mauritius* **5** *Azad Housing Society, No. 128/1-J, Curca, P.O. Goa Velha 403108, India* **6** *Formerly, Department of Botany, Goa University, Goa, 403206, India* **7** *School of Science, Mae Fah Luang University, Chiang Rai 57100, Thailand*

Corresponding author: *Ting-Chi Wen* (tingchiwen@yahoo.com)

Academic editor: *Marc Stadler* | Received 15 June 2018 | Accepted 10 September 2018 | Published 11 October 2018

Citation: Huang S-K, Jeewon R, Hyde KD, Bhat DJ, Chomnunti P, Wen T-C (2018) Beta-tubulin and Actin gene phylogeny supports *Phaeoacremonium ovale* as a new species from freshwater habitats in China. MycoKeys 41: 1–15. https://doi.org/10.3897/mycokeys.41.27536

Abstract

A new species of *Phaeoacremonium*, *P. ovale* (Togniniaceae), was isolated during a diversity study of freshwater fungi from Yunnan Province in China. Morphological and cultural studies of the fungus were carried out and its sexual and asexual morphs (holomorph) are introduced herein. This species is characterised by peculiar long-necked, semi-immersed ascomata with oval to ellipsoid ascospores and ellipsoid to ovoid conidia. Phylogenetic analyses of a combined TUB and ACT gene dataset revealed that strains of *P. ovale* constitute a strongly supported independent lineage and are related to *P. griseo-olivaceum* and *P. africanum*. The number of nucleotide differences, across the genes analysed, also supports establishment of *P. ovale* as a new species.

Keywords

1 new species, Togniniales, Sordariomycetes, Morphology, Phylogeny

Introduction

Lignicolous freshwater fungi are important in nutrient recycling (Hyde et al. 2016). A number of taxonomic studies have focused on the diversity of such fungi in the South East Asian region and these investigations have reported a number of novel species (e.g. Jeewon et al. 2003; Cabanela et al. 2007; Zhang et al. 2008; Luo et al. 2018). In this study, we report a new species of *Phaeoacremonium* isolated from decaying wood from a stream in Yunnan Province, China.

Phaeoacremonium (= *Togninia*), introduced by Crous et al. (1996), is typified by *P. parasiticum* and it belongs to Togniniaceae (Gramaje et al. 2015). *Phaeoacremonium* was reported to be the asexual morph of *Togninia* (Mostert et al. 2003, 2006a; Pascoe et al. 2004). Gramaje et al. (2015) proposed *Phaeoacremonium* over *Togninia* as the correct name based on common usage and this has been listed in Réblová et al. (2016) and followed in Wijayawardene et al. (2018). The species are basically characterised by black ascomata with a long neck and clavate to cylindrical asci with oval to ellipsoid, hyaline ascospores and straight or flexuous mononematous conidiophores with oval to reniform phialo-conidia (Marin-Felix et al. 2018; Spies et al. 2018).

Most species of *Phaeoacremonium* are plant or/and human pathogens and some have been recorded on arthropods or in soil (Groenewald et al. 2001; Guarro et al. 2003; Hemashettar et al. 2006; Mostert et al. 2006a; Damm et al. 2008; Gramaje et al. 2015) while others are causal agents of Petri disease and esca of grapevines (Pascoe et al. 2004; Rooney-Latham et al. 2005a; Mostert et al. 2006b). *Phaeoacremonium* species can also infect a wide range of woody hosts, such as cherry, apricot, olive and peach trees (Rumbos 1986; Di Marco et al. 2004; Kubátová et al. 2004). Recent studies have reported the importance of *Phaeoacremonium* species in causing brown wood streaking of *Olea* spp. and *Prunus* spp. (Mostert et al. 2006b; Damm et al. 2008; Gramaje et al. 2012; Nigro et al. 2013; Olmo et al. 2014; Carlucci et al. 2015). Rooney-Latham et al. (2004, 2005a, b) reported that, in the presence of water, spores in some *Phaeoacremonium* species are forcibly discharged from perithecia through the long neck and exit the ostiole to be dispersed by wind, rain or insects in order to colonise other substrates. Recently Hu et al. (2012) introduced a freshwater inhabiting species, *Phaeoacremonium aquaticum* (= *Togninia aquatica*).

Species of Togniniaceae have been reported to colonise substrates in different types of habitats and recent taxonomic studies have revealed additional new species (Gramaje et al. 2015). We have been studying fungi along a north-south gradient in the Asian region (Hyde et al. 2016) and, in this study, we report on two collections of *Phaeoacremonium* from China. The aim here is to characterise these two strains as one novel species based on morphology as well as to investigate their phylogenetic affinities with previously known Togniniaceae species based on partial TUB and ACT genes.

Materials and methods

Sample collection, morphological studies and isolation

Submerged dead wood was collected from Baoshan, Yunnan Province in China in October 2016, brought to the laboratory in zip lock plastic bags and treated in the laboratory following procedures detailed in Luo et al. (2018). Fruiting bodies were found growing on decaying wood in a sterile plastic box after two weeks of incubation and the fungus was subsequently isolated based on the method of Chomnunti et al. (2014). Specimens were examined by a Motic SMZ 168 stereomicroscope. Micromorphological characters were examined using a Nikon ECLIPSE 80i compound microscope and images were captured with a Canon EOS 600D digital camera. Identification of colours was based on Ridgway (1912). The Taro soft Image Framework programme version 0.9.0.7 was used for measurements. Single spores were isolated and grown on water agar (WA) and potato dextrose agar (PDA) media. Ascospores germinated on PDA within 1 week. The colonies were transferred to WA and PDA to promote sporulation (sporulation occurred after 30 days in PDA). The cultures were checked 2 to 3 times per week and all procedures were performed in a sterile environment and at room temperature. The morphological characters of the asexual morph were examined after sporulation. Specimens are deposited in the Kunming Institute of Botany, Academia Sinica (KUN) and duplicated in Mae Fah Luang University (MFLU) Herbarium, Chiang Rai, Thailand. Facesoffungi numbers (FoF) (http://www.facesoffungi.org/) were obtained as stated in Jayasiri et al. (2015) and Index Fungorum numbers (IF) (http://www.indexfungorum.org/names/IndexFungorumRegisterName.asp).

DNA extraction, PCR amplification and sequencing

Total genomic DNA was extracted from mycelium using a Trelief Plant Genomic DNA Kit following the instructions of the manufacturer. The genomic DNA was amplified by using polymerase chain reaction (PCR) in a 25 µl reaction mixture. Partial regions of the beta-tubulin (TUB) and Actin (ACT) gene were amplified using the primer pairs T1 (O'Donnell and Cigelnik 1997) and Bt2b (Glass and Donaldson 1995), ACT-513F and ACT-783R (Carbone and Kohn 1999), respectively. The internal transcribed spacers (ITS) regions of the rDNA (ITS1-5.8S-ITS2) were also amplified using primer pairs ITS5 and ITS4 (White et al. 1990) but no further analyses were done on these due to lack of sequence data. The PCR conditions for these regions were as follows: an initial denaturation at 94 °C for 3 min, followed by 35 cycles of denaturation at 94 °C for 30 sec, annealing at 51 °C (TUB) or 60 °C (ACT) or 55 °C (ITS) for 50 sec and extension at 72 °C for 1 min, with a final extension at 72 °C for 10 min. PCR products were then sequenced with the primers mentioned above by a commercial sequencing provider (Tsingke Company, Beijing, P.R. China).

Phylogenetic analysis

The quality of the amplified nucleotide sequences was checked and combined by SeqMan version 7.1.0 (44.1) and Finch TV version 1.4.0 (www.geospiza.com). Sequences used by Marin-Felix et al. (2018), Spies et al. (2018) and the closest matches for our strains were retrieved from the National Center for Biotechnology Information (NCBI) by nucleotide BLAST. Sequences were aligned in MAFFT v. 7.310 (http://mafft.cbrc.jp/alignment/server/index.html) (Katoh and Standley 2016) and manually corrected in Bioedit 7.0.9.0 (Hall 1999).

The phylogenetic analyses of combined gene regions (TUB and ACT) were performed using maximum-likelihood (ML) and Bayesian Inference (BI) methods. The best-fit model (GTR+G+I) was obtained using jModelTest 2.1.10 under the Akaike Information Criterion (AIC) calculations (Darriba et al. 2012). The ML analysis was enforced with RAxML-HPC v.8 on XSEDE (Stamatakis 2014; Miller et al. 2015) with 1000 rapid bootstrap replicates. Bayesian inference was implemented by MrBayes v. 3.0b4 (Ronquist and Huelsenbeck 2003). Four simultaneous Markov chains were run for 5,000,000 generations sampling one tree every 1000th generations and other criteria as outlined by Hongsanan et al. (2017). The temperature value was lowered to 0.15, burn-in was set to 0.25. Gaps were treated as missing data with no differential weighting of transitions against transversions and the partition homogeneity test was performed to assess whether datasets from different genes were congruent. Phylogenetic trees were viewed with FigTree v1.4.0 (http:// tree.bio.ed.ac.uk/software/figtree/) and processed by Adobe Illustrator CS5. Alignment and trees were deposited in TreeBASE (submission ID: 22810). The nucleotide sequence data of the new taxon have been deposited in GenBank (Table 1).

Results

Phylogenetic analyses

The combined TUB and ACT sequence dataset comprised 98 strains of *Phaeoacremonium*. The tree was rooted with *Pleurostoma richardsiae* (CBS 270.33) and *Wuestineaia molokaiensis* (CBS 114877). The alignment comprised 947 total characters including gaps (TUB: 646bp; ACT: 301bp). ML and BI analyses yielded trees which were topologically congruent in terms of species groupings. RAxML analysis yielded a best scoring tree with a final optimisation likelihood value of -15310.399369 (Fig. 1). In the phylogenetic tree, two strains of *Phaeoacremonium ovale* forms a well-supported independent subclade (100%, ML/1.00, PP) and closely related to other *Phaeoacremonium* species in Clade I (83%, ML/0.99, PP).

Table 1. Strains and GenBank accession numbers of the isolates used in this study. Isolates from this study are marked with asterisk (*) and the type strains are in bold.

Species	Voucher/Culture	GenBank accession number	
		TUB	ACT
Phaeoacremonium africanum	**CBS 120863**	**EU128100**	**EU128142**
Phaeoacremonium album	**CBS 142688**	**KY906885**	**KY906884**
Phaeoacremonium alvesii	**CBS 110034**	**AY579301**	**AY579234**
Phaeoacremonium alvesii	CBS 729.97	AY579302	AY579235
Phaeoacremonium amstelodamense	**CBS 110627**	**AY579295**	**AY579228**
Phaeoacremonium amygdalinum	**CBS 128570**	**JN191307**	**JN191303**
Phaeoacremonium amygdalinum	CBS H-20507	JN191305	JN191301
Phaeoacremonium amygdalinum	CBS H-20508	JN191306	JN191302
Phaeoacremonium angustius	**CBS 114992**	**DQ173104**	**DQ173127**
Phaeoacremonium angustius	CBS 114991	DQ173103	DQ173126
Phaeoacremonium argentinense	**CBS 777.83**	**DQ173108**	**DQ173135**
Phaeoacremonium armeniacum	**ICMP 17421**	**EU596526**	**EU595463**
Phaeoacremonium aureum	**CBS 142691**	**KY906657**	**KY906656**
Phaeoacremonium australiense	**CBS 113589**	**AY579296**	**AY579229**
Phaeoacremonium australiense	CBS 113592	AY579297	AY579230
Phaeoacremonium austroafricanum	**CBS 112949**	**DQ173099**	**DQ173122**
Phaeoacremonium austroafricanum	CBS 114994	DQ173102	DQ173125
Phaeoacremonium austroafricanum	CBS 114993	DQ173101	DQ173124
Phaeoacremonium bibendum	**CBS 142694**	**KY906759**	**KY906758**
***Phaeoacremonium canadens*e**	**PARC327**	**KF764651**	**KF764499**
Phaeoacremonium cf. mortoniae	**ICMP 18088**	**HM116767**	**HM116773**
Phaeoacremonium cinereum	**CBS 123909**	**FJ517161**	**FJ517153**
Phaeoacremonium cinereum	CBS H-20215	FJ517160	FJ517152
Phaeoacremonium cinereum	CBS H-20213	FJ517158	FJ517150
Phaeoacremonium croatiense	**CBS 123037**	**EU863482**	**EU863514**
Phaeoacremonium fraxinopennsylvanicum	**CBS 101585**	**AF246809**	**DQ173137**
Phaeoacremonium fraxinopennsylvanicum	CBS 110212	DQ173109	DQ173136
Phaeoacremonium fuscum	**CBS 120856**	**EU128098**	**EU128141**
Phaeoacremonium gamsii	**CBS 142712**	**KY906741**	**KY906740**
Phaeoacremonium geminum	**CBS 142713**	**KY906649**	**KY906648**
Phaeoacremonium globosum	**ICMP 16988**	**EU596525**	**EU595466**
Phaeoacremonium globosum	ICMP 17038	EU596521	EU595465
Phaeoacremonium globosum	ICMP 16987	EU596527	EU595459
Phaeoacremonium griseo-olivaceum	**CBS 120857**	**EU128097**	**EU128139**
Phaeoacremonium griseorubrum	**CBS 111657**	**AY579294**	**AY579227**
Phaeoacremonium griseorubrum	CBS 566.97	AF246801	AY579226
Phaeoacremonium hispanicum	**CBS 123910**	**FJ517164**	**FJ517156**
Phaeoacremonium hungaricum	**CBS 123036**	**EU863483**	**EU863515**
Phaeoacremonium inflatipes	**CBS 391.71**	**AF246805**	**AY579259**
Phaeoacremonium inflatipes	CBS 113273	AY579323	AY579260
Phaeoacremonium iranianum	**CBS 101357**	**DQ173097**	**DQ173120**
Phaeoacremonium iranianum	CBS 117114	DQ173098	DQ173121
Phaeoacremonium italicum	**CBS 137763**	**KJ534074**	**KJ534046**
Phaeoacremonium italicum	CBS 137764	KJ534075	KJ534047
Phaeoacremonium italicum	CBS H-21638	KJ534076	KJ534048
Phaeoacremonium junior	**CBS 142697**	**KY906709**	**KY906708**
Phaeoacremonium krajdenii	CBS 110118	AY579324	AY579261
Phaeoacremonium krajdenii	**CBS 109479**	**AY579330**	**AY579267**
Phaeoacremonium longicollarum	**CBS 142699**	**KY906689**	**KY906688**
Phaeoacremonium luteum	**CBS 137497**	**KF823800**	**KF835406**
Phaeoacremonium meliae	**CBS 142710**	**KY906825**	**KY906824**

Species	Voucher/Culture	GenBank accession number	
		TUB	ACT
Phaeoacremonium minimum	**CBS 246.91**	**AF246811**	**AY735497**
Phaeoacremonium minimum	CBS 100397	AF246806	AY735498
Phaeoacremonium mortoniae	CBS 211.97	AF246810	
Phaeoacremonium nordesticola	**CMM4312**	**KY030807**	**KY030803**
Phaeoacremonium novae-zealandiae	**CBS 110156**	**DQ173110**	**DQ173139**
Phaeoacremonium novae-zealandiae	CBS 110157	DQ173111	DQ173140
Phaeoacremonium occidentale	**ICMP 17037**	**EU596524**	**EU595460**
Phaeoacremonium oleae	**CBS 142704**	**KY906937**	**KY906936**
****Phaeoacremonium ovale***	**KUMCC 17-0145**	**MH395327**	**MH395325**
****Phaeoacremonium ovale***	**KUMCC 18-0018**	**MH395328**	**MH395326**
Phaeoacremonium pallidum	**CBS 120862**	**EU128103**	**EU128144**
Phaeoacremonium parasiticum	**CBS 860.73**	**AF246803**	**AY579253**
Phaeoacremonium parasiticum	CBS 113585	AY579307	AY579241
Phaeoacremonium parasiticum	CBS 514.82	AY579306	AY579240
Phaeoacremonium paululum	**CBS 142705**	**KY906881**	**KY906880**
Phaeoacremonium pravum	CBS 142686	KY084246	KY084248
Phaeoacremonium proliferatum	**CBS 142706**	**KY906903**	**KY906902**
Phaeoacremonium prunicola	**CBS 120858**	**EU128095**	**EU128137**
Phaeoacremonium prunicola	CBS 120858	EU128096	EU128138
Phaeoacremonium pseudopanacis	**CPC 28694**	**KY173609**	**KY173569**
Phaeoacremonium roseum	**PARC273**	**KF764658**	**KF764506**
Phaeoacremonium rosicola	**CBS 142708**	**KY906831**	**KY906830**
Phaeoacremonium rubrigenum	**CBS 498.94**	**AF246802**	**AY579238**
Phaeoacremonium rubrigenum	CBS 112046	AY579305	AY579239
Phaeoacremonium santali	**CBS 137498**	**KF823797**	**KF835403**
Phaeoacremonium scolyti	**CBS 113597**	**AF246800**	**AY579224**
Phaeoacremonium scolyti	CBS 113593	AY579293	AY579225
Phaeoacremonium scolyti	CBS 112585	AY579292	AY579223
Phaeoacremonium sicilianum	**CBS 123034**	**EU863488**	**EU863520**
Phaeoacremonium sicilianum	CBS 123035	EU863489	EU863521
Phaeoacremonium sp.	KMU 8592	AB986584	AB986583
Phaeoacremonium spadicum	**CBS 142711**	**KY906839**	**KY906838**
Phaeoacremonium sphinctrophorum	**CBS 337.90**	**DQ173113**	**DQ173142**
Phaeoacremonium sphinctrophorum	CBS 694.88	DQ173114	DQ173143
Phaeoacremonium subulatum	**CBS 113584**	**AY579298**	**AY579231**
Phaeoacremonium subulatum	CBS 113587	AY579299	AY579232
Phaeoacremonium tardicrescens	**CBS 110573**	**AY579300**	**AY579233**
Phaeoacremonium tectonae	**MFLUCC 13-0707**	**KT285563**	**KT285555**
Phaeoacremonium tectonae	MFLUCC 14-1131	KT285570	KT285562
Phaeoacremonium theobromatis	**CBS 111586**	**DQ173106**	**DQ173132**
Phaeoacremonium tuscanicum	**CBS 123033**	**EU863458**	**EU863490**
Phaeoacremonium venezuelense	**CBS 651.85**	**AY579320**	**AY579256**
Phaeoacremonium venezuelense	CBS 110119	AY579318	AY579254
Phaeoacremonium venezuelense	CBS 113595	AY579319	AY579255
Phaeoacremonium vibratile	CBS 117115	DQ649063	DQ649064
Phaeoacremonium viticola	CBS 113065	DQ173105	DQ173128
Phaeoacremonium viticola	CBS 101737	AF246817	DQ173129
Pleurostomophora richardsiae	CBS 270.33	AY579334	AY579271
Wuestneia molokaiensis	CBS 114877	AY579335	AY579272

Abbreviations: **CBS**: CBS-KNAW Collections, Westerdijk Fungal Biodiversity Institute, Utrecht, The Netherlands; **CMM**: Culture Collection of Phytopathogenic Fungi "Prof. Maria Menezes"; **CPC**: Culture collection of Pedro Crous, housed at CBS; **HKUCC**: The University of Hong Kong Culture Collection; **ICMP**: The International Collection of Microorganisms from Plants; **KMU**: Kanazawa Medical University herbarium; **MFLU**: Mae Fah Luang University herbarium, **MFLUCC**: Mae Fah Luang University Culture Collection, Chiang Rai, Thailand; **PARC**: Pacific Agri-Food Research Centre.

Taxonomy

Phaeoacremonium ovale **S.K. Huang, R. Jeewon & K.D. Hyde, sp. nov.**
Index Fungorum number: IF554786
Facesoffungi number: FoF 04685
Fig. 2

Type. CHINA, Yunnan Province, Baoshan, stream along the roadside; saprobic on dead wood, 21 December 2016; Huang S.K. (KUN HKAS99550, holotype; MFLU MFLU18-1076, isotype); ex-type living culture (KUMCC 17-0145; KUMCC 18-0018). GenBank no. (ITS: MH399732, TUB: MH395327, ACT: MH395325; ITS: MH399733, TUB: MH395328, ACT: MH395326)

Etymology. The name *ovale* refers to the oval shaped ascospores.

Description. Sexual morph: *Ascomata* 225–300 µm (n = 5), on wood, perithecial, solitary, semi-immersed, unilocular, subglobose to globose, black, ostiolate, with ostiolar neck erumpent through bark of host when mature. *Neck* 445–645 × 35–45 µm ($\bar{x}$ = 530 × 40 µm, n = 5), centrally ostiolate, contorted, lined with hyaline periphyses. *Peridium* 17–40 µm diam., membranous, composed of dark brown to hyaline cells of *textura angularis*. *Hamathecium* composed of 2–6 µm wide, hyaline, septate paraphyses, slightly constricted at septa and gradually narrowed towards apex. *Asci* 11–20 × 3–6 µm ($\bar{x}$ = 15.5 × 5 µm, n = 30), 8-spored, unitunicate, clavate, with short pedicel, apically rounded. *Ascospores* 3–5 × 1.5–3 µm ($\bar{x}$ = 3.5 × 2 µm, n = 50), bi-seriate, hyaline, oval to ellipsoid, aseptate, smooth-walled, rounded at the ends. **Asexual morph:** *Mycelium* on culture, partly superficial, composed of septate, branched, hyaline, rarely verrucose, hyphae 1.5–3 µm diam., rarely with adelophialides. *Conidiophores* usually arising from hyaline hyphae, mononematous, unbranched, occasionally constricted at basal septum, hyaline. *Phialides* 8–15 × 2–4 µm ($\bar{x}$ = 9.5 × 3 µm, n = 20), terminal, monophialidic, elongate-ampulliform and attenuated at base. *Conidia* 2.5–6 × 1–2.5 µm ($\bar{x}$ = 4 × 2 µm, n = 30), hyaline, ellipsoid to ovoid, aseptate.

Culture characteristics. Ascospore germinating on PDA within 1 week at 23°C, germ tubes produced from ends. Colonies growing on PDA, reaching 2 cm diam. and sporulating after 30 days. Colonies semi-immersed to superficial, irregular in shape, flat, slightly raised, with undulate edge, slightly rough on surface, cottony to fairly fluffy, colony from above, greyish-brown (5F3–5, Ridgway 1912) at the margin, initially write to cream (5A1–3) in the centre, becoming dark brown (5F7–8) at the margin, orange-white (5B1–3) at the centre; from below, initially, greyish-brown at the margin, white at the centre, becoming dark brown at the margin, orange-white at the centre, producing brown pigmentation in agar.

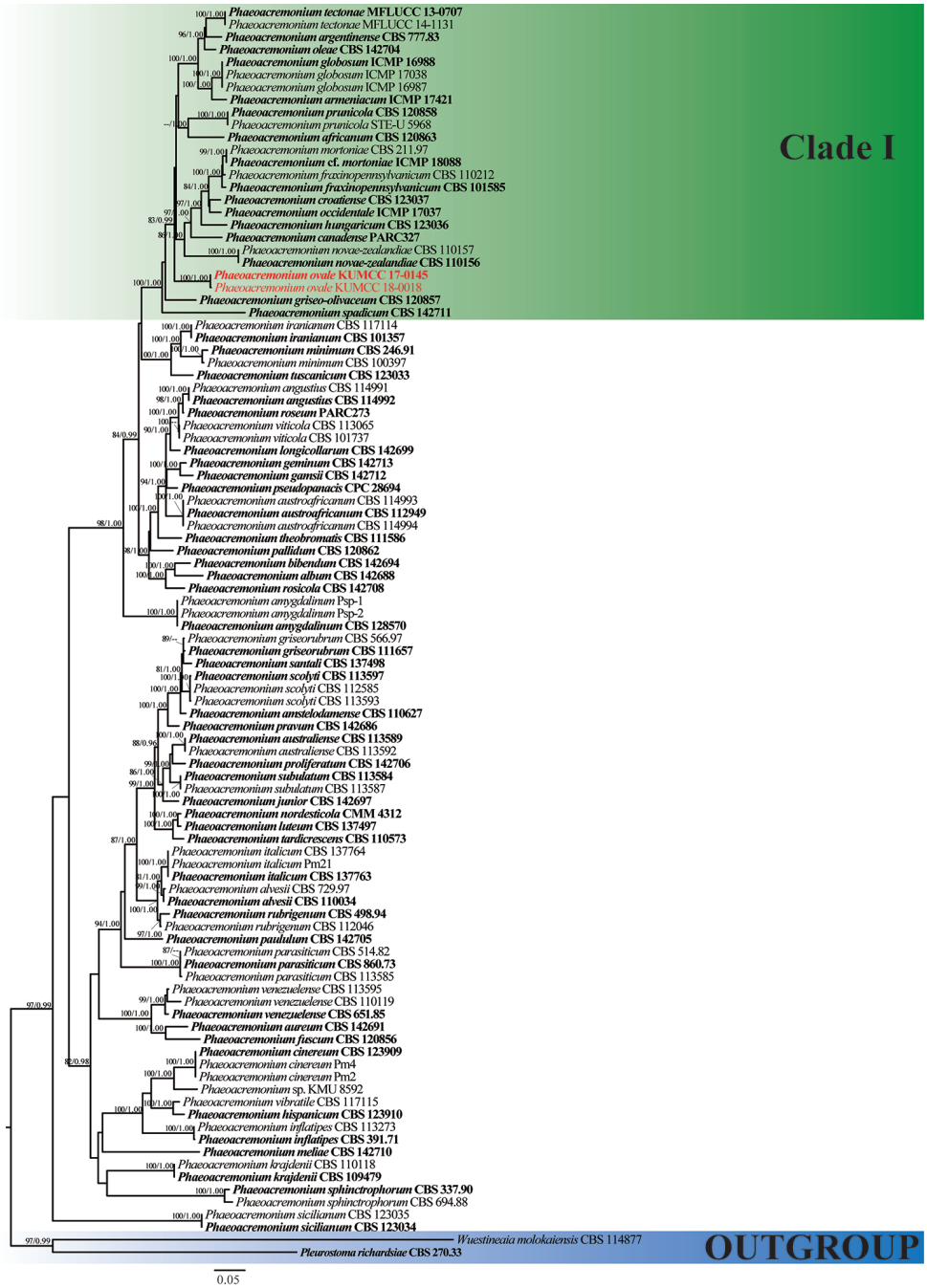

Figure 1. Maximum likelihood phylogenetic tree generated from analysis of a combined TUB and ACT sequences dataset for 98 taxa of Togniniaceae. *Pleurostoma richardsiae* (CBS 270.33) and *Wuestineaia molokaiensis* (CBS 114877) are the outgroup taxa. ML support values greater than 70% (BSML, left) and Bayesian posterior probabilities greater than 0.90 (BYPP, right) are indicated above the nodes. The strain numbers are noted after the species names. Ex-type strains are indicated in **bold**. Isolates from this study are indicated in red.

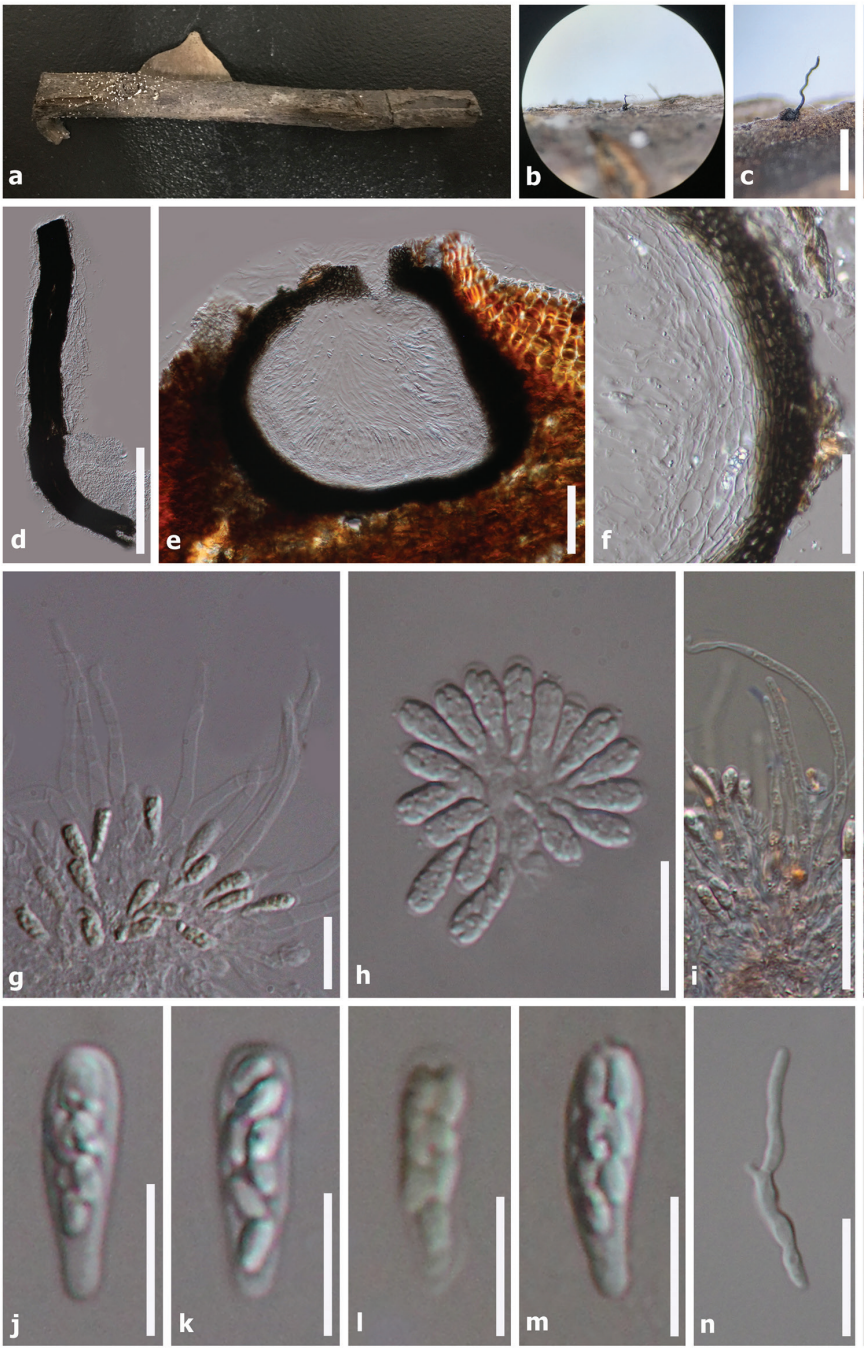

Figure 2. *Phaeoacremonium ovale* (HKAS99550, holotype)**. a** Substrate **b, c** Ascoma on host **d** Squashed neck **e** Ascoma in vertical section **f** Peridium **g** Asci surrounded by paraphyses **h** Asci **i** Septate paraphyses **j–m** Asci with ascospores **n** Germinating ascospores. Note: Fig i stained in Congo red reagent, fig l stained in Melzer's reagent. Scale bars: 500 µm (**c**); 200 µm (**d**); 100 µm (**e**); 50 µm (**f, i**); 30 µm (**n**); 20 µm (**g–h**); 10 µm (**j–m**)

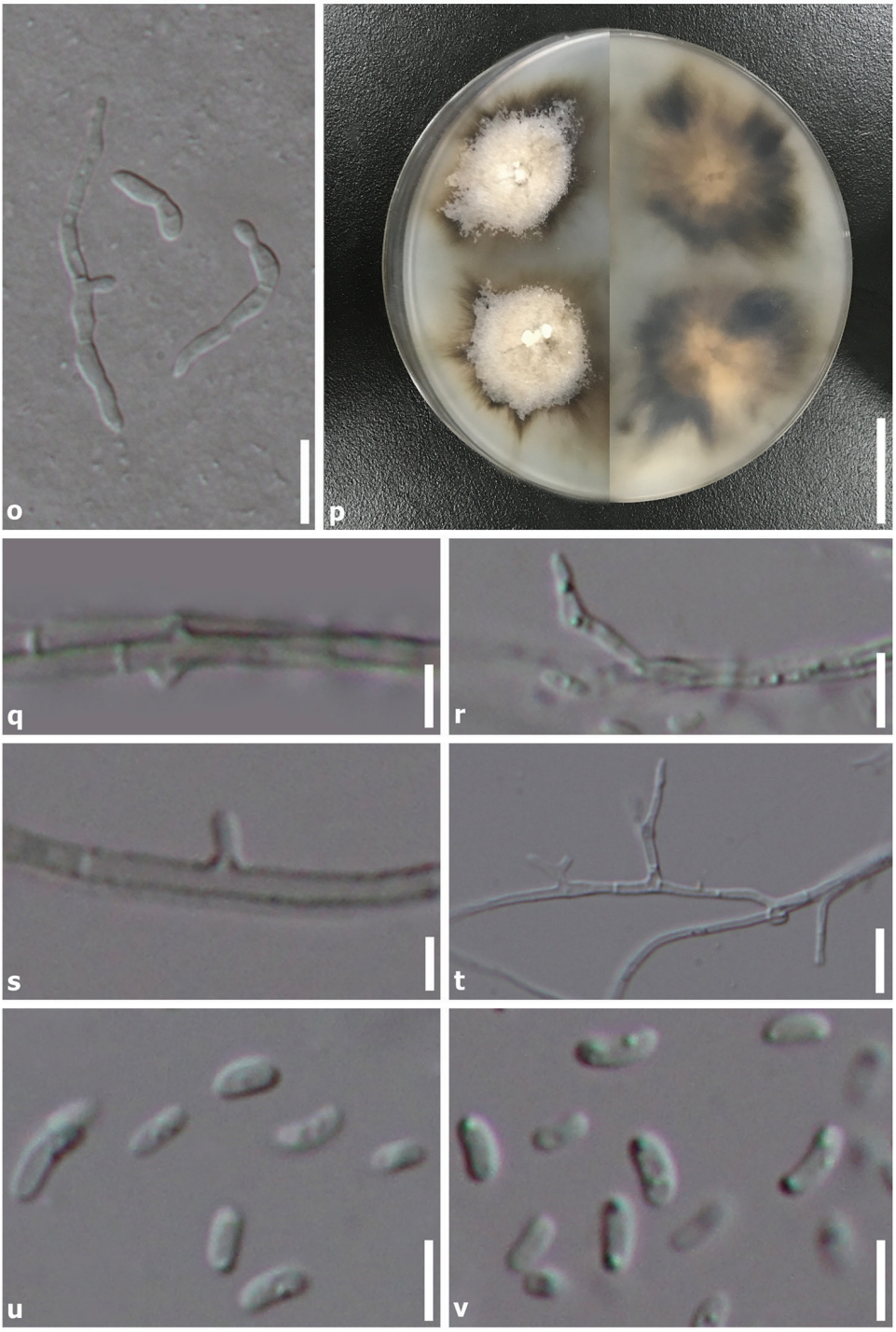

Figure 3. *Phaeoacremonium ovale* (HKAS99550, holotype). **o** Germinating ascospores, **p** 7 weeks of culture plate (above, left/reverse, right), **q** Mycelium with adelophialides **r–t** Branched conidiophores **u–v** Conidia. Scale bars: 20 mm (**p**); 20 µm (**o**); 10 µm (**r, t**); 5 µm (**q, s, u–v**).

Discussion

Phaeoacremonium is currently accommodated in the monogeneric family Togniniaceae (Wijayawardene et al. 2018). To date, 65 species are accepted in this genus (Mostert et al. 2006b; Gramaje et al. 2015; Marin-Felix et al. 2018; Spies et al. 2018). While most of the species are commonly isolated as asexual morphs, some taxa have been recovered in their sexual morph state, viz. *Phaeoacremonium aquaticum* (= *Togninia aquatica*), *P. viticola* (= *T. viticola*), *P. novae-zealandiae* (= *T. novae-zealandiae*) (Hausner et al. 1992; Mostert et al. 2006a; Hu et al. 2012).

In this study, we introduce a novel taxon of *Phaeoacremonium* from dead wood collected in a stream in the Yunnan Province, China and describe its sexual and asexual morph. Examination of morphological characters reveal that our species is sufficiently distinct from extant species to establish it as a new species. Analyses of the combined DNA sequence dataset from partial TUB and ACT genes also support that this taxon is a *Phaeoacremonium* species and phylogenetically distinct from other species (Fig. 1). The two strains of *P. ovale* constitute a strongly supported independent lineage close to other species as depicted in Clade I. Phylogeny also reveals a close relationship to *P. griseo-olivaceum*, but with low support. To further support *P. ovale* as a new species, we compared nucleotide differences with other related species as recommended by Jeewon and Hyde (2016). Comparison of the 533 nucleotides across the TUB region reveals 43 bp (10%) differences, 256 bp of the ACT region reveals 22 bp (8.5%) differences and 517 bp of the ITS region reveals 4 bp (1%) differences compared to *P. griseo-olivaceum* (CBS 120857). Examination of the TUB region reveals 59 bp (11%) difference compared to *P. africanum* (CBS 120863) while the ACT region reveals 19 bp (7%) and ITS region reveals 17 bp (3%) differences, but the latter clusters in a different subclade in our phylogeny and is therefore considered distinct. There are also some morphological similarities between *P. ovale* and *P. africanum* in terms of black ascomata with a long neck, clavate asci and small, oval to ellipsoid ascospores in sexual morph and ellipsoid to ovoid, aseptate conidia in asexual morph (Damm et al. 2008). Despite a morphological resemblance to *P. africanum* and close relationship to *P. griseo-olivaceum*, there are other differences across these species. *Phaeoacremonium ovale* was collected from an aquatic habitat and from dead wood in China whereas the former two species were collected from *Prunus* spp. in South Africa (Damm et al. 2008). In addition, conidial size of *P. africanum* and *P. griseo-olivaceum* are 5–12 × 1.5–2 µm and 5–8 × 1.5–2 µm, whereas conidia of *P. ovale* measure 2.5–6 × 1–2.5 µm (Damm et al. 2008; Fig. 3). No sequence data of the TUB and ACT gene are available for *P. aquaticum* and *P. leptorrhynchum* and therefore we provide ITS sequences of our strains and compare them with those two species. Comparison of ITS regions reveals 61 bp (12%) differences with *P. aquaticum* (IFRDCC 3035) and 11 bp (2%) differences with *P. leptorrhynchum* (UAMH9590). In addition, our new species is also morphologically different from them. *Phaeoacremonium ovale* is morphologically different as ascospores of *P. aquaticum* and *P. leptorrhynchum* are reniform (ascospores of *P. ovale* are oval/ellipsoid) and measure 5–6 × 1–1.5 µm and 7–10 × 1–1.5 µm, respectively. *Phaeoacremonium inconspicuum* as described by Gramaje et al. (2015) also appears morphologically

similar to *P. ovale* in terms of clavate asci and hyaline, aseptate ascospores (Eriksson and Yue 1990), but could not be included in our analyses as DNA sequences are unavailable. However, the ascospore shape and size of *P. inconspicuum* is different (allantoid, measuring 7–10 × 1.5–2 μm) (Eriksson and Yue 1990; Réblová 2011).

Acknowledgements

This work was supported by the National Natural Science Foundation of China (No. 31760014), the Science and Technology Foundation of Guizhou Province (No. [2016]2863 & [2017]5788). Dr. Qi Zhao is acknowledged for his support and thanks to Dr. Sajeewa Maharachchikumbura for his valuable help in phylogenetic analyses. Shaun Pennycook is thanked for checking and correcting the Latin name.

References

Cabanela MV, Jeewon R, Hyde KD (2007) Morphotaxonomy and phylogeny of *Paoayensis lignicola* gen et sp. nov. (ascomycetes) from submerged wood in Paoay Lake, Ilocos Norte, the Philippines. Cryptogamie, Mycologie 28: 301–310.

Carbone I, Kohn LM (1999) A method for designing primer sets for speciation studies in filamentous ascomycetes. Mycologia 91(3): 553–556. https://doi.org/10.2307/3761358

Carlucci A, Lops F, Cibelli F, Raimondo ML (2015) *Phaeoacremonium* species associated with olive wilt and decline in southern Italy. European Journal of Plant Pathology 141(4): 717–729. https://doi.org/10.1007/s10658-014-0573-8

Chomnunti P, Hongsanan S, Aguirre-Hudson B, Tian Q, Peršoh D, Dhami MK, Alias AS, Xu JC, Liu XZ, Stadler M, Hyde KD (2014) The sooty moulds. Fungal Diversity 66: 1–36. https://doi.org/10.1007/s13225-014-0278-5

Crous PW, Gams W, Wingfield MJ, van Wyk PS (1996) *Phaeoacremonium* gen. nov. associated with wilt and decline diseases of woody hosts and human infections. Mycologia 88(5): 786–796. https://doi.org/10.1080/00275514.1996.12026716

Damm U, Mostert L, Crous PW, Fourie PH (2008) Novel *Phaeoacremonium* species associated with necrotic wood of *Prunus* trees. Persoonia 20: 87–102. https://doi.org/10.3767/003158508X324227

Darriba D, Taboada GL, Doallo R, Posada D (2012) jModelTest 2: more models, new heuristics and parallel computing. Nature Methods 9(8): 772. https://doi.org/10.1038/nmeth.2109

Di Marco S, Calzarano F, Osti F, Mazzullo A (2004) Pathogenicity of fungi associated with a decay of kiwifruit. Australasian Plant Pathology 33: 337–342. https://doi.org/10.1071/AP04024

Eriksson O, Yue JZ (1990) Notes on bambusicolous pyrenomycetes. No.s 1-10. Mycotaxon 38: 201–220.

Glass NL, Donaldson GC (1995) Development of primer sets designed for use with the PCR to amplify conserved gene from filamentous Ascomycetes. Applied and Environmental Microbiology 61: 1323–1330.

Gramaje D, García-Jiménez J, Armengol J (2012) Fungal trunk pathogens in Spanish grapevine nurseries: a survey of current nursery management practices in Spain. Phytopathologia Mediterranea 51: 411–412.

Gramaje D, Mostert L, Groenewald JZ, Crous PW (2015) *Phaeoacremonium*: From esca disease to phaeohyphomycosis. Fungal Biology 119: 759–783. https://doi.org/10.1016/j.funbio.2015.06.004

Groenewald M, Kang JC, Crous PW, Gams W (2001) ITS and β-tubulin phylogeny of *Phaeoacremonium* and *Phaeomoniella* species. Mycological Research 105: 651–657. https://doi.org/10.1017/S0953756201004282

Guarro J, Alves SH, Gené J, Grazziotin NA, Muzzuco R, Dalmagro C, Capilla J, Zaror L, Mayayo E (2003) Two cases of subcutaneous infection due to *Phaeoacremonium* spp. Journal of Clinical Microbiology 41: 1332–1336. https://doi.org/10.1128/JCM.41.3.1332-1336.2003

Hall T (1999) BioEdit: a user-friendly biological sequence alignment editor and analysis program for Windows 95/98/NT. Nucleic Acids Symposium Series 41: 95–98.

Hausner G, Eyjólfsdóttir GG, Reid J, Klassen GR (1992) Two additional species of the genus *Togninia*. Canadian Journal of Botany 70(4): 724–734. https://doi.org/10.1139/b92-093

Hemashettar BM, Siddaramappa B, Munjunathaswamy BS, Pangi AS, Pattan J, Andrade AT, Padhye AA, Mostert L, Summerbell RC (2006) *Phaeoacremonium krajdenii*, a cause of white grain eumycetoma. Journal of Clinical Microbiology 44: 4619–4622. https://doi.org/10.1128/JCM.01019-06

Hongsanan S, Maharachchikumbura SSN, Hyde KD, Samarakoon MC, Jeewon R, Zhao Q, Al-Sadi AM, Bahkali AH (2017) An updated phylogeny of Sordariomycetes based on phylogenetic and molecular clock evidence. Fungal Diversity 84: 25–41. https://doi.org/10.1007/s13225-017-0384-2

Hu DM, Cai L, Hyde KD (2012) Three new ascomycetes from freshwater in China. Mycologia 104(6): 1478–1489. https://doi.org/10.3852/11-430

Hyde KD, Fryar S, Tian Q, Bahkali AH, Xu JC (2016) Lignicolous freshwater fungi along a north-south latitudinal gradient in the Asian/Australian region; can we predict the impact of global warming on biodiversity and function? Fungal Ecology 19: 190–200. https://doi.org/10.1016/j.funeco.2015.07.002

Jayasiri SC, Hyde KD, Ariyawansa HA, Bhat J, Buyck B, Cai L, Dai YC, Abd-Elsalam KA, Ertz D, Hidayat I, Jeewon R, Jones EBG, Bahkali AH, Karunarathna SC, Liu JK, Luangsa-ard JJ, Lumbsch HT, Maharachchikumbura SSN, McKenzie EHC, Moncalvo JM, GhobadNejhad M, Nilsson H, Pang KL, Pereira OL, Phillips AJL, Raspé O, Rollins AW, Romero AI, Etayo J, Selçuk F, Stephenson SL, Suetrong S, Taylor JE, Tsui CKM, Vizzini A, Abdel-Wahab MA, Wen TC, Boonmee S, Dai DQ, Daranagama DA, Dissanayake AJ, Ekanayaka AH, Fryar SC, Hongsanan S, Jayawardena RS, Li WJ, Perera RH, Phookamsak R, de Silva NI, Thambugala KM, Tian Q, Wijayawardene NN, Zhao RL, Zhao Q, Kang JC, Promputtha I (2015) The Faces of Fungi database: fungal names linked with morphology, phylogeny and human impacts. Fungal Diversity 74: 3–18. https://doi.org/10.1007/s13225-015-0351-8

Jeewon R, Cai L, Zhang K, Hyde KD (2003) *Dyrithiopsis lakefuxianensis* gen et sp. nov. from Fuxian Lake, Yunnan, China and notes on the taxonomic confusion surrounding *Dyrithium*. Mycologia 95: 911–920. https://doi.org/10.1080/15572536.2004.11833050

Jeewon R, Hyde KD (2016) Establishing species boundaries and new taxa among fungi: recommendations to resolve taxonomic ambiguities. Mycosphere 7: 1669–1677. https://doi.org/10.5943/mycosphere/7/11/4

Katoh K, Standley DM (2016) A simple method to control over-alignment in the MAFFT multiple sequence alignment program. Bioinformatics 32(13): 1933–1942. https://doi.org/10.1093/bioinformatics/btw108

Kubátová A, Kolarik M, Pazoutová S (2004) *Phaeoacremonium rubrigenum*–hyphomycete associated with bark beetles found in Czechia. Folia Microbiology 49: 99–104. https://doi.org/10.1007/BF02931381

Luo ZL, Hyde KD, Bhat DJ, Jeewon R, Maharachchikumbura SSN, Bao DF, Li WL, Su XJ, Yang XY, Su HY (2018) Morphological and molecular taxonomy of novel species *Pleurotheciaceae* from freshwater habitats in Yunnan, China. Mycological Progress 17(5): 511–530. https://doi.org/10.1007/s11557-018-1377-6

Marin-Felix Y, Hernández-Restrepo M, Wingfield MJ, Akulov A, Carnegie AJ, Cheewangkoon R, Gramaje D, Groenewald JZ, Guarnaccia V, Halleen F, Lombard L, Luangsaard J, Marincowitz S, Moslemi A, Mostert L, Quaedvlieg W, Schumacher RK, Spies CFJ, Thangavel R, Taylor PWJ, Wilson AM, Wingfield BD, Wood AR, Crous PW (2018) Genera of phytopathogenic fungi: GOPHY 2. Studies in Mycology. https://doi.org/10.1016/j.simyco.2018.04.002

Miller AM, Schwartz T, Pickett BE, He S, Klem EB, Scheuermann RH, Passarotti M, Kaufman S, O'Leary MA (2015) A RESTful API for access to phylogenetic tools via the CIPRES science gateway. Evol Bioinform 11: 43–48. https://doi.org/10.4137/EBO.S21501

Mostert L, Crous PW, Groenewald JZE, Gams W, Summerbell RC (2003) *Togninia* (Calosphaeriales) is confirmed as teleomorph of *Phaeoacremonium* by means of morphology, sexual compatibility and DNA phylogeny. Mycologia 95(4): 646–659. https://doi.org/10.1080/15572536.2004.11833069

Mostert L, Groenewald JZ, Summerbell RC, Gams W, Crous PW (2006a) Taxonomy and pathology of *Togninia* (Diaporthales) and its *Phaeoacremonium* anamorphs. Studies in Mycology 54: 1–115. https://doi.org/10.3114/sim.54.1.1

Mostert L, Halleen F, Fourie P, Crous PW (2006b) A review of *Phaeoacremonium* species involved in Petri disease and esca of grapevines. Phytopathologia Mediterranea 45: 12–29.

Nigro F, Boscia D, Antelmi I, Ippolito A (2013) Fungal species associated with a severe decline of olive in Southern Italy. Journal of Plant Pathology 95(3): 668–668.

O'Donnell K, Cigelnik E (1997) Two divergent intragenomic rDNA ITS2 types within a monophyletic lineage of the fungus *Fusarium* are nonorthologous. Molecular Phylogenetics and Evolution 7: 103–116. https://doi.org/10.1006/mpev.1996.0376

Olmo D, Gramaje D, Agustí-Brisach C, Leon M, Armengol J (2014) First report of *Phaeoacremonium venezuelense* associated with decay of apricot trees in Spain. Plant Disease 98(7): 1001. https://doi.org/10.1094/PDIS-12-13-1198-PDN

Pascoe IG, Edwards J, Cunnington JH, Cottral E (2004) Detection of the *Togninia* teleomorph of *Phaeoacremonium aleophilum* in Australia. Phytopathologia Mediterranea 43: 51–58.

Réblová M (2011) New insights into the systematics and phylogeny of the genus *Jattaea* and similar fungi of the *Calosphaeriales*. Fungal Diversity 49: 167–198. https://doi.org/10.1007/s13225-011-0099-8

Réblová M, Miller AN, Rossman AY, Seifert KA, Crous PW, Hawksworth DL, Abdel-Wahab MA, Cannon PF, Daranagama DA, De Beer ZW, Huang SK, Hyde KD, Jayawardena R, Jaklitsch W, Jones EB, Ju YM, Judith C, Maharachchikumbura SS, Pang KL, Petrini LE, Raja HA, Romero AI, Shearer C, Senanayake IC, Voglmayr H, Weir BS, Wijayawarden NN (2016) Recommendations for competing sexual-asexually typified generic names in Sordariomycetes (except Diaporthales, Hypocreales, and Magnaporthales). IMA Fungus 7(1): 131–153. https://doi.org/10.5598/imafungus.2016.07.01.08

Ridgway R (1912) Color Standards and Color Nomenclature. Washington, DC. https://doi.org/10.5962/bhl.title.144788

Ronquist F, Huelsenbeck JP (2003) Mrbayes 3: Bayesian phylogenetic inference under mixed models. Bioinformatics 19: 1572–1574. https://doi.org/10.1093/bioinformatics/btg180

Rooney-Latham S, Eskalen A, Gubler WD (2004) Ascospore discharge and occurrence of *Togninia minima* (anamorph = *Phaeoacremonium aleophilum*) in California vineyards. (Abstr.) Phytopathology 94: S57.

Rooney-Latham S, Escalen A, Gubler WD (2005a) Teleomorph formation of *Phaeoacremonium aleophilum*, cause of esca and grapevine decline in California. Plant Disease 89: 177–184. https://doi.org/10.1094/PD-89-0177

Rooney-Latham S, Eskalen A, Gubler WD (2005b) Ascospore release of *Togninia minima*, cause of esca and grapevine decline in California. Online. Plant Health Progress. https://doi.org/10.1094/PHP-2005-0209-01-RS

Rumbos IC (1986) *Phialophora parasitica*, causal agent of cherry dieback. Journal of Phytopathology 117: 283–287. https://doi.org/10.1111/j.1439-0434.1986.tb00944.x

Spies CFJ, Moyo P, Halleen F, Mostert L (2018) *Phaeoacremonium* species diversity on woody hosts in the Western Cape Province of South Africa. Persoonia 40: 26–62. https://doi.org/10.3767/persoonia.2018.40.02

Stamatakis A (2014) RAxML version 8: a tool for phylogenetic analysis and post-analysis of large phylogenies. Bioinformatics 30: 1312–1313. https://doi.org/10.1093/bioinformatics/btu033

Wijayawardene NN, Hyde KD, Lumbsch HT, Liu JK, Maharachchikumbura SSN, Ekanayaka AH, Tian Q, Phookamsak R (2018) Outline of Ascomycota: 2017. Fungal Diversity 88: 167–263. https://doi.org/10.1007/s13225-018-0394-8

White TJ, Bruns T, Lee S, Taylor J (1990) Amplification and direct sequencing of fungal ribosomal RNA genes for phylogenetics. In: Innis MA, Gelfand DH, Sninsky JJ, White TJ. (Eds) PCR Protocols: A Guide to Methods and Applications. Academic Press, San Diego, 315–322.

Zhang Y, Jeewon R, Fournier J, Hyde KD (2008) Multi-gene phylogeny and morphotaxonomy of *Amniculicola lignicola*: novel freshwater fungus from France and its relationships to the Pleosporales. Fungal Biology 112: 1186–1194.

MycoKeys 41: 17–27 (2018)
doi: 10.3897/mycokeys.41.28130
http://mycokeys.pensoft.net

RESEARCH ARTICLE

A peer-reviewed open-access journal
MycoKeys
Launched to accelerate biodiversity research

Description and distribution of *Tuber incognitum* sp. nov. and *Tuber anniae* in the Transmexican Volcanic Belt

Carolina Piña Páez[1], Gregory M. Bonito[2], Gonzalo Guevara-Guerrero[3], Michael A. Castellano[4], Roberto Garibay-Orijel[1], James M. Trappe[4], Rafael Peña Rámirez[3]

1 *Instituto de Biología, Universidad Nacional Autónoma de México, Tercer Circuito s/n, Ciudad Universitaria Delegación Coyoacán, A.P. 70-233, C.P. 04510 Ciudad de México, México* **2** *Department of Plant, Soil and Microbial Sciences, Michigan State University, East Lansing, MI 48824, USA* **3** *Instituto Tecnológico de Ciudad Victoria. Av. Portes Gil 1301 Poniente, 87010 Ciudad Victoria, Tamaulipas, México* **4** *US Department of Agriculture, Forest Service, Northern Research Station, Forestry Sciences Laboratory, Corvallis, Oregon, 97331, USA*

Corresponding author: *Roberto Garibay-Orijel* (rgaribay@ib.unam.mx)

Academic editor: *K. Hyde* | Received 3 July 2018 | Accepted 12 September 2018 | Published 11 October 2018

Citation: Piña Páez C, Bonito GM, Guevara-Guerrero G, Castellano MA, Garibay-Orijel R, Trappe JM, Rámirez RP (2018) Description and distribution of *Tuber incognitum* sp. nov. and *Tuber anniae* in the Transmexican Volcanic Belt. MycoKeys 41: 17–27. https://doi.org/10.3897/mycokeys.41.28130

Abstract

The genus *Tuber* is a lineage of diverse ectomycorrhizal, hypogeous, sequestrate ascomycete fungi that are native to temperate forests in the Northern Hemisphere. Recently, many new species of *Tuber* have been described in North America and Asia, based on morphological characteristics and molecular data. Here we describe and illustrate a new species, *Tuber incognitum*, based upon phylogenetic analysis and morphological description. We also present a new record for *Tuber anniae* in México. These two *Tuber* species are distributed in the Transmexican Volcanic Belt in the states of México, Michoacán, Guanajuato, Querétaro and Tlaxcala at altitudes between 2,000 and 3,200 meters. These species are associated with *Pinus* (*T. anniae*) and *Quercus* forests (*T. incognitum*).

Keywords

Sequestrate fungi, truffles, Ascomycota, Systematics, new species

Introduction

Fungal species, within the genus *Tuber,* produce hypogeous, sequestrate ascomata, that are more commonly known as truffles. These fungi are ectomycorrhizal (EcM) symbionts of angiosperm or gymnosperm hosts, including many species of trees as well as orchids. Plant hosts provide their EcM symbionts with carbohydrates in exchange for greater access to water and nutrients (Wurzburger et al. 2001; Bidartondo et al. 2004; Walker et al. 2005; Shefferson et al. 2008). The genus *Tuber* has been studied intensively over the past century, largely due to its economic importance as an edible fungus. Most of these efforts have been directed towards European species with economic value (e.g. *Tuber melanosporum*, *Tuber magnatum*, *Tuber aestivum*), which reside in a few clades, neglecting most of the diversity in this genus. Reference and environmental sequences data were recently used to infer a minimum of 180–230 species of *Tuber* worldwide (Bonito et al. 2010) and substantiate that most *Tuber* diversity resides within less studied and non-economically important lineages delimitated as the Rufum, Puberulum and Maculatum clades. In México, eighteen *Tuber* species are known and have been formally described. The majority of the collections of these described species are from northeast and central México. In this study, we propose the new species *Tuber incognitum* and provide the first report of *T. anniae* in México based on morphological characteristics and phylogenetic analyses.

Materials and methods

Morphological observation

Ascomata were collected from the states of Guanajuato, México, Michoacán, Querétaro, Tlaxcala and were deposited in herbaria at Oregon State University (OSC), Herbario Nacional de México (MEXU) and Herbario José Castillo Tovar (ITCV). Macroscopic characters were recorded from fresh specimens and microscopic characters were described from both sections of fresh specimens and dried specimens mounted in 5% potassium hydroxide (KOH) following protocols from Castellano et al. (1989).

DNA sequencing and phylogenetic analyses

DNA was extracted from ascomata of collections OSC157842 and OSC150066 using a CTAB chloroform extract protocol and ITS rDNA was amplified and sequenced as previously described (Bonito et al. 2010). Tissue samples from collections MEXU 26504, MEXU 26541, MEXU 26218 and MEXU25995 were sent to the Canadian Center of Barcoding (CCDB) for extraction, amplification, sequencing and barcoding of the Internal Transcribed Spacers (ITS). The ITS region was amplified with ITS1f and ITS4 primers (White et al. 1990). The sequences were edited in Geneious

7.1 (http://www.geneious.com, Kearse et al. 2012). The distribution and ecology of these species was complemented with soil DNA data from central and south México through a BLASTn search against the Mexican Soil Fungi Database in Geneious 7.1. This database includes ITS2 sequences of soil fungi (total DNA soil extractions) from central and southern México as part of an ongoing project, which has been partially published by Argüelles-Moyao and Garibay-Orijel (2018).

DNA sequences were manually trimmed and edited with Sequencher 4.0 (Gene Codes Corp., Ann Arbor, Michigan). ITS sequences were queried against the NCBI public database GenBank by use of the BLASTn algorithm to retrieve similar sequences (Altschul et al. 1990). Collated DNA sequences were aligned with MUSCLE in Mesquite 3.04 (Maddison and Maddison 2015; Edgar 2004). Ambiguously aligned regions were excluded from the alignment. Phylogenetic analyses were conducted on ITS rDNA alignments through the CIPRES portal (www.phylo.org, Miller et al. 2010). Maximum Likelihood (ML) searches were conducted with RAxML v.7.2.8 using rapid bootstrapping of 1,000 pseudoreplicates (Stamatakis 2014). Bayesian Inference (BI) was carried out with MrBayes v3.2.6 (Ronquist and Huelsenbeck 2003). To estimate posterior probabilities, 20,000,000 Markov chain Monte Carlo (MCMC) simulation generations were run in two parallel searches on four chains, with trees sampled every 1,000th generation, with the first 5,000 trees discarded as burn-in (convergence of parallel runs). Bootstrap support, based on 1,000 iterations, was considered informative where it was ≥ 70% and posterior probability was considered significant where it was ≥ 99%. Sequences, generated in this study, are available on GenBank under the accession numbers GQ221447, KC152267, KC152256, KJ595013, KJ595014 and MH174661 (Table 1) and in the BOLD systems database (www.barcodinglife.org).

Results

Descriptions

***Tuber incognitum* Piña Páez, Bonito, Guevara & Castellano, sp. nov.**
MycoBank: MB 824931
BOLD systems: ECMTM112, ECMCU046.
Fig. 1a–d

Type. MÉXICO, State of Querétaro, Huimilpan, San Pedro, under *Quercus crassifolia* Humb. and Bonpl., *Quercus* spp., hypogeous, gregarious, 24 September 1996, M.A. Castellano (Holotype: OSC 150066), GB GQ221447. State of Michoacán, Zinapécuaro, el Jaral, under *Quercus polymorpha* Schltdl. and Cham., hypogeous, solitary or in groups of two, 2380 m alt., 19°46'48"N, -100°47'24"W, 4 September 2008, R. Garibay-Orijel (Paratype: MEXU 25995), GB KJ595014. State of México, Temascaltepec, under *Quercus* spp., hypogeous, solitary, 2011 m alt., 19°04'12"N, -100°01'48"W, 8 July 2009, R. Garibay-Orijel (Paratype: MEXU 26218), GB KJ595013.

Table 1. Accession and voucher numbers of sequences generated in this paper.

Taxon	GenBank	Voucher	Origin	Reference
T. incognitum Piña Páez. Bonito, Guevara & Castellano	GQ221447	OSC 150066	Ascoma	This paper
	KJ595013	MEXU 26218	Ascoma	This paper
	KJ595014	MEXU 25995	Ascoma	This paper
	MH174661	–	EcM	This paper
	MH447961	ITCV 1695	Ascoma	This paper
T. anniae W. Colgan & Trappe	MH174660	OSC 157842	Ascoma	This paper
T. bonitoi G. Guevara & Trappe	KC152256	MEXU 26541	Ascoma	Guevara et al. 2015
Tuber sp. 3	KJ152267	MEXU 26504	Ascoma	This paper

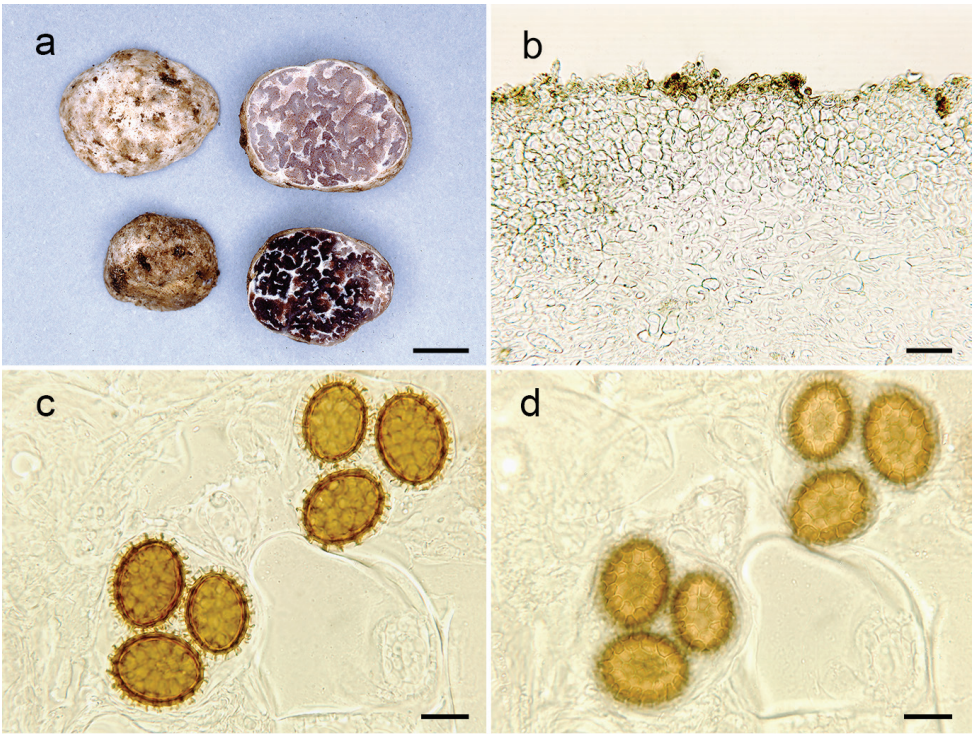

Figure 1. *Tuber incognitum* (Holotype, OSC 150066). **a** Ascoma, surface and cross-section view **b** Peridium in cross-section **c** Light microscopy of spores in cross-sectional view, highlighting the spines and ornamentation **d** Light microscopy of spores in surface view, highlighting the surface and reticulum. Scale bars: 5 mm (**a**), 20 µm (**b**), 15 µm (**c, d**).

Diagnosis. *Tuber incognitum* is distinctive in the structure of its peridium (two-layered) and spore size (25–55 × 20–44 µm), which separates it from the rest of the species within the Puberulum clade reported from México.

Etymology. Incognitum is Latin for unknown. The name incognitum is not derived from its morphology, rather from the fact that it was overlooked for so long. The holotype was collected in 1996 and not described until now.

Description. ***Ascomata*** 10–15 mm broad, subglobose to slightly irregular, white with light brown areas when dry, glabrous, with canals that continue with the veins into the gleba. Gleba pinkish to purplish pale-brown in youth, dark brown at maturity, marbled with white veins. Odour fruity, pleasant.

Peridium two-layered, when handled the upper layer is lost and only the inner layer is observable under the light microscope, 350–400 µm thick, pellis 175–240 µm thick, composed of isodiametric or angular cells, 6–15 µm broad, walls 1.75–2.0 µm thick, yellowish hyaline in KOH. Subpellis 110–140 µm thick, composed of septate, interwoven hyphae (*textura intricata*), 4.5–7.0 µm broad, thin walled < 1 µm thick, hyaline in KOH. Gleba composed of septate, interwoven hyphae (*textura epidermoidea*), 5.0–7.5 µm broad, thin walled < 1 µm thick, hyaline in KOH. ***Ascospores*** broadly ellipsoid; excluding their alveolate-reticulate ornamentation, in 1-spored asci 45–55 × 34–44 µm (Q = 1.3), 2-spored 37–43 × 29–34 µm (Q = 1.25–1.36), 3-spored 30–42 × 26–31 µm (Q = 1.2–1.37), 4-spored 28–33 × 24–28 µm (Q = 1.09–1.25) and 5-spored 25–28 × 20–28 µm (Q = 1.2–1.25), spore colour orange-yellow in KOH, the walls > 2 µm thick; reticulum with 3–8 alveolae across the spore surface; the alveolar walls 3.5–4.0 µm tall. ***Asci*** globose, subglobose to broadly ellipsoid, pyriform, 88–100 × 70–95 µm, pedicel lacking to prominent, hyaline in KOH, hyphae around the asci prostrated or interwoven, cylindrical, 3.5–6.0 µm broad at the septa, thin walled, hyaline in KOH.

Distribution and ecology. Only known from central and southwest México (Querétaro, Michoacán, State of México, Guanajuato and Hidalgo). Ascocarps always associated with *Quercus* species (*Q. crassifolia*, *Q. polymorpha*). An EcM association with *Quercus* has been verified (MH174661) and its DNA has been recovered only from soil in *Quercus* forest in Hidalgo, México.

Additional collections examined. MÉXICO, State of Guanajuato, Guanajuato, Las Palomas, under *Quercus* spp., hypogeous, in groups of two, 2534 m alt., 21°03'50"N, -101°13'23"W, 10 October 2016, R. Peña-Ramirez (ITCV 1695).

Taxonomic comments. *Tuber incognitum* resembles *Tuber pseudoseparans* in the colour of the peridium and the lack of dermatocystidia but differs by the size of the spores (being smaller in *T. incognitum*, 31–50 × 24–37 µm vs. *T. pseudoseparans*, 46–65 × 34–46 µm) and in the thickness of the peridium (being thinner in *T. pseudoseparans*, by ± 250 µm). *Tuber incognitum* is similar to *Tuber bonitoi* in spore size and ornamentation, but differs by the presence of dermatocystidia, which are absent in *T. incognitum* and the thickness of the peridium, being thicker in *T. bonitoi* (200–500 µm). *Tuber incognitum* is similar to *Tuber guzmanii* in the peridial organisation, both species have a well differentiated two-layered peridium but differ in the thickness (being thinner in *T. guzmanii*, 100–160 µm) and spore ornamentation (alveolate reticulum, 2–4 µm tall) and the size of the spores (being larger in *T. guzmanii*, 27–68 × 30–50 µm). The collection from Guanajuato represents a young developmental stage of *T. incognitum*, this collection has a thinner peridium (130–345 µm) and smaller spores (1-spored asci 23–35 × 19–25 µm, Q = 1.09 1.59; 2-spored 18–29 × 17–22 µm, Q = 1.0–1.61; 3-spored 30–42 × 26–31 µm, Q = 1.11–1.2; 4-spored 23–27 × 19–25 µm, Q = 1.08–1.26). These differences represent morphological variation within the species and its identity was confirmed with molecular data.

***Tuber anniae* W. Colgan & Trappe**
Fig. 2a–d

Description. ***Ascomata*** subglobose to slightly irregular, 10–12 mm broad, white, cream, light brown when dry. Peridium thin, < 0.2 mm, smooth to velvety, irregularly roughened, furrows with depressions continuing as canals into the gleba. Gleba solid, brown, marbled with white veins that emerge as depressions on the peridium. Odour and taste not recorded.

Peridium 85–140 µm thick; pellis a pseudoparenchyma, 40–65 µm thick, cells 6–18 µm broad, versiform, isodiametric, squared, rectangular or angular, hyaline to yellowish in KOH, thick walled (> 1.0 µm), dermatocystidia absent; subpellis 45–75 µm thick, of hyaline, septate, interwoven hyphae (*textura epidermoidea*), 4.0–5.5 µm broad, thin walled, < 1 µm thick. Gleba of hyaline, interwoven, sinuous hyphae, 5.0–7.5 µm broad, constrained at the septum, 3.0–4.5 µm broad at the septa, thin-walled (< 1.0 µm).

Ascospores subglobose; excluding their alveolate-reticulate ornamentation, 1-spored asci 40–50 × 30–46 µm (Q= 1.03–1.15), 2-spored 28–38 × 26–35 µm (Q = 1.05–1.13), 3-spored 26–33 × 24–30 µm (Q = 1.04–1.15), spore colour orange-yellowish in KOH; walls > 2 µm thick, yellow; reticulum with 5–6 aveolae across the spore surface; the alveolar walls 3–4.5 µm tall. ***Asci*** subglobose, 84–105 × 75–85 µm, pedicel lacking to prominent, walls with 2–3 layers, hyaline in KOH; hyphae around the asci interwoven, 3.5–5.5 µm broad at the septum, thin walled (< 1.0 µm), hyaline in KOH.

Distribution and ecology. Wang et al. (2013) reported from Europe; Colgan and Trappe 1997; Bonito et al. (2010) reported in North America. Here, we extended the distribution to central México (State of México and Tlaxcala). In Finland, *T. anniae* has been confirmed to establish association with *P. sylvestris* L. (Wang et al. 2013). In Washington, this species has been confirmed to establish association with *Pseudotsuga menziesii* (Mirbel) Franco (Bonito et al. 2010). In México, sporocarps always collected co-occurring with *Pinus leiophylla* Schiede and Deppe and *Abies religiosa* (Kuntch) Schldl. and Cham. In México, the only environmental DNA of this species has been recovered from soil in conifer forests in Tlaxcala associated with *Pinus montezumae* and in State of México associated with *A. religiosa* (Argüelles-Moyao and Garibay-Orijel 2018).

Collections examined. MÉXICO, State of Tlaxcala, Huamantla, cañada central, La Malinche National Park, under *Pinus leiophylla* Schiede and Deppe and *Abies religiosa* (Kunth) Schltdl. and Cham., hypogeous, solitary, 3220 m alt., 19°14'7"N, -97°59'9"W, 23 September 2007, G.M. Bonito (OSC 157842), GB MH174660.

Taxonomic comments. *Tuber anniae* is similar to *Tuber pacificum* Trappe, Castellano and Bushnell, however, the latter species has narrower, ellipsoid spores (23–15 × 16–35 µm) and a thicker peridium (250–400 µm) than the former. *T. pacificum* has also been found co-occurring with *Pseudotsuga menziesii* and *Tsuga heterophylla* (Raf.) Sarg. along costal Oregon, while *T. anniae* has been found co-occurring with *P. leiophylla* and *A. religiosa.*

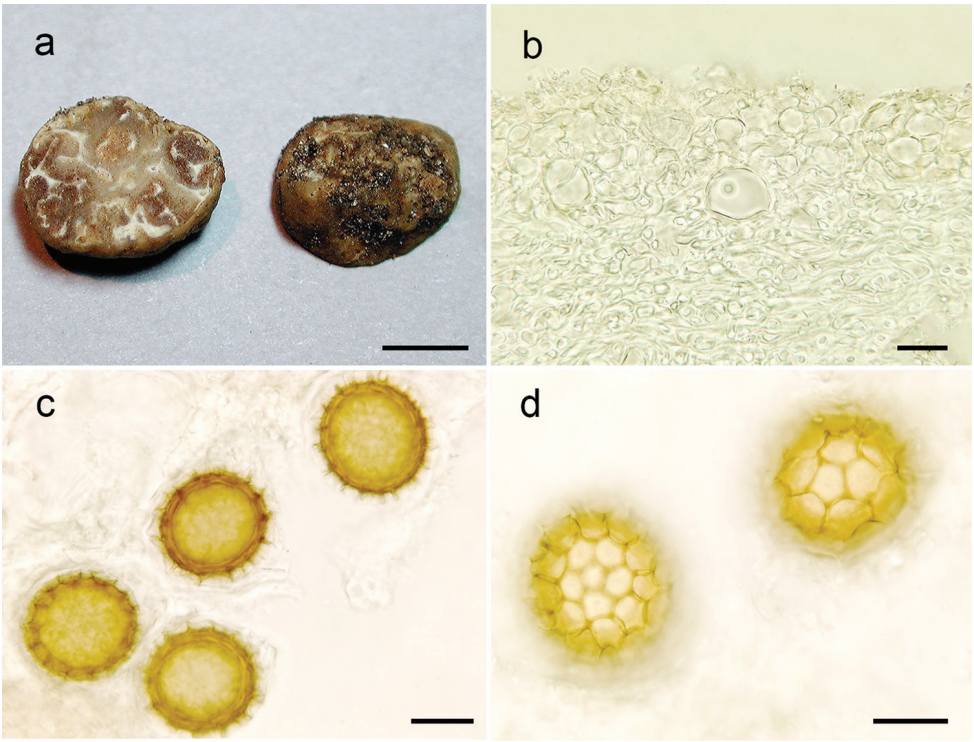

Figure 2. *Tuber anniae* (OSC 157842). **a** Ascoma, surface and cross-section view **b** Peridium in cross-section **c** Light microscopy of spores in cross-sectional view, highlighting the spines and ornamentation **d** Light microscopy of spores in surface view, highlighting the surface and reticulum. Scale bars: 5 mm (**a**), 15 µm (**b, c, d**).

Tuber anniae was first described by Colgan and Trappe (1997). The holotype (from Washington) and the other collections reported were from the Pacific Northwest in the US and reported co-occurring with *P. menziesii*. The *T. anniae* complex of species has been proposed based on phylogenetic analysis using ITS region (Wang et al. 2013). The collection from México is very similar to the holotype collection, however, the latter has a brown to dark olive-brown peridium and its spores have thicker (up to 5 µm) spore walls than the former. Additionally, *T. anniae,* as described by Colgan and Trappe (1997), has mostly globose spores with 10–16 alveolae across the spores. The Finnish collections exhibit subtle morphological differences in comparison with the collections from North America. The Finnish specimens have a smooth peridial surface, except along the grooves and around the pits (Wang et al. 2013), while the holotype specimen was reported to be smooth and lack dermatocystidia (Colgan and Trappe 1997). It seems that the presence of dermatocystida only along the grooves and/or at the bottom of pits in *Tuber* collections is likely the result of handling of the ascoma during processing (Dr. D. Luoma, personal communication). Additionally, the spores from the Finnish specimens have larger dimensions (27–60 × 27–56 µm; Q = (1.00) 1.05–1.20 (1.33)) than the specimens described for *T. anniae* by Colgan and Trappe from Washington (1997).

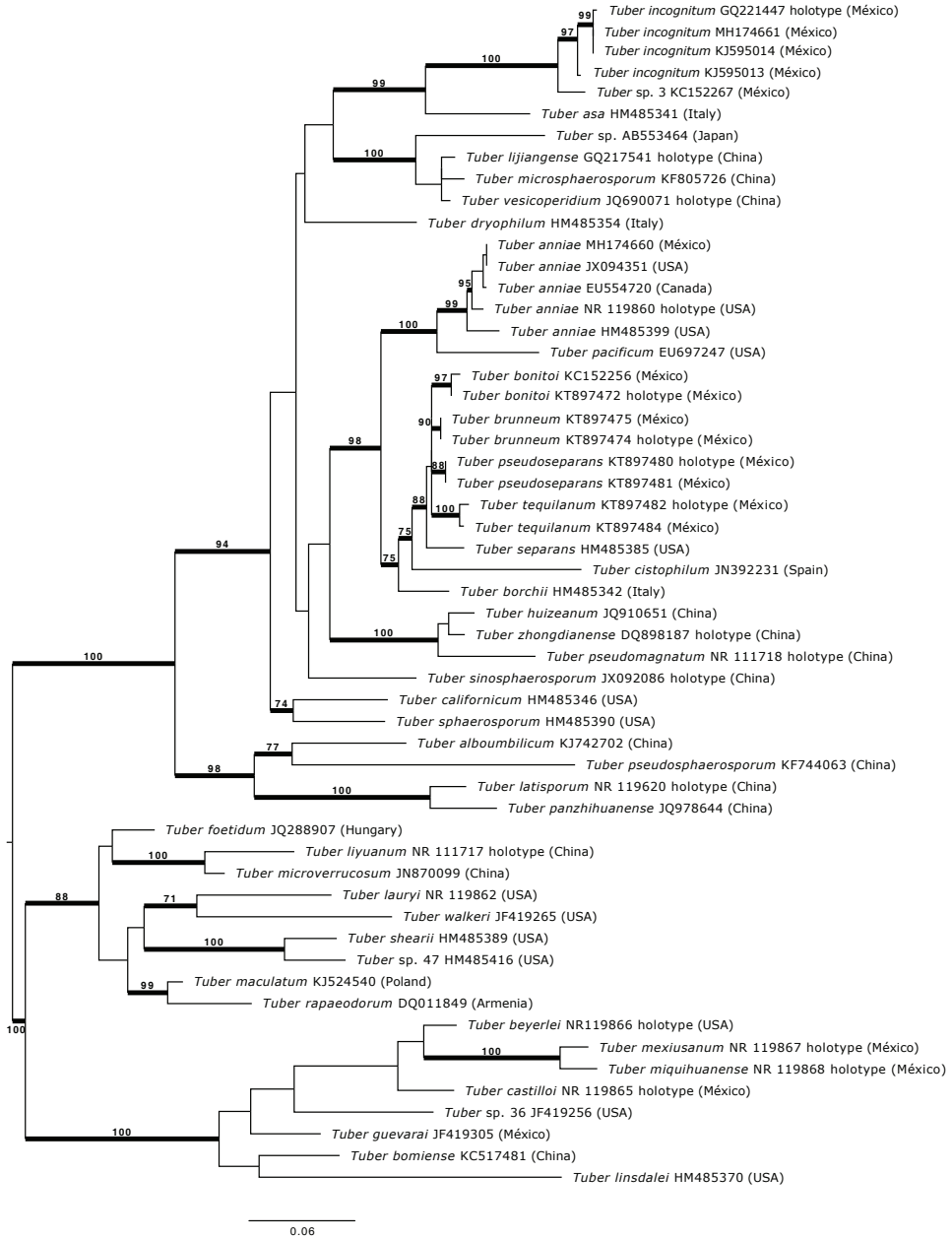

Figure 3. Most likely tree based on maximum likelihood phylogenetic inference showing the placement of *Tuber incognitum* within the Puberulum clade. Bootstrap values ≥ 70% are labelled above nodes. Nodes with posterior probabilities ≥ 99% are blacked. Holotype collections are labelled. The phylogeny is rooted with species belonging to the Maculatum clade. Scale bar corresponds to the mean number of nucleotides substitutions per site.

Discussion

Species in Puberulum clade can be found in North America, Europe and Asia and some regions of North Africa and South America (Bonito et al. 2010, 2013; Jeandroz et al. 2008; Payen et al. 2014). There are some records of species in the Puberulum clade (e.g. *Tuber rapaeodorum*) that have been introduced into Australia and New Zealand (Bonito et al. 2010). Species in this clade show a wider range of host associations than other species within the Rufum, Excavatum, Aestivum, Maculatum and Gennadii clades (Payen et al. 2014). Species within the Puberulum clade commonly form associations with angiosperms and conifers (Bidartondo et al. 2004; Bonito et al. 2010). In México, twenty species of *Tuber* have been reported, including the two species from this study. Eight of the twenty belong to the Puberulum clade. Both the Maximum Likelihood and Bayesian analyses (Figure 3) show that *T. incognitum* forms a strongly supported clade (Maximum Likelihood bootstrap= 97), which includes sequences from both voucher collections and EcM root tip collections. This clade is placed as a sister taxon of the undescribed species *Tuber* sp. 3 (KC152267) also from México. This study combines sporocarp anatomy, molecular analyses and phylogenetic analyses to support the erection of *T. incognitum* as a unique species within the Puberulum clade.

The *T. anniae* species complex is recovered as a strongly supported clade. There is an internal structure in this clade, with different branch lengths and nested subclades, but additional markers are needed to resolve relationships within this species complex. The Mexican specimens' group with those from Alaska (JX094351), form a nested clade that is closely related to a collection from Canada (EU554720). The members in the *T. anniae* species complex are closely related to *T. pacificum* from Oregon, USA. Given the relatively high ITS similarity, phylogenetic position and similar morphology to the *T. anniae* holotype collection, we have identified the Mexican collection as *T. anniae,* extending its known range and southernmost distribution of this species in North America.

Acknowledgements

This research was made possible through NSF award number 0641297, REVSYS: Phylogenetic and Revisionary Systematics of North American Truffles (*Tuber*). GB thanks AgBioResearch MICL02416 for research support. DNA sequencing was supported by the MEXBOL network project CONACYT 280896. CPP thanks the North American Truffling Society for research support, Daniel Luoma, Javier Tabima and Antonio Gómez who provided insight and expertise that greatly assisted the research. GG thanks CONACYT and TecNM for research support. We thank the herbaria of ITCV, MEXU and OSC for accessing their collections.

References

Altschul SF, Gish W, Miller W, Myers EW, Lipman DJ (1990) Basic local alignment search tool. Journal of Molecular Biology 215(3): 403–10. http://dx.doi.org/10.1016/S0022-2836(05)80360-2

Argüelles-Moyao A, Garibay-Orijel R (2018) Ectomycorrhizal fungal communities in high mountain conifer forests in central México and their potential use in the assisted migration of Abies religiosa. Mycorrhiza 28: 509. http://dx.doi.org/10.1007/s00572-018-0841-0

Bidartondo MI, Burghardt B, Gebauer G, Bruns TD, Read DJ (2004) Changing partners in the dark: isotopic and molecular evidence of ectomycorrhizal liaisons between forest orchids and trees. Proceedings of the Royal Society of London B: Biological Sciences 271(1550): 1799–806. http://dx.doi.org/10.1098/rspb.2004.2807

Bonito GM, Gryganskyi AP, Trappe JM, Vilgalys R (2010) A global meta-analysis of *Tuber* ITS rDNA sequences: species diversity, host associations and long-distance dispersal. Molecular Ecology 19(22): 4994–5008. https://doi.org/10.1111/j.1365-294X.2010.04855.x

Bonito G, Smith ME, Nowak M, Healy RA, Guevara G, Cázares E, Kinoshita A, Nouhra ER, Domínguez LS, Tedersoo L, Murat C (2013) Historical biogeography and diversification of truffles in the Tuberaceae and their newly identified southern hemisphere sister lineage. PloS One 8(1): e52765. https://doi.org/10.1371/journal.pone.0052765

Castellano MA, Trappe JM, Maser C (1989) Key to spores of the genera of hypogeous fungi of north temperate forests with special reference to animal mycophagy. Mad River Press, 186 pp.

Colgan III W, Trappe JM (1997) NATS truffle and truffle-like fungi. 7. *Tuber anniae* sp. nov. (Ascomycota). Mycotaxon 64: 437–442.

Edgar RC (2004) MUSCLE: multiple sequence alignment with high accuracy and high throughput. Nucleic Acids Research 32(5): 1792–1797. http://dx.doi.org/10.1093/nar/gkh340

Guevara G, Bonito G, Cázares-González E, Healy R, Vilgalys R, Trappe JM (2015) Novel *Tuber* spp. (Tuberaceae, Pezizales) in the Puberulum group from México. Ascomycete.org 7(6): 367–74. https://doi.org/10.25664/art-0161

Jeandroz S, Murat C, Wang Y, Bonfante P, Tacon FL (2008) Molecular phylogeny and historical biogeography of the genus *Tuber*, the 'true truffles'. Journal of Biogeography 35(5): 815–29. https://doi.org/10.1111/j.1365-2699.2007.01851.x

Kearse M, Moir R, Wilson A, Stones-Havas S, Cheung M, Sturrock S, Buxton S, Cooper A, Markowitz S, Duran C, Thierer T (2012) Geneious Basic: an integrated and extendable desktop software platform for the organization and analysis of sequence data. Bioinformatics 28(12): 1647–9. http://dx.doi.org/10.1093/bioinformatics/bts199

Maddison WP, Maddison DR (2015) Mesquite: a modular system for evolutionary analysis. http://mesquiteproject.org [Version 3.04]

Miller MA, Pfeiffer W, Schwartz T (2010) Creating the CIPRES Science Gateway for inference of large phylogenetic trees. Gateway Computing Environments Workshop (GCE): 14 Nov 2010, New Orleans, 1–8. http://dx.doi.org/10.1109/GCE.2010.5676129

Payen T, Murat C, Bonito G (2014) Truffle phylogenomics: new insights into truffle evolution and truffle life cycle. Advances in Botanical Research 70: 211–234. http://dx.doi.org/10.1016/B978-0-12-397940-7.00007-0

Ronquist F, Huelsenbeck JP (2003) MrBayes 3: Bayesian phylogenetic inference under mixed models. Bioinformatics 19(12): 1572–4. http://dx.doi.org/10.1093/bioinformatics/btg180

Shefferson RP, Kull T, Tali K (2008) Mycorrhizal interactions of orchids colonizing Estonian mine tailings hills. American Journal of Botany 95(2): 156–64. http://dx.doi.org/10.3732/ajb.95.2.156

Stamatakis A (2014) RAxML version 8: a tool for phylogenetic analysis and post-analysis of large phylogenies. Bioinformatics 30(9): 1312–3. http://dx.doi.org/10.1093/bioinformatics/btu033

Wang XH, Benucci GM, Xie XD, Bonito G, Leisola M, Liu PG, Shamekh S (2013) Morphological, mycorrhizal and molecular characterization of Finnish truffles belonging to the *Tuber anniae* species-complex. Fungal Ecology 6(4): 269–80. http://dx.doi.org/10.1016/j.funeco.2013.03.002

Walker JF, K Miller OR, Horton JL (2005) Hyperdiversity of ectomycorrhizal fungus assemblages on oak seedlings in mixed forests in the southern Appalachian Mountains. Molecular Ecology 14(3): 829–38. http://dx.doi.org/10.1111/j.1365-294X.2005.02455.x

White TJ, Bruns T, Lee SJ, Taylor JL (1990) Amplification and direct sequencing of fungal ribosomal RNA genes for phylogenetics. PCR Protocols: A Guide to Methods and Applications 18(1): 315–22. http://dx.doi.org/10.1016/B978-0-12-372180-8.50042-1

Wurzburger N, Bidartondo MI, Bledsoe CS (2001) Characterization of *Pinus* ectomycorrhizas from mixed conifer and pygmy forests using morphotyping and molecular methods. Canadian Journal of Botany 79(10): 1211–6. http://dx.doi.org/10.1139/b01-079

MycoKeys 41: 29–38 (2018)
doi: 10.3897/mycokeys.41.28485
http://mycokeys.pensoft.net

RESEARCH ARTICLE

A peer-reviewed open-access journal
MycoKeys
Launched to accelerate biodiversity research

Dentipellis tasmanica sp. nov. (Hericiaceae, Basidiomycota) from Australia

Xiao-Hong Ji[1], Qian Chen[1], Genevieve Gates[2], Ping Du[3]

1 *Institute of Microbiology, PO Box 61, Beijing Forestry University, Beijing 100083, China* **2** *Tasmanian Institute of Agriculture, Private Bag 54, Hobart, Tasmania 7001, Australia* **3** *College of Life Science and Technology, Yangtze Normal University, Chongqing 408100, China*

Corresponding authors: *Xiao-Hong Ji* (xhji2010@163.com); *Ping Du* (duping7374@163.com)

Academic editor: *Zai-Wei Ge* | Received 19 July 2018 | Accepted 18 September 2018 | Published 11 October 2018

Citation: Ji X-H, Chen Q, Gates G, Du P (2018) *Dentipellis tasmanica* sp. nov. (Hericiaceae, Basidiomycota) from Australia. MycoKeys 41: 29–38. https://doi.org/10.3897/mycokeys.41.28485

Abstract

Dentipellis tasmanica **sp. nov.** is described and illustrated from Tasmania, Australia based on rDNA evidence and morphological characters. It is characterised by an annual growth habit; resupinate basidiocarps up to 100 cm long; spines cream when fresh and cinnamon when dry, up to 3 mm long and a few glued at tips when dry; distinct white fibrillous to cottony margin; a monomitic hyphal structure with non-amyloid, non-dextrinoid and cyanophilous generative hyphae; the presence of gloeoplerous hyphae and gloeocystidia which become dark blue in Melzer's reagent; the presence of chlamydospores in the subiculum and rough basidiospores measuring 3.5–4.5 × 2.4–3.2 µm. A molecular study based on the combined ITS (internal transcribed spacer region) and 28S (the large nuclear ribosomal RNA subunit) dataset supports the new species in *Dentipellis*. A key to species of *Dentipellis* sensu stricto is provided.

Keywords

hydnoid fungi; *Russulales*; taxonomy; wood-inhabiting fungi

Introduction

Dentipellis Donk, typified by *D. fragilis* (Pers.) Donk, is a hydnaceous genus in the Russulales and is characterised by a wood-inhabiting resupinate fruiting body with soft spines, a monomitic hyphal structure with clamp connections on the generative hyphae and amyloid, rough basidiospores (Ginns 1986, Dai et al. 2009, Zhou and Dai 2013). Zhou and Dai (2013) demonstrated that *Dentipellis* was polyphyletic and segregated

Dentipellis leptodon (Mont.) Maas Geest. and *Dentipellis taiwaniana* Sheng H. Wu from *Dentipellis* to a new genus of *Dentipellicula* Y.C. Dai & L.W. Zhou based on ITS and 28S rDNA sequences. Besides, *Dentipellopsis* Y.C. Dai & L.W. Zhou is erected as a new genus and characters are provided in a generic key to distinguish *Dentipellicula*, *Dentipellis* and *Dentipellopsis* that morphologically are highly similar, as well as a key to the current species in *Dentipellis* (Zhou and Dai 2013). Recently, based on molecular and morphological analyses, more new taxa were described in *Dentipellis* sensu lato (Zhou and Dai 2013, Chen et al. 2015, Shen and Wang 2017, Yuan et al. 2018) and, indeed, all *Dentipellis* spp. were found from the northern Hemisphere (Ginns 1986, Dai et al. 2009, Zhou and Dai 2013, Shen and Wang 2017, Yuan et al. 2018).

During a field trip to Tasmania, the island state of Australia, three wood-inhabiting specimens with soft spines were collected and, based on the morphological characters, they belong to *Dentipellis*. After phylogenetic analysis of ITS and 28S sequences and examination of the morphology in the laboratory, they turn out to represent a new species. This is so far the first species of *Dentipellis* found in the southern Hemisphere. In this paper, we present an illustrated description and an identification key to accepted species of *Dentipellis* worldwide.

Materials and methods

Morphological studies

Thin sections were studied microscopically according to Chen et al. (2016) at magnifications ≤1000× using a Nikon Eclipse 80i microscope with phase contrast illumination. Drawings were made with the aid of a drawing tube. Microscopic features, measurements and drawings were made from sections stained with Cotton Blue and Melzer's reagent. Spores were measured from sections cut from the tubes. To present spore size variation, the 5% of measurements excluded from each end of the range are given in parentheses. Basidiospore apiculus lengths were not included in the measurements.

Abbreviations include:

IKI	Melzer's reagent,	L	mean spore length (arithmetic average of all spores),
IKI–	negative in Melzer's reagent,		
IKI+	amyloid in Melzer's reagent,	W	mean spore width (arithmetic average of all spores),
KOH	5% potassium hydroxide,		
CB	Cotton Blue,	Q	the L/W ratio,
CB+	cyanophilous,	n	number of spores measured from the given number of specimens.
CB–	acyanophilous,		

Colour terms follow Petersen (1996). The studied specimens are deposited in the herbaria as cited below; herbarium abbreviations follow Thiers (2014).

Molecular study and phylogenetic analysis

A CTAB rapid plant genome extraction kit (Aidlab Biotechnologies, Beijing) was used to obtain PCR products from dried specimens, according to the manufacturer's instructions with some modifications (Wu et al. 2017). The primer pair ITS4 and ITS5 was used for amplification of the ITS region (White et al. 1990), while the primer pair LR0R and LR7 (http://www.biology.duke.edu/fungi/mycolab/primers.htm) was used for providing the D1-D4 regions of the 28S (https://unite.ut.ee/primers.php). The PCR procedure for ITS was as follows: initial denaturation at 95 °C for 3 min, followed by 35 cycles at 94 °C for 40 s, 54 °C for 45 s and 72 °C for 1 min, with a final extension of 72 °C for 10 min. The PCR procedure for 28S was as follows: initial denaturation at 94 °C for 1 min, followed by 35 cycles at 94 °C for 30 s, 50 °C for 1 min and 72 °C for 1.5 min, with a final extension of 72 °C for 10 min. The PCR products were purified and sequenced in Beijing Genomics Institute, China with the same primers.

New sequences, deposited in GenBank (Table 1), were aligned with additional sequences retrieved from GenBank (Table 1) using BioEdit 7.0.5.3 (Hall 1999) and ClustalX 1.83 (Chenna et al. 2003). *Bondarzewia podocarpi* Y.C. Dai & B.K. Cui and *B. occidentalis* Jia J. Chen, B.K. Cui & Y.C. Dai were chosen as outgroups, consulting Dai et al. (2010) and Zhou and Dai (2013). Prior to phylogenetic analysis, ambiguous regions at the start and the end of the alignment were deleted and gaps were manually adjusted to optimise the alignment. The edited alignment was deposited at TreeBase (submission ID 22975; www.treebase.org).

The method of phylogenetic analysis followed Chen et al. (2016). Maximum parsimony (MP) analysis was performed in PAUP* version 4.0b10 (Swofford 2002). All characters were equally weighted and gaps were treated as missing data. Trees were inferred using the heuristic search option with tree-bisection reconnection (TBR) branch swapping and 1,000 random sequence additions. Max-trees were set to 5,000, branches of zero length were collapsed and all parsimonious trees were saved. Clade robustness was assessed using a bootstrap (BT) analysis with 1,000 replicates (Felsenstein 1985). Phylogenetic trees were visualised using Treeview (Page 1996).

MrModeltest 2.3 (Posada and Crandall 1998, Nylander 2004) was used to determine the best-fit evolution model of the combined dataset for Bayesian Inference (BI). BI was calculated with MrBayes 3.1.2 (Ronquist and Huelsenbeck 2003) with a general time reversible (GTR) model of DNA substitution and an invgamma distribution rate variation across sites. Four Markov chains were performed for 2 runs from random starting trees for 500,000 generations of the combined ITS and 28S dataset and trees were sampled every 100 generations. The burn-in was set to discard the first 25% of the trees. A majority rule consensus tree of all remaining trees was calculated. Nodes that received BT support ≥50% and Bayesian posterior probabilities (BPP) ≥0.95 were considered as significantly supported.

Table 1. Specimens and GenBank accession number of sequences used in this study.

Species	Sample no.	Locality	GenBank accession no.	
			ITS	nLSU
Bondarzewia occidentalis	DAOM F-415	Canada	DQ200923	DQ234539
B. podocarpi	Dai 9261	China	KJ583207	KJ583221
Dentipellicula austroafricana	Dai 12580	South Africa	KJ855274	KJ855275
D. leptodon	GB 011123	Uganda	EU118625	EU118625
D. taiwaniana	Dai 10867	China	JQ349115	JQ349101
	Cui 8346	China	JQ349114	JQ349100
Dentipellis coniferarum	Cui 10063	China	JQ349106	JQ349092
	Yuan 5623	China	JQ349107	JQ349093
D. dissita	NH 6280	Canada	AF506386	AF506386
D. fragilis	Dai 12550	China	JQ349110	JQ349096
	Dai 9009	China	JQ349108	JQ349094
D. longiuscula	He 20120717-5	China	KR108235	KR108238
	He 20120717-7	China	KR108234	KR108239
D. microspora	Cui 10035	China	JQ349112	JQ349098
D. rhizomorpha	Dai 17474	China	MG020134	MG020137
	Dai 17477	China	MG020135	MG020138
	Dai 17481	China	MG020136	MG020139
D. tasmanica	**Dai 18737**	**China**	**MH571698**[a]	**MH571701**[a]
	Dai 18767	**China**	**MH571699**[a]	**MH571702**[a]
	Dai 18768	**China**	**MH571700**[a]	**MH571703**[a]
D. tropicalis	Cui 8545	China	KR108236	KR108240
	He 1993	China	KR108237	KR108241
Dentipellopsis dacrydicola	Dai 12004	China	JQ349104	JQ349089
D. dacrydicola	Dai 12010	China	–	JQ349090
Hericium abietis	NH 6990	Canada	AF506456	AF506456
H. alpestre	NH 13240	Russia	AF506457	AF506457
H. americanum	DAOM F-21467	Canada	AF506458	AF506458
H. coralloides	NH 282	Sweden	AF506459	AF506459
H. erinaceus	NH 12163	Russia	AF506460	AF506460
Laxitextum bicolor	NH 5166	Sweden	AF310102	AF310102
Pseudowrightoporia japonica	Dai 7221	China	FJ644289	KM107882
Wrightoporiopsis biennis	Cui 8457	China	KJ807066	KJ807074

[a] Sequences newly generated in this study; the new species is shown in bold.

Results

The combined ITS and 28S dataset included sequences from 31 fungal collections representing 22 species. The dataset had an aligned length of 1792 characters, of which 1218 characters are constant, 126 are variable and parsimony-uninformative and 448 (37%) are parsimony-informative. MP analysis yielded 2 equally parsimonious trees (TL = 1343, CI = 0. 653, RI = 0.793, RC = 0.518, HI = 0.347). The best-fit model for the combined ITS and 28S sequences dataset estimated and applied in the Bayesian analysis: GTR+I+G, lset nst = 6, rates = invgamma; prset statefreqpr = dirichlet (1,1,1,1). BI

resulted in a similar topology with an average standard deviation of split frequencies = 0.006203 to MP analysis and, thus, only the MP tree was provided. Both BT values (≥50%) and BPPs (≥0.95) are shown at the nodes (Fig. 1).

Three sampled specimens of the new species, *Dentipellis tasmanica*, formed a well-supported lineage (100% MP and 1 BPPs), indicating they are phylogenetically distinct from other species (Fig. 1).

Taxonomy

***Dentipellis tasmanica* Y.C. Dai, G.M. Gates, X.H. Ji & P. Du, sp. nov.**
MycoBank: MB 827073
Figs 1, 2

Diagnosis. Differs from other *Dentipellis* species by its gloeoplerous hyphae and gloeocystidia that become dark blue in Melzer's reagent and the presence of chlamydospores in subiculum.

Holotype. AUSTRALIA. Tasmania: Arve River Streamside Reserve, 43°10'S, 146°48.5'E, elev. 160 m, on fallen trunk of *Nothofagus* sp., 15 May 2018, *Dai 18767* (M, isotype in BJFC; ITS GenBank accession number: MH571699, 28S GenBank accession number: MH571702).

Etymology. *Tasmanica* (Lat.): referring to the species collected from Tasmania of Australia.

Basidiomata. Annual, resupinate, inseparable from substratum, soft corky, without odour or taste when fresh, fragile upon drying, up to 100 cm long, 40 cm wide and 3.5 mm thick at centre. Hymenophore with spines, cream when fresh and cinnamon when dry, spines up to 3 mm long, 2–3 per mm across base, soft corky to fragile, a few glued at tips when dry; margin distinct, white, fibrillous to cottony, up to 5 mm wide; spines, cream, becoming fragile and clay-buff when dry, up to 3 mm long. Subiculum very thin, soft corky, white to cream, <1 mm thick.

Hyphal structure. Hyphal system monomitic; generative hyphae with clamp connections, IKI–, CB+; the colour and size unchanged in KOH.

Subiculum. Generative hyphae colourless, thin- to slightly thick-walled, frequently branched, flexuous, interwoven, 3–4.5 μm in diam. Gloeoplerous hyphae occasionally present, dark blue in Melzer's reagent. Chlamydospores present, ellipsoid, thick-walled, 5–5.6 × 2.8–3.3 μm.

Hymenophoral trama. Generative hyphae colourless, thin-walled, frequently branched, straight, parallel along the spines, 2.8–4 μm in diam. Gloeocystidia abundant, colourless, thin- to slightly thick-walled, clavate, contents oily and dark blue in Melzer's reagent, rooting deep from the trama, up to a few hundred microns long, the cystidia-like apical part 30–45 × 5–8 μm. Oily material abundant amongst trama.

Hymenium. Cystidioles colorless, thin-walled, ventricose with elongated apical portion, bearing some irregular crystals, 30–45 × 5–8 μm; basidia clavate with four

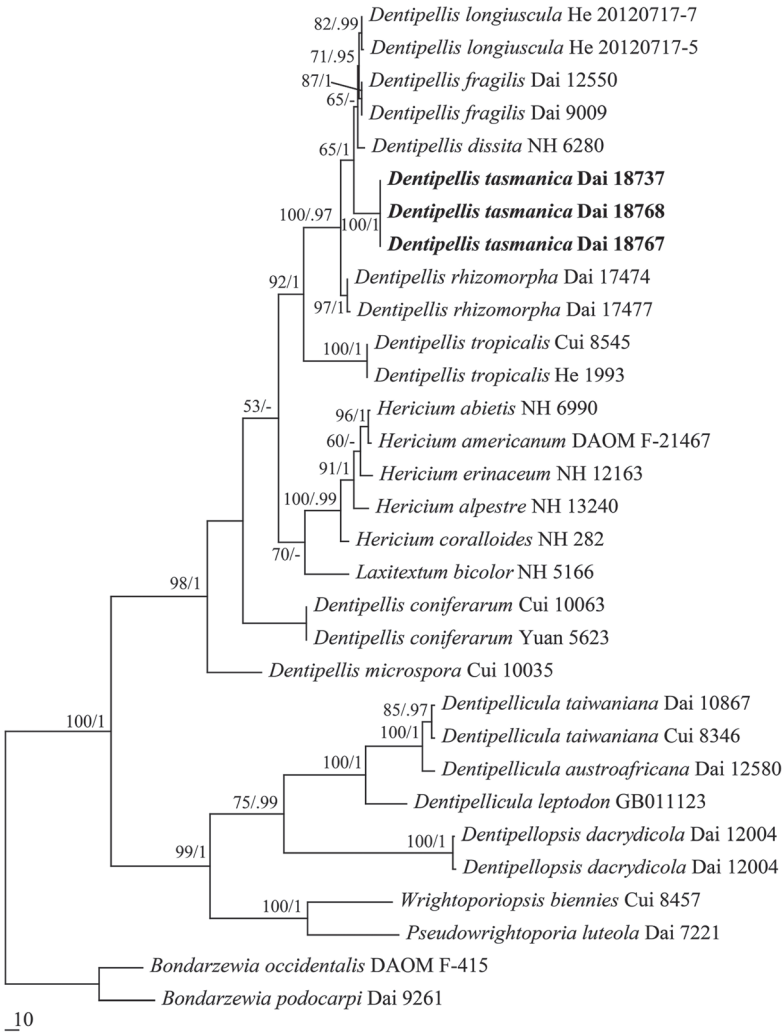

Figure 1. Strict consensus tree illustrating the phylogenetic position of *Dentipellis tasmanica*, generated by the maximum parsimony method based on ITS+28S sequence data. Branches are labelled with parsimony bootstrap values ≥50% and Bayesian posterior probabilities ≥0.95. *Bondarzewia podocarpi* and *B. occidentalis* are used to root the tree. Branch lengths reflect expected changes per site as indicated by the scale.

sterigmata and a basal clamp connection, 20–26 × 3–4.5 µm. Basidiospores ellipsoid, coloruless, thin-walled, densely echinulate, IKI+, CB+, (3.4–)3.5–4.5(–4.8) × 2.4–3.2(–3.5) µm, L = 3.99 µm, W = 2.92 µm, Q = 1.36–1.39 (n = 90/3).

Additional specimens examined (paratypes). AUSTRALIA. Tasmania: Arve River Streamside Reserve, on fallen trunk of *Nothofagus* sp., 15 May 2018, *Dai 18768* (M, duplicate in BJFC; ITS GenBank accession number: MH571700, 28S GenBank accession

Figure 2. A fresh basidiocarp of *Dentipellis tasmanica* (holotype). Scale bar: 1 cm.

number: MH571703); Mt Field National Park, 42°41'S, 146°42'E, elev., 180 m, on fallen trunk of *Nothofagus* sp., 14 May 2018, *Dai 18737* (M, duplicate in BJFC; ITS GenBank accession number: MH571698, 28S GenBank accession number: MH571701).

Discussion

Morphologically, *Dentipellis tasmanica* is characterised by spines, cream when fresh; distinct white fibrillous to cottony margin; a monomitic hyphal structure with generative hyphae bearing clamp connections; the presence of gloeoplerous hyphae and gloeocystidia which become dark blue in Melzer's reagent and presence of chlamydospores in the subiculum. Phylogenetically, three samples of *D. tasmanica* formed a distinct lineage with strong support (100 % MP, 1.0 BPPs) and are distant from other taxa (Fig. 1). Both morphology and rDNA sequence data confirmed that *D. tasmanica* is a new species in *Dentipellis*.

Dentipellis tasmanica was considered as *Dentipellicula leptodon* (Mont.) Y.C. Dai & L.W. Zhou (Gates and Ratkowsky 2016) as having similar basidiospores (3.5–4.5 × 2.4–3.3 µm

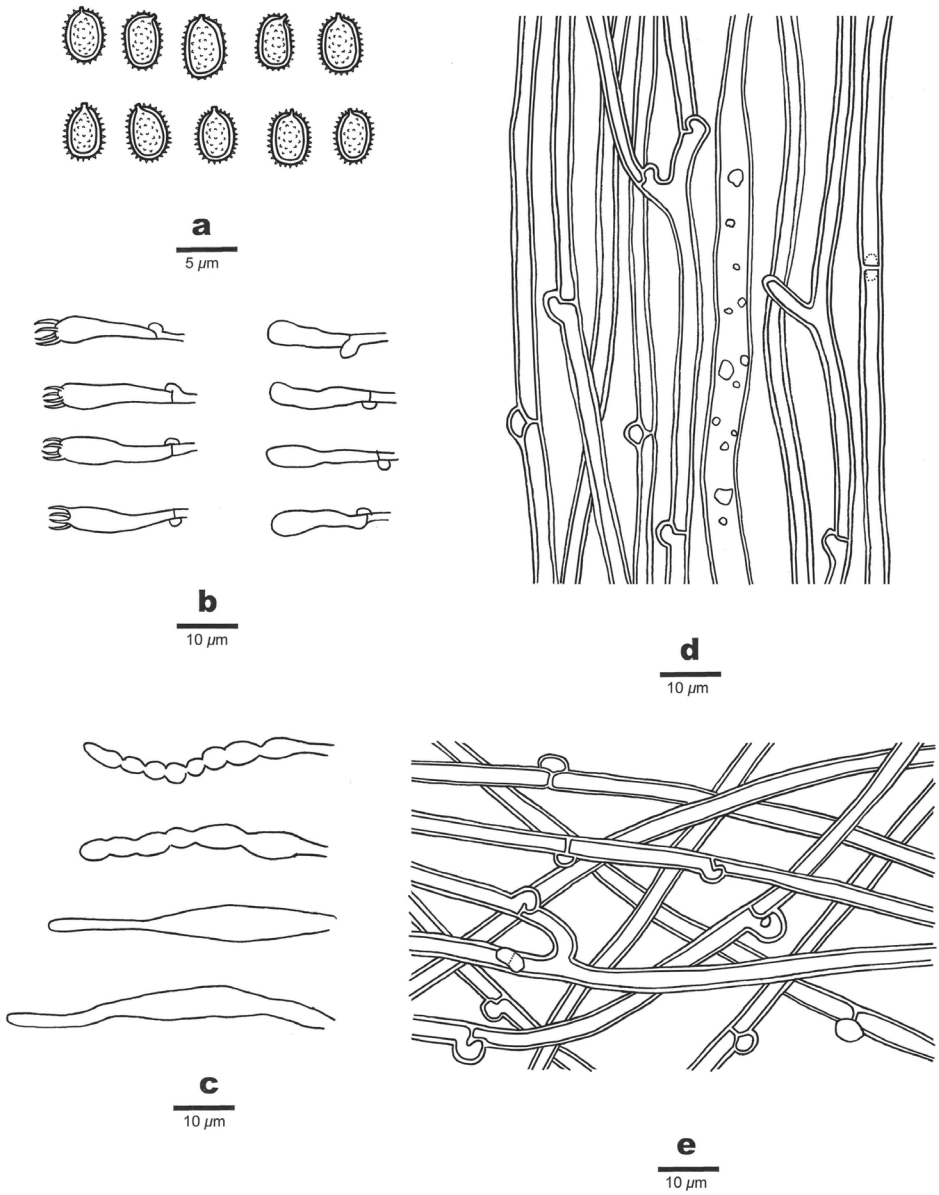

Figure 3. Microscopic structures of *Dentipellis tasmanica* (holotype). **a** Basidiospores **b** Basidia and basidioles **c** Gloeocystidia and Cystidioles **d** Hyphae from trama **e** Hyphae from subiculum.

vs. 3.2–4 1 × 2.4–3 μm, Ginns 1986), but gloeocystidia and gloeoplerous hyphae in *D. leptodon* are yellowish in Melzer's reagent and it lacks chlamydospores in subiculum.

Phylogenetically, *Dentipellis tasmanica* is more closely related to *D. rhizomorpha* Yuan & Y.C. Dai, *D. fragilis*, *D. dissita* and *D. longiuscula* (Fig.1). However, *D. rhizomorpha* has denser spines (5–7 per mm vs. 2–3 per mm in *D. tasmanica*), lacks gloeoplerous hyphae

and gloeocystidia. *D. fragilis* and *D. dissita* differ from *D. tasmanica* in having larger basidiospores (5–5.8 × 4.1–4.9 µm in *D. fragilis*, 4.2–4.7 × 3.2–3.7 µm in *D. dissita*; Dai et al. 2009). *D. longiuscula* is distinguished from *D. tasmanica* by lacking gloeoplerous hyphae and gloeocystidia and having larger basidiospores (5–6 × 3–3.6 µm; Shen and Wang 2017).

Key to species of *Dentipellis*

1	Gloeoplerous hyphae absent	**2**
–	Gloeoplerous hyphae present	**5**
2	Basidiospores <5 µm long	**3**
–	Basidiospores ≥5 µm long	**4**
3	Basidiospores <3.2 µm long, <2.2 µm wide-	***D. microspora***
–	Basidiospores >3.2 µm long, >2.2 µm wide-	***D. rhizomorpha***
4	Gloeocystidia absent	***D. longiuscula***
–	Gloeocystidia present	***D. tropicalis***
5	Basidiocarps becoming brown when bruised	***D. coniferarum***
–	Basidiocarps unchanged when bruised	**6**
6	Gloeocystidia absent	***D. ohiensis***
–	Gloeocystidia present	**7**
7	Gloeocystidia dark blue in IKI, basidiospores <3.2 µm wide	***D. tasmanica***
–	Gloeocystidia yellowish in IKI, basidiospores >3.2 µm wide	**8**
8	Basidiospores 5–5.8 × 4.1–4.9 µm	***D. fragilis***
–	Basidiospores 4.2–4.7 × 3.2–3.7 µm	***D. dissita***

Acknowledgements

We would like to express our deep thanks to Prof. Yu-Cheng Dai (Beijing Forestry University) who allowed us to study his specimens. The research is supported by the National Natural Science Foundation of China (Project No. 31750001).

References

Chen JJ, Cui BK, Dai YC (2016) Global diversity and molecular systematics of *Wrightoporia* s. l. (Russulales, Basidiomycota). Persoonia 37: 21–36. https://doi.org/10.3767/003158516X689666

Chen JJ, Cui BK, He SH, Cooper JA, Barrett MD, Chen JL, Dai YC (2016) Molecular phylogeny and global diversity of the remarkable genus *Bondarzewia* (Basidiomycota, Russulales). Mycologia 108: 697–708. https://doi.org/10.3852/14-216

Chen JJ, Shen LL, Dai YC (2015) *Dentipellicula austroafricana* sp. nov. supported by morphological and phylogenetic analyses. Mycotaxon 130: 17–25. https://doi.org/10.5248/130.17

Chenna R, Sugawara H, Koike T, Lopez R, Gibson TJ, Higgins DG, Thompson JD (2003) Multiple sequence alignment with the Clustal series of programs. Nucleic Acids Research 31: 3497–3500. https://doi.org/10.1093/nar/gkg500

Dai YC, Cui BK, Liu XY (2010) *Bondarzewia podocarpi*, a new and remarkable polypore from tropical China. Mycologia 102: 881–886. https://doi.org/10.3852/09-050

Dai YC, Xiong HY, Wu SH (2009) Notes on *Dentipellis* (Russulales, Basidiomycota). Mycosystema 28: 668–671.

Felsenstein J (1985) Confidence intervals on phylogenetics: an approach using bootstrap. Evolution 39: 783–791. https://doi.org/10.2307/2408678

Gates G, Ratkowsky D (2016) A field guide to Tasmanian fungi. Tasmanian Field Naturalists Club, Hobart, 1–249.

Ginns J (1986) The genus *Dentipellis* (Hericiaceae). Windahlia 16: 35–45.

Hall TA (1999) Bioedit: a user-friendly biological sequence alignment editor and analysis program for Windows 95/98/NT. Nucleic Acids Symp Ser 41: 95–98

Nylander JAA (2004) MrModeltest v2. Program distributed by the author. Evolutionary Biology Centre, Uppsala University.

Page RMD (1996) Treeview: An application to display phylogenetic trees on personal computers. Comput Appl Biosci 12: 357–358.

Petersen JH (1996) The Danish Mycological Society´s color-chart. Foreningen til Svampekundskabens Fremme, Greve, 1–6.

Posada D, Crandall KA (1998) Modeltest: testing the model of DNA substitution. Bioinformatics 14: 817–818. https://doi.org/10.1093/bioinformatics/14.9.817

Ronquist F, Huelsenbeck JP (2003) MRBAYES 3: Bayesian phylogenetic inference under mixed models. Bioinformatics 19: 1572–1574. https://doi.org/10.1093/bioinformatics/btg180

Shen LL, Wang M (2017) Morphological characteristics and molecular data reveal two new species of *Dentipellis* from China. Phytotaxa 323: 69. https://doi.org/10.11646/phytotaxa.323.1.5

Swofford DL (2002) PAUP*: Phylogenetic analysis using parsimony (*and other methods). Version 4.0b10. Sinauer Associates, Sunderland, Massachusetts.

Thiers B (2014) Index Herbariorum: A global directory of public herbaria and associated staff. New York Botanical Garden's Virtual Herbarium.

White TJ, Bruns TD, Lee S, Taylor J (1990) Amplification and direct sequencing of fungal ribosomal RNA genes for phylogenetics. In: Innis MA, Gelfand DH, Sninsky JJ, White TJ (Eds) PCR protocols, a guide to methods and applications. Academic, San Diego, 315–322. https://doi.org/10.1016/B978-0-12-372180-8.50042-1

Wu, F, Chen JJ, Ji XH, Vlasák J, Dai YC (2017) Phylogeny and diversity of the morphologically similar polypore genera *Rigidoporus, Physisporinus, Oxyporus* and *Leucophellinus*. Mycologia 109: 749–765. https://doi.org/10.1080/00275514.2017.1405215

Yuan Y, Ren GJ, Dai YC (2018) *Dentipellis rhizomorpha* sp. nov. supported by morphological and phylogenetic analyses. Nova Hedwigia 107: 131–140. https://doi.org/10.1127/nova_hedwigia/2018/0459

Zhou LW, Dai YC (2013) Taxonomy and phylogeny of hydnoid Russulales: two new genera, three new species and two new combination species. Mycologia 105: 636–649. https://doi.org/10.3852/12-011

MycoKeys 41: 39–50 (2018)
doi: 10.3897/mycokeys.41.28454
http://mycokeys.pensoft.net

RESEARCH ARTICLE

A peer-reviewed open-access journal
MycoKeys
Launched to accelerate biodiversity research

The first smut fungus, *Thecaphora anthemidis* sp. nov. (Glomosporiaceae), described from *Anthemis* (Asteraceae)

Julia Kruse[1], Volker Kummer[2], Roger G. Shivas[1], Marco Thines[3,4,5]

1 *Centre for Crop Health, Institute for Agriculture and the Environment, University of Southern Queensland, Toowoomba 4350, Queensland, Australia* **2** *University Potsdam, Institute for Biochemistry and Biology, Maulbeerallee 1, D-14469 Potsdam, Germany* **3** *Goethe University Frankfurt am Main, Department of Biosciences, Institute of Ecology, Evolution and Diversity, Max-von-Laue-Str. 9, D-60438 Frankfurt am Main, Germany* **4** *Biodiversity and Climate Research Centre (BiK-F), Senckenberg Gesellschaft für Naturforschung, Senckenberganlage 25, D-60325 Frankfurt am Main, Germany* **5** *Integrative Fungal Research Cluster (IPF), Georg-Voigt-Str. 14-16, D-60325 Frankfurt am Main, Germany*

Corresponding author: *Julia Kruse* (Julia.Kruse@usq.edu.au)

Academic editor: *T. Lumbsch* | Received 18 July 2018 | Accepted 12 September 2018 | Published 11 October 2018

Citation: Kruse J, Kummer V, Shivas RG, Thines M (2018) The first smut fungus, *Thecaphora anthemidis* sp. nov. (Glomosporiaceae), described from *Anthemis* (Asteraceae). MycoKeys 41: 39–50. https://doi.org/10.3897/mycokeys.41.28454

Abstract

There are 63 known species of *Thecaphora* (Glomosporiaceae, Ustilaginomycotina), a third of which occur on Asteraceae. These smut fungi produce yellowish-brown to reddish-brown masses of spore balls in specific, mostly regenerative, plant organs. A species of *Thecaphora* was collected in the flower heads of *Anthemis chia* (Anthemideae, Asteraceae) on Rhodes Island, Greece, in 2015 and 2017, which represents the first smut record of a smut fungus on a host plant species in this tribe. Based on its distinctive morphology, host species and genetic divergence, this species is described as *Thecaphora anthemidis* **sp. nov.** Molecular barcodes of the ITS region are provided for this and several other species of *Thecaphora*. A phylogenetic and morphological comparison to closely related species showed that *Th. anthemidis* differed from other species of *Thecaphora*. *Thecaphora anthemidis* produced loose spore balls in the flower heads and peduncles of *Anthemis chia* unlike other flower-infecting species.

Keywords

Glomosporiaceae, host specificity, internal transcribed spacer, molecular phylogenetics, smut fungi

Introduction

Thecaphora species belong to the Glomosporiaceae (Urocystidales, Ustilaginomycotina). The type species is *Th. seminis-convolvuli* described from *Convolvulus arvensis* (Convolvulaceae) collected in France (Desmazièrs 1827). Until now, 63 species of *Thecaphora* have been recognised (Vánky 2012), infecting host plant species in 16 different eudicot families (Vánky and Lutz 2007, Roets et al. 2008, Vánky et al. 2008, Vánky 2012). Species of *Thecaphora* produce sori in flowers, fruits, seeds, stems, leaves or roots, often in galls or pustules. The granular to powdery spore balls are yellowish-brown to reddish-brown, but never black. The majority of *Thecaphora* species produce loose or permanent spore balls without sterile cells. An exception to this is *Th. smallanthi*, which was reported to have large spore balls with outer spores and an internal layer of hyaline (sterile) cells (Piepenbring 2001). Three species have single spores (not united in spore balls), namely, *Th. thlaspeos*, *Th. oxalidis* (Vánky et al. 2008) and *Th. capensis* (Roets et al. 2008).

The Asteraceae is the largest family of eudicots with an estimated number of 30,000 species (Funk et al. 2009). The Asteraceae is divided into 13 subfamilies, including four (Asteroideae, Cichorioideae, Carduoideae and Mutisioideae) that contain about 99% of all taxa. *Anthemis* is a large genus in the tribe Anthemideae (subfamily Asteroideae), along with *Cota*, *Gonospermum* (including *Lugoa*), *Nananthea*, *Tanacetum* and *Tripleurospermum* (Bremer and Humphries 1993, Oberprieler et al. 2009, Presti et al. 2010). Species of *Anthemis* are distributed in western Eurasia, including the Mediterranean region, northern Africa and a small part of eastern Africa (Oberprieler 1998, 2001, Oberprieler et al. 2009, Presti et al. 2010). There are 62 species of *Anthemis* in Europe. *Anthemis chia* belongs to the section *Chiae* and is a Mediterranean species common on Rhodes Island, Greece.

About 20 species of *Thecaphora* infect host plant species in six tribes of the Asteraceae. Taxa of the tribes Astereae and Heliantheae in the subfamily Asteroideae are often hosts of several *Thecaphora* species. Some less species-rich tribes, e.g. Coreopsideae, Millerieae, Polymnieae and Cynareae (subfamily Carduoideae) are also hosts of *Thecaphora* species. The species of *Thecaphora* on Asteraceae have not been studied by molecular phylogenetic methods, in contrast to species of *Thecaphora* on Caryophyllaceae (Vánky and Lutz 2007), Polygonaceae (Vasighzadeh et al. 2014) and Oxalidaceae (Roets et al. 2008, 2012).

Plants of *Anthemis chia* with distorted flower heads containing mostly ligulate (ray) florets and swollen peduncles were collected near Tsambika, Rhodes Island, Greece, in 2015 and 2017. The swollen flower heads contained reddish-brown granular to powdery spore ball masses, typical of species of *Thecaphora*. The aim of this study was to identify the fungus and to determine its taxonomic assignment based on morphological and phylogenetic analyses of the internal transcribed spacer (ITS, barcoding locus) sequence data.

Materials and methods

Specimens

Herbarium specimens (23) of *Thecaphora* on a range of host plant species from across Europe and North America were examined (Tables 1, 2). The ITS sequences of specimens available on GenBank (19) and published in previous studies (Table 2) were included in the phylogenetic analysis. The nomenclature of the host plant species follows Euro+Med PlantBase (http://www.emplantbase.org/home.html) and the nomenclature of the fungi is according to Vánky (2012).

The morphology of the spore balls and spores of one specimen (GLM-F112531) of *Thecaphora* on *Anthemis chia* was microscopically examined at 1000× in 80% lactic acid heated to the boiling point on a glass slide. Measurements of 30 spore balls and 100 spores were made with the Zeiss AxioVision software and micrographs were taken with an Olympus FE-120 camera on a Seben SBX-5 compound microscope (Seben GmbH, Berlin). The measurements are reported as maxima and minima in parentheses and the means are placed in italics.

DNA extraction, amplification and sequencing

Genomic DNA was extracted from 23 herbarium specimens of *Thecaphora* (Table 1) using the methods reported by Kruse et al. (2017). The ITS nrDNA was amplified by PCR as reported in Kruse et al. (2018), using M-ITS1 (Stoll et al. 2003) as forward primer and either smITS-R1 or smITS-R2 (Kruse et al. 2017) as reverse primer. The ITS of host plants was amplified using primer pair ITS1P/ITS4 (Ridgway et al. 2003) with an annealing temperature of 53 °C. The resulting amplicons were sequenced at the Senckenberg Biodiversity and Climate Research Centre (BiK-F, Senckenberg) using the ITS4 primer (White et al. 1990). Sequences were deposited in GenBank (Table 2).

Phylogenetic analysis

In total, 42 ITS sequences from 21 *Thecaphora* species were used in the phylogenetic analyses. Sequences were aligned with MAFFT v.7 (Katoh and Standley 2013) employing the G-INS-I algorithm and leading and trailing gaps were trimmed. The resulting alignment length was 534 bp. The methods of phylogenetic analysis were according to Kruse et al. (2018) using Minimum Evolution (ME), Maximum Likelihood (ML) and Bayesian Inference (BA). *Thecaphora italica* and allied species were selected as an outgroup, on the basis of the phylogeny presented by Vánky and Lutz (2007).

Table 1. Collection records for specimens of *Thecaphora* examined in this study.

Species	Host	Country	Location	Date	Collector	Herbarium accession no.*
Thecaphora affinis	*Astragalus glycyphyllos*	Slovenia	Lower Styria, region Savinjska, N of Ljubno ob Savinjii, trail to Mt. Greben Smrekovec-Komen from Primož pri Ljubnem, wayside, 46°24'21"N, 14°49'54"E, 1150 m asl	14 July 2015	J. Kruse	GLM F112522
	A. glycyphyllos	Germany	Saxony-Anhalt, SW of Zschornewitz, forestry trail nearby SW-shore of „Gürke“ (Zschornewitzer Lake)	26 June 2007	H. Jage	GLM F094059
Th. anthemidis	*Anthemis chia*	Greece	Island Rhodes, 3.5 km NE Archangelos, Tsambika, way up to monastery, northeastslope, 36°14'03"N, 28°09'19"E, 90 m asl	26 April 2017	V. Kummer	GLM F112531
Th. haumanii	*Iresine diffusa*	Costa Rica	Prov. Guanacaste, 6 km NW de la barrada de la Laguna de Arenal	1 April 1992	R. Berndt, M. Piepenbring	M 0236177
Th. leptideum	*Chenopodium album*	France	Lotharingia, Forbach, Kreuzberg Mt.	Aug.-Oct. 1912/1913	A. Ludwig	M 0230099
Th. molluginis	*Mollugo cerviana*	Romania	Bratovesti, Oltenia	15 July 1963	K. Lug. Eliart	M 0236178
	M. cerviana	Romania	Oltenia, Timburesti	19 Sept. 1958	L. Pop	M 0236180
Th. oxalidis	*Oxalis stricta*	Austria	Upper Austria, Braunau at Inn, Hagenau Inncounty, Hagenauer Street, wayside, 48°16'24"N, 13°06'03"E, 340 m asl	18 Aug. 2014	J. Kruse	GLM F112523
	O. stricta	Germany	Bavaria, Upper Franconia, Fichtelmountains, Fichtelberg, Sandgrubenway, cemetery, 605 m asl	17 Sept. 2012	J. Kruse	GLM F112524
	O. stricta	Germany	Saxony-Anhalt, county Anhalt-Bitterfeld, Bitterfeld-Wolfen, Mühlstreet, allotment garden area „Kühler Grund“, 51°37'23"N, 12°20'08"E	13 July 2014	J. Kruse & H. Jage	GLM F112525
Th. pustulata	*Bidens pilosa*	Puerto Rico, USA	Mayagüez	13 Mar. 1920	H. H. Whetzel, E. W. Olive	CUP PR000458
Th. seminis-convolvuli	*Convolvulus arvensis*	Germany	Saxony, Middlesaxony, Freiberg, Halsbrücker Street, roadside, 50°55'31"N, 13°20'56"E, 400 m asl	11 Aug. 2017	J. Kruse	GLM F112527
	C. arvensis	Germany	Hesse, c. 8.5 km SE Eschwege, Weißenborn, Sandhöfe, path, 51°07'35"N, 10°07'25"E, 250 m asl	22 July 2017	J. Kruse	GLM F112528
	C. arvensis	Germany	Saxony-Anhalt, SSE Seeben, at Franzosenstein, wayside	26 Aug. 2002	H. Jage	GLM F065278
	Calystegia sepium	Germany	Mecklenburg-Western Pomerania, county Vorpommern-Rügen, 1,5 km NE of Barth, Glöwitz, rest area, 54°22'15"N, 12°45'38"E, 0 m asl	24 Aug. 2014	J. Kruse	GLM F112526
	C. sepium	Germany	North Rhine-Westphalia, county Steinfurt, Rheine, castle grounds Bentlage, between parking area and Gradierwerk, 52°17'49"N, 07°25'11"E, 35 m asl	14 July 2017	J. Kruse	GLM F112529

Species	Host	Country	Location	Date	Collector	Herbarium accession no.*
Th. seminis-convolvuli	*C. sepium*	Germany	Schleswig-Holstein, county Schleswig-Flensburg, Schaalby, W of Winningmay, parking area at „Reesholm“, wayside, 54°31'44"N, 09°37'53"E, 2 m asl	30 Aug. 2014	J. Kruse	GLM F112530
Th. thlaspeos	*Arabis ciliata*	Austria	Tyrol, district Kufstein, county Walchsee, Kaiserwinkel, track from hickinghut towards Niederkaseralm, over Hintere Abendpoit, eastslope Mt. Hochköpfl, 47°41'25"N, 12°19'37"E, 1300 m asl	21 July 2014	J. Kruse	GLM F112533
	A. ciliata	Germany	Bavaria, Chiemgauer Alps, county Rosenheim, Priener Hut, track 8,20, way up towards Kampenwand, alpine meadow, 47°42'29"N, 12°19'27"E, 1570 m asl	18 July 2014	J. Kruse	GLM F112536
	A. ciliata	Germany	Bavaria, Chiemgauer Alps, county Traunstein, Priener Hut, track 8,20 towards Priener Hut, alpine meadow, 47°42'07"N, 12°20'36"E, 1310 m asl	19 July 2014	J. Kruse	GLM F112537
	A. hirsuta	Germany	Hesse, Meißnerfoothills, Werra-Meißner-county, Großalmerode, S of Weißenbach, “Bühlchen”, calcareous grassland, 51°14'55"N, 09°51'08"E, 500 m asl	13 June 2015	J. Kruse	GLM F112532
	A. hirsuta	Germany	Bavaria, county Donau-Ries, Harburg, N of Ronheim, dry grassland, 435 m asl	20 June 2013	J. Kruse	GLM F112534
	A. hirsuta	Germany	Bavaria, Upper Bavaria, county Weilheim, N of Pähl, E at Hartschimmelhof, N „Goaslweide“, wayside, 720 m asl	20 July 2013	J. Kruse	GLM F112535

* Acronyms: GLM = Herbarium Senckenbergianum, Görlitz, Germany; CUP = Plant Pathology Herbarium, Cornell University, New York, USA; M = Botanische Staatssammlung, Munich, Germany.

Host plant species determination was verified by comparison with published sequences from Asteraceae deposited in GenBank (https://www.ncbi.nlm.nih.gov/genbank/) using BLASTN (Altschul et al. 1997).

Results

Molecular phylogenetic reconstruction

The ML and BA trees yielded consistent topologies with the ME tree (Fig. 1). The *Thecaphora* sp. on *Anthemis chia*, together with three Asteracious species (*Th. pustulata*, *Th. hennenea* and *Th. spilanthis*) and *Th. solani* from *Solanum lycopersicum* (Solanaceae), formed a sister clade to the species on other host plant families with strong to intermediate bootstrap support (83% in ME, 93% in ML). The *Thecaphora* sp. on *Anthemis chia*

Table 2. Specimens and GenBank sequences used for phylogenetic analyses. Sequences generated in this study are shown in bold.

Thecaphora species	Host	Herbarium accession no. [1]	ITS GenBank accession no.	Reference
Th. affinis	*Astragalus glycyphyllos*	GLM F112522	**MH399748**	this paper
		GLM F094059	**MH399749**	this paper
Th. alsinearum	*Stellaria holostea*	HUV 10535	EF200032	Vánky and Lutz 2007
Th. amaranthi	*Amaranthus hybridus*	HUV 20727	EF200013	Vánky and Lutz 2007
Th. anthemidis	*Anthemis chia*	GLM F112531	**MH399758**	this paper
Th. frezii	*Arachis hypogaea*	Sa-EM1*	KP994420	Cazón et al. 2016
		Cba-GD2*	KP994419	Cazón et al. 2016
Th. haumanii	*Iresine diffusa*	M 0236177	**MH399764**	this paper
Th. hennenea	*Melampodium divaricatum*	HUV 14434	EF200014	Vánky and Lutz 2007
Th. italica	*Silene italica*	HUV 20345	EF200026	Vánky and Lutz 2007
		HUV 20344	EF200025	Vánky and Lutz 2007
Th. leptideum	*Chenopodium album*	M 0230099	**MH399756**	this paper
Th. melandrii	*Silene alba*	HUV 12677	EF200024	Vánky and Lutz 2007
Th. molluginis	*Mollugo cerviana*	M 0236178	**MH399762**	this paper
		M 0236180	**MH399763**	this paper
Th. oxalidis	*Oxalis stricta*	GLM F112524	**MH399759**	this paper
		GLM F112523	**MH399760**	this paper
		GLM F112525	**MH399761**	this paper
Th. oxytropis	*Oxytropis pilosa*	Kummer P 1146/3*	KF640685	Kummer et al. 2014
		Kummer P 1146/2*	KF640684	Kummer et al. 2014
Th. pustulata	*Bidens pilosa*	CUP PR000458	**MH399757**	this paper
Th. saponariae	*Saponaria officinalis*	TUB 012796	EF200022	Vánky and Lutz 2007
Th. schwarzmaniana	*Rheum ribes*	BASU 4242	JX006079	Vasighzadeh et al. 2014
		KRAM F-49788	KF297811	Vasighzadeh et al. 2014
Th. seminis-convolvuli	*Calystegia sepium*	GLM F112529	**MH399742**	this paper
		GLM F112526	**MH399743**	this paper
		GLM F112530	**MH399744**	this paper
	Convolvulus arvensis	GLM F112527	**MH399745**	this paper
		GLM F112528	**MH399746**	this paper
		GLM F065278	**MH399747**	this paper
Th. solani	*Solanum lycopersicum*	HUV 11180	EF200037	Vánky and Lutz 2007
Th. sp.	*Rheum palmatum*	S. Wang 1991*	KJ579177	Piątek et al. unpublished
		Y. Wang 2013*	KJ579176	Piątek et al. unpublished
		HUV 21117	KF297812	Vasighzadeh et al. 2014
Th. spilanthis	*Acmella* sp.	AFTOL 1913	DQ832243	Matheny et al. 2006
Th. thlaspeos	*Arabis hirsuta*	GLM F112532	**MH399752**	this paper
		TUB 015857	KJ579178	Vasighzadeh et al. 2014
		GLM F112534	**MH399750**	this paper
		GLM F112535	**MH399751**	this paper
	Arabis ciliata	GLM F112537	**MH399753**	this paper
		GLM F112533	**MH399754**	this paper
		GLM F112536	**MH399755**	this paper

[1] Acronyms: AFTOL = Assembling the Fungal Tree Of Life, http://aftol.org; BASU: Herbarium of Bu-Ali Sina University, Iran; CUP = Plant Pathology Herbarium, Cornell University, New York, USA; GLM = Herbarium Senckenbergianum, Görlitz, Germany; HUV = Herbarium Ustilaginales Vánky, deposited in BRIP = Queensland Plant Pathology Herbarium, Brisbane, Australia; KRAM F = Mycological Collection of the W. Szafer Institute of Botany, Polish Academy of Sciences, Kraków, Poland; M = Botanische Staatssammlung, Munich, Germany; TUB = Herbarium Tubingense, Eberhard-Karls-Universität Tübingen, Germany; * not deposited in any public herbaria.

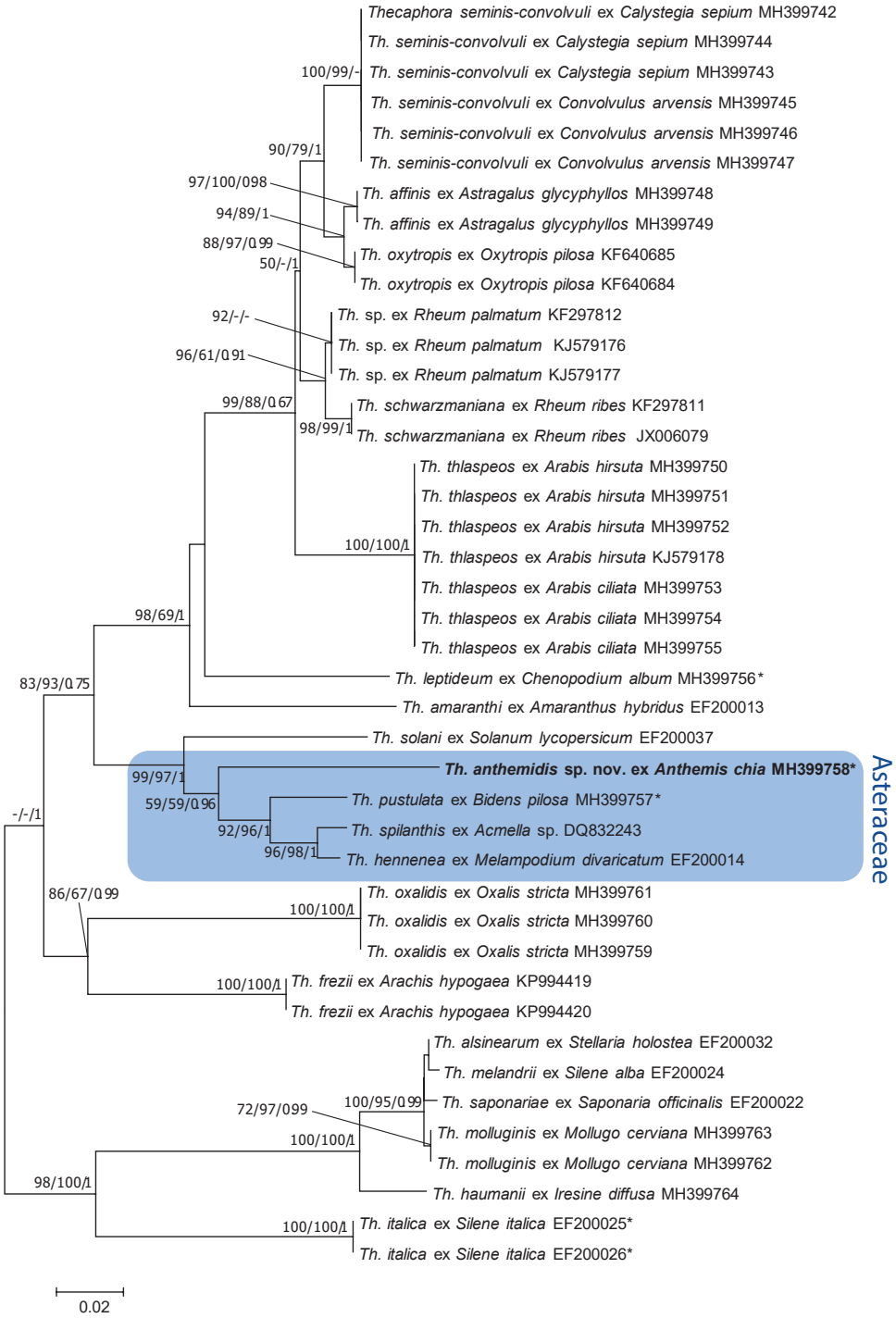

Figure 1. Phylogenetic tree of *Thecaphora* species based on ME analysis of the ITS locus. Numbers on branches denote support in ME, ML and BA, respectively. Values below 50% are denoted by '–'. The bar indicates the number of substitutions per site. Ex-type sequences are highlighted with an asterisk.

was sister to the other Asteracious species with low bootstrap support (59% in ME, 59% in ML), but high Bayesian posterior probability (96%). The *Thecaphora* species on Fabaceae were polyphyletic, with *Th. frezii* on *Arachis hypogaea* sister to *Th. oxalidis* on *Oxalis stricta* (Oxalidaceae). *Thecaphora frezii* was distant to a monophyletic lineage on *Oxytropis pilosa* and *Astragalus glycyphyllos*, which was sister to *Th. seminis-convolvuli*, the type of the genus. All specimens of *Th. seminis-convolvuli* collected on *Calystegia sepium* and *Convolvulus arvensis* (Convolvulaceae) had identical ITS sequences, as was the case with *Thecaphora thlaspeos* on *Arabis hirsuta* and *A. ciliata* (Brassicaceae). Within the clade of mostly Caryophyllaceae-infecting species, two species of *Thecaphora* infected other families of the Caryophyllales, namely *Th. molluginis* on *Mollugo cerviana* (Molluginaceae) and *Th. haumanii* on *Iresine diffusa* (Amaranthaceae).

Taxonomy

***Thecaphora anthemidis* J. Kruse, V. Kumm. & Thines, sp. nov.**
MycoBank: MB827067
Figure 2A–H

Type. GREECE, Rhodes Island, 3.5 km NE Archangelos, Tsambika, on path to monastery, northeast slope, 36°14'03"N, 28°09'19"E, 90 m a.s.l, on *Anthemis chia*, 26 Apr. 2017, V. Kummer. Holotype GLM-F112531, isotype Herbarium V. Kummer P 1971/chia4; ITS sequence GenBank MH399758.

Etymology. From the host plant genus *Anthemis*.

Description. Sori in swollen and distorted flower heads and peduncles; spore ball mass initially white, later reddish-brown, granular to powdery; spore balls subglobose to ellipsoidal, rarely ovoid, mostly regular in shape, (31–) 36–*41*–47 (–52) × (28–) 31–*38*–44 (–50) µm, length/width ratio 0.9–*1.1*–1.2 (n=30), under light microscopy yellowish-brown to pale yellowish-brown, composed of 2–10 (–12) loosely united spores that separate easily; spores ellipsoidal, subglobose, ovoid or cuneiform, (18–) 20–*21*–23 (–25) × (14–) 17–*18*–20 (–23) µm, length/width ratio of 1.1–*1.2*–1.4 (n=100), with flattened contact surfaces and rounded exposed surfaces; wall at contact surface up to 0.5 µm thick, wall at free surface up to 3 µm thick, densely verrucose with warts 0.5–1 µm high, often confluent and sometimes irregular.

Host range. *Anthemis chia*.

Distribution. Greece.

Notes. *Thecaphora anthemidis* has sori in the flower heads and the peduncles, which differentiates it from the following species that produce pustules, galls or swellings on the stems of Asteraceae: *Th. ambrosiae*, *Th. denticulata*, *Th. heliopsidis*, *Th. hennenea*, *Th. melampodii*, *Th. mexicana*, *Th. neomexicana*, *Th. piluliformis*, *Th. polymniae*, *Th. pulcherrima*, *Th. pustulata*, *Th. smallanthi* and *Th. spilanthis*. Four of the seven previously known species of *Thecaphora* that infect the flower heads of Asteraceae, namely *Th. arnicae*, *Th. burkartii*, *Th. californica* and *Th. cuneata* have firmly united spores that only separate after considerable pressure, which differentiate them from *Th. anthemidis* that has loose spore

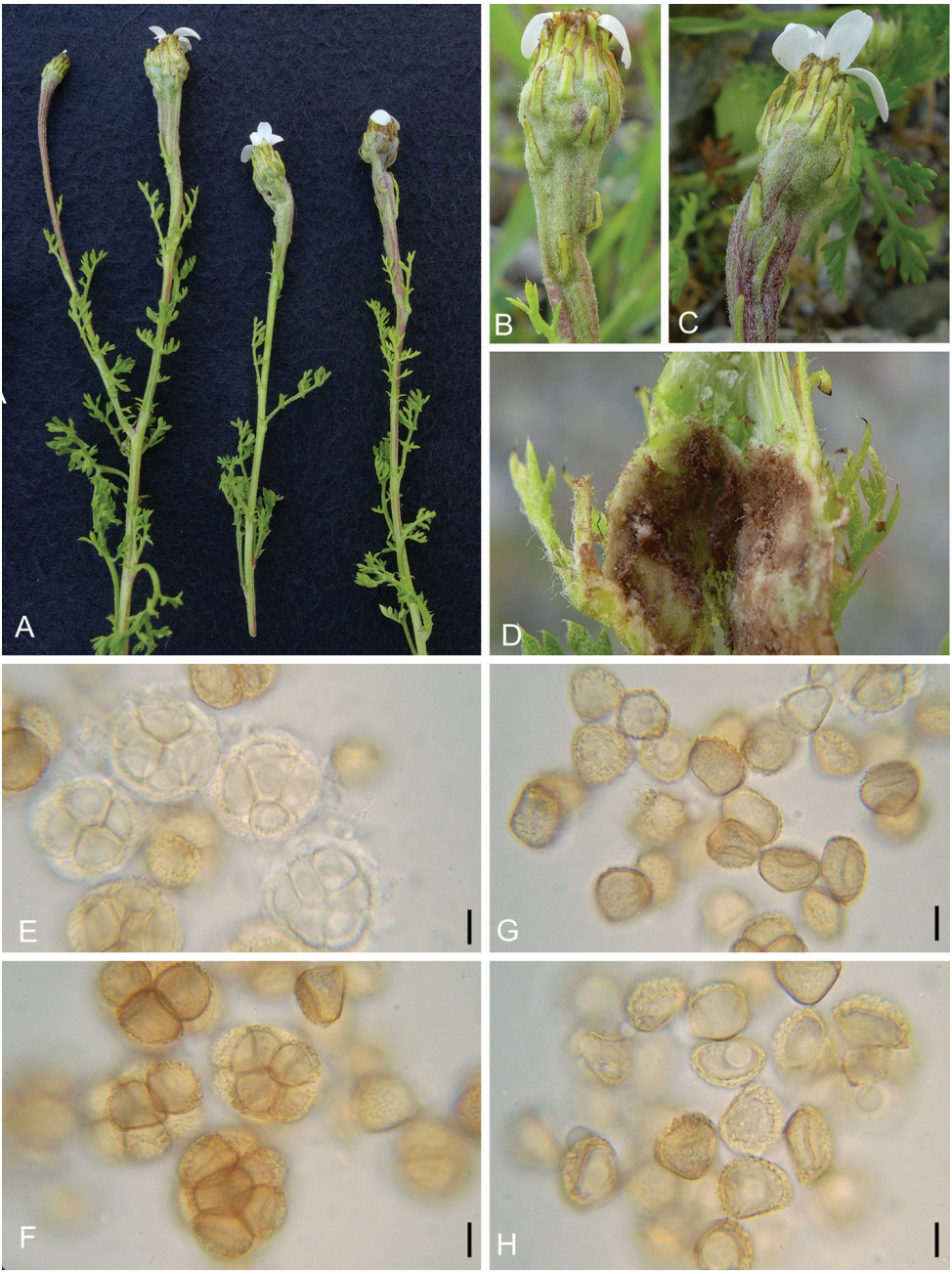

Figure 2. Sori, spore balls and spores of *Thecaphora anthemidis* on *Anthemis chia* (GLM-F112531) (**A–H**), **A** habit **B–C** swollen flower heads and peduncles **D** dissected flower head with reddish granular powdery spore ball mass **E** young spore balls **F** mature spore balls **G–H** single spores. Scale bars: 10 µm.

balls. Further, *Th. arnicae* (spore balls comprised of up to 25 spores), *Th. californica* (6–20 spores) and *Th. solidaginis* (8 to 50 or more spores) have larger spore balls with larger numbers of spores than *Th. anthemidis*. The spores of *Th. cuneata* are radially arranged

within the spore balls and *Th. burkartii* has spores with an outer wall 5–9 µm thick, which is more than three times thicker than in *Th. anthemidis*. *Thecaphora lagenophorae* and *Th. trailii* are morphologically most similar to *Th. anthemidis*. *Thecaphora lagenophorae* is only known to infect *Solenogyne gunnii* (tribe Astereae) in Australia (Vánky 2012). *Thecaphora trailii* infects species of *Carduus*, *Cirsium* and *Saussurea* (Asteraceae, tribe Cynareae, Carduoideae) (Vánky 2012) and further differs from *Th. anthemidis* by having smaller spore balls (12–30 µm) and fewer spores (2–8) per spore ball.

Discussion

The present study is the first to identify a species of *Thecaphora* on a host plant species in the tribe Anthemideae (Asteraceae) (see Vánky 2012). *Thecaphora anthemidis* was recovered in a monophyletic group of *Thecaphora* species on Asteraceae, sister to *Thecaphora solani* on *Solanum lycopersicum* (Solanaceae). Our phylogenetic hypothesis, based on the ITS region, was similar to the analyses of the LSU locus of these taxa in Vánky and Lutz (2007) and Roets et al. (2008). In the latter study, *Thecaphora polymniae*, which is known only from the type collection on *Polymnia riparia* (Polymnieae, Asteroideae, Asteraceae) from South America (Vánky 2012), clustered within a clade of taxa that infect Fabaceae, Caryophyllaceae and Amaranthaceae (Roets et al. 2008). *Thecaphora polymniae* has spores with a reticulate ornamentation and this may be evidence of a host jump from one of these plant families to Asteraceae. Host jumps have been reported before in the Ustilaginomycotina (e.g. Begerow et al. 2002, Piątek et al. 2017) and are thought to be a driver of plant pathogen diversification (Choi and Thines 2015).

Previously, only two ITS sequences of *Thecaphora* species infecting Asteraceae (*Th. spilanthis* and *Th. hennenea*) were available on GenBank, which together with the new sequences reported in this study, represents only 20% of all *Thecaphora* species known to occur on Asteraceae. In addition to the sequence of *Th. anthemidis*, we have provided barcode sequences of the ITS region for eight other taxa not previously available on GenBank (Table I). Future studies should address whether species of *Thecaphora* that infect the flower heads of Asteraceae form a monophyletic group.

Acknowledgements

The authors are grateful to Ulrike Damm and Michaela Schwager of the Herbarium Senckenbergianum Görlitz (GLM) for providing us with herbarium numbers for private collections and to the curators Dagmar Triebel of the Herbarium Munich (M), Ulrike Damm of the Herbarium Senckenbergianum Görlitz (GLM) and Scott LaGreca of the Cornell University New York (CUP) for loaning specimens from their keeping. We also thank all private collectors of the specimens investigated in this study for giving material to public herbaria. Furthermore, we want to thank the Ministry for Environment and Energy, Directorate for Forest Management for the collection permission in Rhodes (Greece). Alistair McTaggart is thanked for proofreading the paper and helpful advice.

References

Altschul SF, Madden TL, Schäffer AA, Zhang J, Zhang Z, Miller W, Lipman DJ (1997) Gapped BLAST and PSI-BLAST: a new generation of protein database search programs. Nucleic Acids Research 25: 3389–3402. https://doi.org/10.1093/nar/25.17.3389

Begerow D, Lutz M, Oberwinkler F (2002) Implications of molecular characters for the phylogeny of the genus *Entyloma*. Mycological Research 106: 1392–1399. https://doi.org/10.1017/S0953756202006962

Bremer K, Humphries CJ (1993) Generic monograph of the Asteraceae-Anthemideae. Bulletin of the British Museum (Natural History) Botany series 23: 71–177.

Cazón I, Conforto C, Fernández FD, Paredes JA, Rago AM (2016) Molecular detection of *Thecaphora frezii* in peanut (*Arachis hypogaea* L.) seeds. Journal of Plant Pathology 98: 327–330. http://www.jstor.org/stable/44280452

Choi YJ, Thines M (2015) Host jumps and radiation, not co-divergence drives diversification of obligate pathogens. A case study in downy mildews and Asteraceae. PLoS One. 10: https://doi.org/10.1371/journal.pone.0133655

Desmazières JBHJ (1827) Plantes cryptogames du Nord de la France (Cryptogamic plants of France). Edn 1: No. 274. Exsiccata, 44 fascicles.

Funk, VA, Susanna A, Stuessy TF, Robinson HE (2009) Classification of Compositae. In: Funk VA, Susanna A, Stuessy T, Bayer R (Eds) Systematics, Evolution, and Biogeography of Compositae. International Association for Plant Taxonomy, Vienna, 171–189.

Katoh K, Standley DM (2013) MAFFT multiple sequence alignment software version 7: improvements in performance and usability. Molecular Biology and Evolution 30: 772–780. https://doi.org/10.1093/molbev/mst010

Kruse J, Choi YJ, Thines M (2017) New smut-specific primers for the ITS barcoding of Ustilaginomycotina. Mycological Progress 16: 213–221. https://doi.org/10.1007/s11557-016-1265-x

Kruse J, Dietrich W, Zimmermann H, Klenke F, Richter U, Richter H, Thines M (2018) *Ustilago* species causing leaf-stripe smut revisited. IMA Fungus 9: 49–73. https://doi.org/10.5598/imafungus.2018.09.01.05

Kummer V, Lutz M, Richter U, Ristow M, Zimmermann H (2014) *Thecaphora oxytropis* – erste Nachweise in Europa. Boletus 35: 5–15.

Matheny PB, Gossmann JA, Zalar P, Kumar TA, Hibbett DS (2006) Resolving the phylogenetic position of the Wallemiomycetes: an enigmatic major lineage of Basidiomycota. Botany 84: 1794–1805. https://doi.org/10.1139/b06-128

Oberprieler C (1998) The systematics of *Anthemis* L. (Compositae, Anthemideae) in W and C North Africa. Bocconea 9: 1–328.

Oberprieler C (2001) Phylogenetic relationships in *Anthemis* L. (Compositae, Anthemideae) based on nrDNA ITS sequence variation. Taxon 50: 745–762. https://doi.org/10.2307/1223705

Oberprieler C, Himmelreich S, Källersjö M, Valles J, Vogt R (2009) Anthemideae. In: Funk VA, Susanna A, Stuessy TF, Bayer R (Eds) Systematics, evolution, and biogeography of Compositae. International Association for Plant Taxonomy,Vienna, 631–666.

Oberprieler C, Himmelreich S, Vogt R (2007) A new subtribal classification of the tribe Anthemideae (Compositae). Willdenowia 37: 89–114. https://doi.org/10.3372/wi.37.37104

Piątek M, Lutz M, Sousa FMP, Santos ARO, Félix CR, Landell MF, Gomes FCO, Rosa CA (2017) *Pattersoniomyces tillandsiae* gen. et comb. nov.: linking sexual and asexual morphs of the only known smut fungus associated with Bromeliaceae. Organisms Diversity & Evolution 17: 531–543. https://doi.org/10.1007/s13127-017-0340-8

Piepenbring M (2001) New species of smut fungi from the neotropics. Mycological Research 105: 757–767. https://doi.org/10.1017/S0953756200004135

Presti RML, Oppolzer S, Oberprieler C (2010) A molecular phylogeny and a revised classification of the Mediterranean genus *Anthemis* sl (Compositae, Anthemideae) based on three molecular markers and micromorphological characters. Taxon 59: 1441–1456. http://www.jstor.org/stable/20774040

Ridgway KP, Duck JM, Young JPW (2003) Identification of roots from grass swards using PCR-RFLP and FFLP of the plastid trn L (UAA) intron. BMC Ecology 3: 8. https://doi.org/10.1186/1472-6785-3-8

Roets F, Dreyer LL, Wingfield MJ, Begerow D (2008) *Thecaphora capensis* sp. nov., an unusual new anther smut on *Oxalis* in South Africa. Persoonia 21: 147–152. https://doi.org/10.3767/003158508X387462

Roets F, Curran H, Dreyer LL (2012) Morphological and reproductive consequences of an anther smut fungus on *Oxalis*. Sydowia 64: 267–280. https://doi.org/10.4102/sajs.v107i3/4.653

Stoll M, Piepenbring M, Begerow D, Oberwinkler F (2003) Molecular phylogeny of *Ustilago* and *Sporisorium* species (Basidiomycota, Ustilaginales), based on internal transcribed spacer (ITS) sequences. Canadian Journal of Botany 81: 976–984. https://doi.org/10.1017/S0953756204002229

Vánky K, Lutz M (2007) Revision of some *Thecaphora* species (Ustilaginomycotina) on Caryophyllaceae. Mycological Research 111: 1207–1219. https://doi.org/10.1016/j.mycres.2007.06.007.

Vánky K, Lutz M, Bauer R (2008) About the genus *Thecaphora* (Glomosporiaceae) and its new synonyms. Mycological Progress 7: 31–39. https://doi.org/10.1007/s11557-007-0550-0

Vánky K (2012) Smut Fungi of the World. APS Press, St Paul, Minnesota, 1458 pp.

Vasighzadeh A, Zafari D, Selçuk F, Hüseyin E, Kurşat M, Lutz M, Piątek M (2014) Discovery of *Thecaphora schwarzmaniana* on *Rheum ribes* in Iran and Turkey: implications for the diversity and phylogeny of leaf smuts on rhubarbs. Mycological Progress 13: 881–892. https://doi.org/10.1007/s11557-014-0972-4

White TJ, Bruns T, Lee SJWT, Taylor JL (1990) Amplification and direct sequencing of fungal ribosomal RNA sequences for phylogenetics. In: Innis N, Gelfand D, Sninsky J, White T (Eds) PCR Protocols: a guide to methods and applications. San Diego, Academic Press, 315–322.

MycoKeys 41: 51–63 (2018)
doi: 10.3897/mycokeys.41.27694
http://mycokeys.pensoft.net

RESEARCH ARTICLE

A peer-reviewed open-access journal
MycoKeys
Launched to accelerate biodiversity research

Ravenelia piepenbringiae and *Ravenelia hernandezii*, two new rust species on *Senegalia* (Fabaceae, Mimosoideae) from Panama and Costa Rica

M. Ebinghaus[1], D. Begerow[1]

1 *AG Geobotanik, Ruhr-Universität Bochum, Germany*

Corresponding author: *M. Ebinghaus* (malte.ebinghaus@gmx.de)

Academic editor: *Marco Thines* | Received 21 June 2018 | Accepted 19 September 2018 | Published 23 October 2018

Citation: Ebinghaus M, Begerow D (2018) *Ravenelia piepenbringiae* and *Ravenelia hernandezii*, two new rust species on *Senegalia* (Fabaceae, Mimosoideae) from Panama and Costa Rica. MycoKeys 41: 51–63. https://doi.org/10.3897/mycokeys.41.27694

Abstract

Two new rust species, *Ravenelia piepenbringiae* and *R. hernandezii* (Pucciniales) on *Senegalia* spp. (Fabaceae) are described from the Neotropics (Panama, Costa Rica). A key to the species on neotropical *Senegalia* spp. is provided. Molecular phylogenetic analyses based on 28S rDNA sequence data suggest that the representatives of *Senegalia* rusts distributed in the neotropics evolved independently from species known from South Africa. This is further supported by the teliospore morphology, which is characterised by uniseriate cysts in the neotropical *Senegalia* rusts and contrasting multiseriate cysts in the paleotropic *Ravenelia* species that infect this host genus.

Keywords

Senegalia rust, rust fungi, Phylogeny, Taxonomy

Introduction

With more than 200 described species, the genus *Ravenelia* is amongst the most speciose genera within the rust fungi (Pucciniales) (Cummins and Hiratsuka 2003). In the tropics and subtropics, members of this genus parasitise a diverse range of hosts of the legume family (Fabaceae), including Caesalpinioideae, Faboideae and Mimosoideae. Numerous species of *Ravenelia* are known from the neotropics, mostly from Mexico

(Cummins 1978), Brazil (Dianese et al. 1993, Rezende and Dianese 2001; Hennen et al. 2005) and Argentina (Hernández and Hennen 2002).

However, in the neotropics, occurrence of *Ravenelia* species is poorly known in other countries such as Panama and Costa Rica. Preliminary checklists of abundant fungi in Central America report only a single species of *Ravenelia* in Panama (*R. entadae*) (Piepenbring 2006) and 18 species of *Ravenelia* in Costa Rica, respectively (Berndt 2004).

Specimens of a rust fungus on *Senegalia hayesii* (Benth.) Britton and Rose were collected in Panama in 2013. Another species of *Ravenelia* was discovered through the analysis of herbarium specimens of the U.S. National Fungal Collections (BPI) on *Senegalia tenuifolia* (L.) Britton and Rose. On the basis of morphological and molecular data, these two specimens were herein analysed and described respectively as *Ravenelia piepenbringiae* and *R. hernandezii*.

Material and methods

Light- and electron microscopic investigations

Spores representing different spore stages were scraped from the leaf surfaces of dried herbarium specimens and stained in lactophenol solution on microscope slides. For the analysis of soral structures, hand sections were prepared under a stereomicroscope. Samples were microscopically studied with a Zeiss Axioplan Light Microscope and Zeiss AxioCam. Cellular structures were measured using ZEN 2 (Blue Edition) Software. Infected leaflets of the herbarium specimens were mounted on double-sided sticky carbon tape on metal stubs and coated with gold in a Sputtercoater BAL-TEC SCD OSO (Capovani Brothers Inc, USA). Superficial ornamentation of spores was investigated using a ZEISS Sigma VP scanning electron microscope at the Ruhr-University Bochum, Germany.

DNA extraction and PCR

Genomic DNA extractions were carried out using the INNUPrep Plant DNA Kit (Analytic Jena, Germany) according to the manufacturer's protocol. Spores were milled in a Retsch Schwingmühle MM2000 (F. Kurt Retsch GmbH &Co KG, Haan, Germany), using two steel beads and liquid nitrogen in three consecutive cycles. An amount of 40 ml of lysis buffer was added to loosen spore remnants by vortexing from the Eppendorf tube lid, followed by centrifuging in a final cycle. Polymerase chain reaction (PCR) of 28S rDNA was conducted using the Taq-DNA-Polymerase Mix (PeqLab, Erlangen, Germany). To compensate for small amounts of spores applied for DNA extractions up to 5ml of genomic DNA extraction were used as the template in 25 ml reactions. Primer pair LR0R (Moncalvo et al. 1995) and LR6 (Vilgalys and Heester 1990) were used to obtain sequences of the 28S rDNA, with thermal cycling conditions set at 96 °C (3 min) followed by 40 cycles of 30 sec at 95 °C, 40 sec at 49 °C and 1 min at 72 °C, with a final extension for 7 min at 72 °C. PCR products, which

Table 1. Specimens analysed in this study, including GenBank Accession Numbers. Published references are given for sequences obtained from GenBank. †: BPI (U.S. National Fungus Collections, USA); ‡: KR (Staatliches Museum für Naturkunde Karlsruhe, Germany); $: PREM (Plant Protection Research Institute, South Africa); |: Z+ZT (Universität Zürich, Switzerland and Eidgenössische Technische Hochschule Zürich, Switzerland); ¶: BRIP (Department of Agriculture and Fisheries, Australia); #: PMA (Universidad de Panamá, Panama).

Voucher	Species	Substrate	Reference	Origin	LSU GenBank
BPI841185†	*Ravenelia cohniana* Henn.	*Senegalia praecox* (Grieseb.) Seigler & Ebinger	This work	Catamarca Province, Argentina	MG954487
BPI841034†	*Ravenelia echinata* var. *ectypa* (Arthur & Holw.) Cummins	*Calliandra formosa* (Kunth) Benth.	Scholler and Aime, 2006	Tucuman Province, Argentina	DQ323925*
KR-M-0043650‡	*Ravenelia escharoides* Syd.	Senegalia burkei (Benth.) Kyal. & Boatwright	This work	Mpumalanga, South Africa	MG954480
KR-M-0043651‡	*Ravenelia escharoides* Syd.	*Senegalia burkei* (Benth.) Kyal. & Boatwright	This work	Limpopo, South Africa	MG954481
KR-M-0043652‡	*Ravenelia escharoides* Syd.	*Senegalia burkei* (Benth.) Kyal. & Boatwright	This work	Limpopo, South Africa	MG954482
PREM61223$	*Ravenelia evansii* Syd.	*Vachellia sieberiana* (Burtt Davy) Kyal. & Boatwr.	This work	KwaZulu-Natal, South Africa	MG945988
PREM61228$	*Ravenelia evansii* Syd.	*Vachellia sieberiana* (Burtt Davy) Kyal. & Boatwr.	This work	KwaZulu-Natal, South Africa	MG945989
PREM61855$	*Ravenelia halsei* Doidge	*Senegalia ataxacantha* (D.C) Kyal. & Boatwright	This work	Mpumalanga, South Africa	MG954484
Z+ZT RB5788|	*Ravenelia havanensis* Arthur	*Enterolobium contortisiliquum* (Vell.) Morong	Aime, 2006	Tucuman Province, Argentina	DQ354557*
BPI872308†	*Ravenelia hernandezii* Ebinghaus & Begerow	*Senegalia tenuifolia* (L.) Britton & Rose	This work	Guanacaste, Costa Rica	MG954488
PREM61222$	*Ravenelia macowaniana* Pazschke	*Vachellia karroo* (Hayne) Banfi & Galasso	This work	Limpopo Province, South Africa	MG946007
PREM61210$	*Ravenelia macowaniana* Pazschke	*Vachellia karroo* (Hayne) Banfi & Galasso	This work	Eastern Cape Province, South Africa	MG946004
PREM61221$	*Ravenelia macowaniana* Pazschke	*Vachellia karroo* (Hayne) Banfi & Galasso	This work	North-West Province, South Africa	MG946005
BPI841195†	*Ravenelia macrocarpa* Syd. & Syd.	*Senna subulata* (Griseb.) H.S. Irwin & Barneby	Scholler and Aime 2006	Argentina	DQ323926*
BRIP56908¶	*Ravenelia neocaledoniensis* Huguenin	*Vachellia farnesiana* (L.) Wight & Arn.	McTaggart et al. 2015	Kununurra, Australia	KJ862348*
BRIP56907¶	*Ravenelia neocaledoniensis* Huguenin	*Vachellia farnesiana* (L.) Wight & Arn.	McTaggart et al. 2015	Northern Territory, Australia	KJ862347*
KR-M-0045114‡	*Ravenelia pienaarii* Doidge	*Senegalia caffra* (Thunb.) P.J.H. Hurter & Mabb.	This work	Gauteng, South Africa	MG954483
PREM61892$	*Ravenelia pienaarii* Doidge	*Senegalia caffra* (Thunb.) P.J.H. Hurter & Mabb.	This work	KwaZulu-Natal, South Africa	MG954482
MP5157 (PMA)#	*Ravenelia piepenbringiae* Ebinghaus & Begerow	*Senegalia hayesii* (Benth.) Britton & Rose	This work	Chiriquí Province, Panama	MG954489
BRIP56904¶	*Ravenelia* sp.	*Cassia* sp. Mill.	McTaggart et al. 2015	Northern Territory, Australia	KJ862349*
PREM61858$	*Ravenelia transvaalensis* Doidge	*Senegalia mellifera* (Vahl) Seibler & Ebinger	This work	North-West Province, South Africa	MG954485
PREM61893$	*Ravenelia transvaalensis* Doidge	*Senegalia mellifera* (Vahl) Seibler & Ebinger	This work	North-West Province, South Africa	MG954486
BRIP56539¶	*Endoraecium auriculiforme* McTaggart & Shivas	*Acacia difficilis* Maiden	McTaggart et al., 2015	Northern Territory, Australia	KJ862398*
BRIP27071¶	*Endoraecium tierneyi* (Walker & Shivas) Scholler & Aime	*Acacia harpophylla* F.Muell. ex Benth.	McTaggart et al. 2015	Queensland, Australia	KJ862335*
BRIP56557¶	*Endoraecium tropicum* McTaggart & Shivas	*Acacia tropica* (Maiden & Blakely) Tindale	McTaggart et al. 2015	Northern Territory, Australia	KJ862337*
BRIP56545¶	*Endoraecium violae-faustiae* Berndt	*Acacia difficilis* Maiden	McTaggart et al. 2015	Northern Territory, Australia	KJ862344*

showed only weak bands on agarose gels, were purified with Zymo Research DNA Clean & Concentrator-5 Kit (ZymoResearch Corp., Irvine, USA), according to the manufacturer's protocol. The remaining PCR products were purified using Sephadex G-50 columns (Sigma-Aldrich Chemie GmbH, Taufkirchen, Germany). Sequencing was carried out in both directions using the same primers as in PCR at the sequencing service of the Faculty of Chemistry and Biochemistry of the Ruhr-University Bochum, Germany and by GATC (GATC Biotech, Konstanz, Germany)

Phylogenetic analyses

Sequences were screened against the NCBI Genbank using the BLAST algorithm to check for erroneously amplified contaminations and were afterwards edited manually using Sequencher 5.0 software (Gene Codes Corp., Michigan, USA). In total, 26 sequences were included (Table 1) to construct an alignment of the 28S rDNA-sequence data using MAFFT v6.832b (Katoh and Standley 2013). Maximum likelihood (ML) analyses were performed with RxML 8.0.26 (Stamatakis 2014) using RAxML GUI v. 1.31 (Silvestro and Michalak 2012) based on the General Time Reversible model of nucleotide substitution plus gamma distribution (GTR+G; Rodriguez et al. 1990) and 1000 generations. Four representative species of *Endoraecium* (KJ862335, KJ862298, KJ862337, KJ862344) were set as multiple outgroups. Maximum Parsimony (MP) analyses were carried out using MEGA6 (Tamura et al. 2013) using the heuristic search option with tree bisection-reconnection (TBR) branch swapping algorithm with 10 initial trees using random step-wise addition. The reliability of topology was tested using the bootstrap method with 1000 replicates.

Results

Phylogenetic analyses

The alignment of the 28S rDNA sequence data consisted of 26 sequences representing 18 taxa and had a total length of 1015 nucleotides with 305 variable characters, 250 parsimony-informative sites and 55 singletons. The tree topologies of MP and ML analyses were identical and thus only the ML tree is shown. A clade, comprising rusts on neotropical *Senegalia* species, i.e. *R. cohniana*, *R. hernandezii* sp. nov. and *R. piepenbringiae* sp. nov., displays a robustly supported sister-group (MLBS/MPBS = 99/100) to two neotropically distributed rusts which infect non-*Senegalia* hosts (i.e. *R. echinata* var. *ectypa* on *Calliandra formosa*, DQ323925 and *R. havanensis* on *Enterolobium contortisiliquum* DQ354557) (Scholler and Aime 2006, Aime 2006). A second clade, based on sequences obtained from *Ravenelia* species on *Senegalia* spp. with paleotropical origin, appeared only distantly related to the former species cluster (MLBS/MPBS = 100/99) (Figure 1).

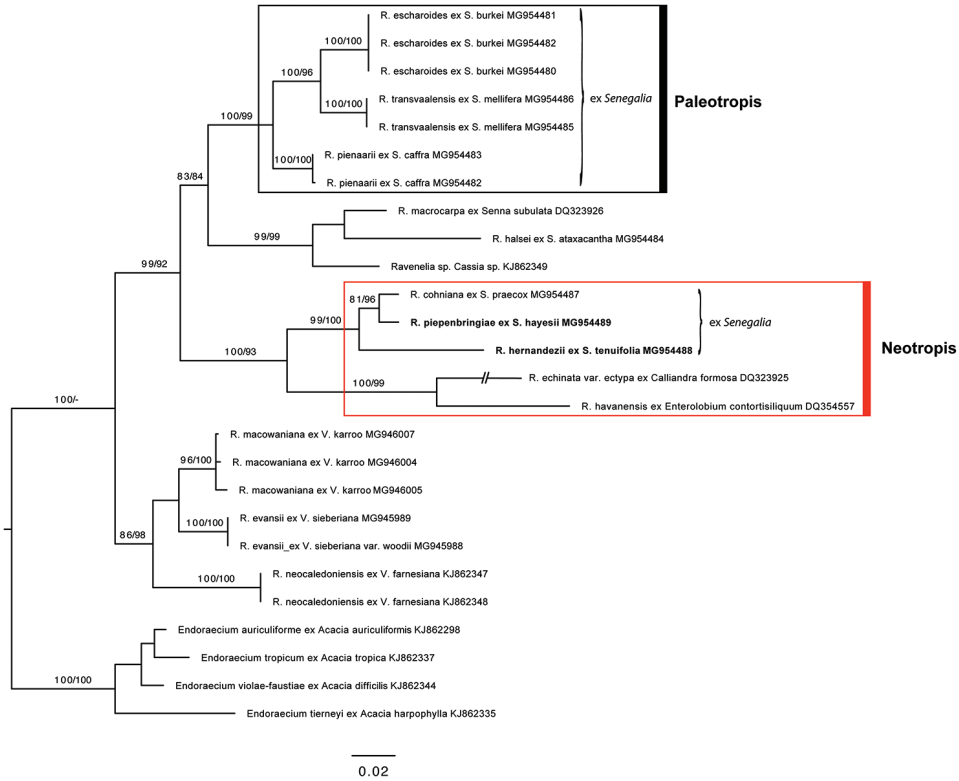

Figure 1. Maximum likelihood reconstruction of *Ravenelia* spp. based on 28S rDNA sequence data. Bootstrap values are shown above branches based on 1000 replicates (MLBS and MPBS, respectively), values below 75 are not shown. Names of species collected on neotropical *Senegalia* hosts including *R. piepenbringiae* and *R. hernandezii* are highlighted (bold, red box). For paleotropically distributed species of *Senegalia* rusts, see black box.

Taxonomy

Ravenelia piepenbringiae Ebinghaus & Begerow, sp. nov. on *Senegalia hayesii* (Benth.) Britton & Rose (Mimosoideae, Leguminosae)

Mycobank: MB 824297
Fig. 2

Type. Panama, Chiriquí Province, Dolega District, Los Algarrobos, Casa de la Alemana, Bosquecito, approx. 150 m a.s.l., 8°29'45.31"N, 82°25'56.24"W on *Senegalia hayesii* (Benth.) Britton and Rose, 17 February 2013, coll. M. Piepenbring MP 5157 [**holotype**: s.n. (PMA), isotypes: KR-M-0043654 (KR). M-0141345 (M)]

Etymology. Named after M. Piepenbring, who discovered the rust fungus in her garden and provided the specimens.

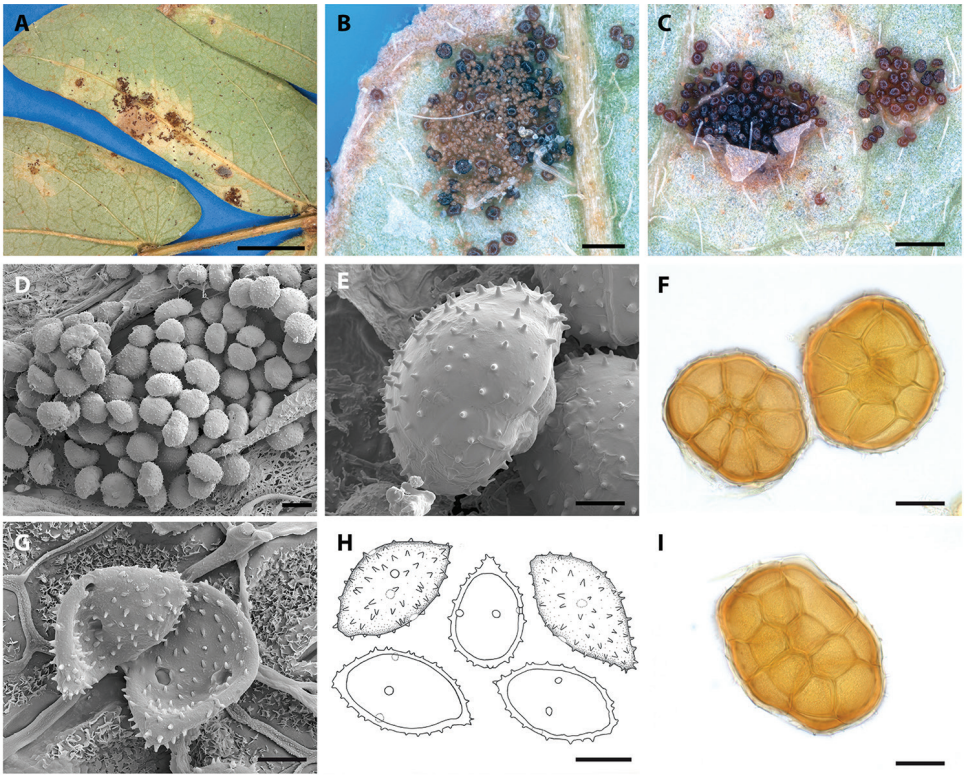

Figure 2. *Ravenelia piepenbringiae*. **A** Telia in chlorotic spots associated with infection of *Senegalia hayesii* **B, C** sori showing uredinio- and teliospores and teliospores, respectively **D** SEM image of a telium **E** SEM view of a teliospore **F, I** LM images of teliospores **G** SEM image of urediniospores showing equatorially arranged germ pores **H** drawings of urediniospores. Scale bars: 3 mm (**A**); 0.1 mm (**B**); 0.2 mm (**C**); 40 mm(**D**); 10 mm (**E**); 20 mm(**F**); 5 mm(**G**); 10 mm(**H**); 20 mm(**I**).

Spermogonia and aecia not seen. Uredinia hypophyllous, single or in irregular groups, light brown, often associated with necrotic spots that are also evident on the adaxial surface, 0.1–0.8 mm in diameter, aparaphysate, subepidermal, covered by the epidermis when young, later erumpent. Urediniospores obovoidal, ellipsoidal or slightly curved, often limoniform with an acuminate apex, ochraceous brown, (18)21–25(29) × 12–15(20) mm; spore wall laterally 1–1.5 mm thick, apically and basally often slightly thickened, distinctly verrucose to echinulate; aculei 1.0–1.5 mm high, distances between aculei about 2 mm, germ pores 4–7, in equatorial position. Telia replacing uredinia or developing independently from uredinia, chestnut to dark brown, sometimes confluent. Teliospores roundish to broadly ellipsoidal to oblong in planar view, hemispherical in lateral view, with 4–6 probasidial cells across, single-layered, each teliospore formed by 9–13 probasidial cells, (44)58–73(78) mm in diameter, single probasidial cells (19)22–26(31) × (11)17–22(28) mm; cell wall thickened at the surface of the teliospore (epispore), 2–4(5) mm thick, often with a thin and hyaline outer layer, each probasidial cell with 7–11 rod-shaped, straight spines that are (1)2–3(4.5) mm long; cysts at the

basis of the teliospores, uniseriate and in the same position and number as the peripheral probasidial cells, globose, hyaline, swelling in water, slightly swelling in lactophenol.

Further specimens. Type locality, 22 January 2014, M. Piepenbring 5203 [M-0141344 (M), s.n. (UCH)]. Type locality, 12 January 2017, M. Piepenbring & I. D. Quiroz González 5333 (UCH, s.n.).

***Ravenelia hernandezii* Ebinghaus & Begerow, sp. nov. on *Senegalia tenuifolia* (L.) Britton and Rose (Mimosoideae, Leguminosae)**

Mycobank: MB 824298

Fig. 3

Type. Costa Rica, Guanacaste, Area de Conservación Guanacaste, Sendero Bosque húmedo (10°50.702'N, 85°36.450'W) on *Senegalia tenuifolia* (L.) Britton and Rose, coll. J.R. Hernandez, 1. December 2003. Holotype: BPI 872308 (BPI).

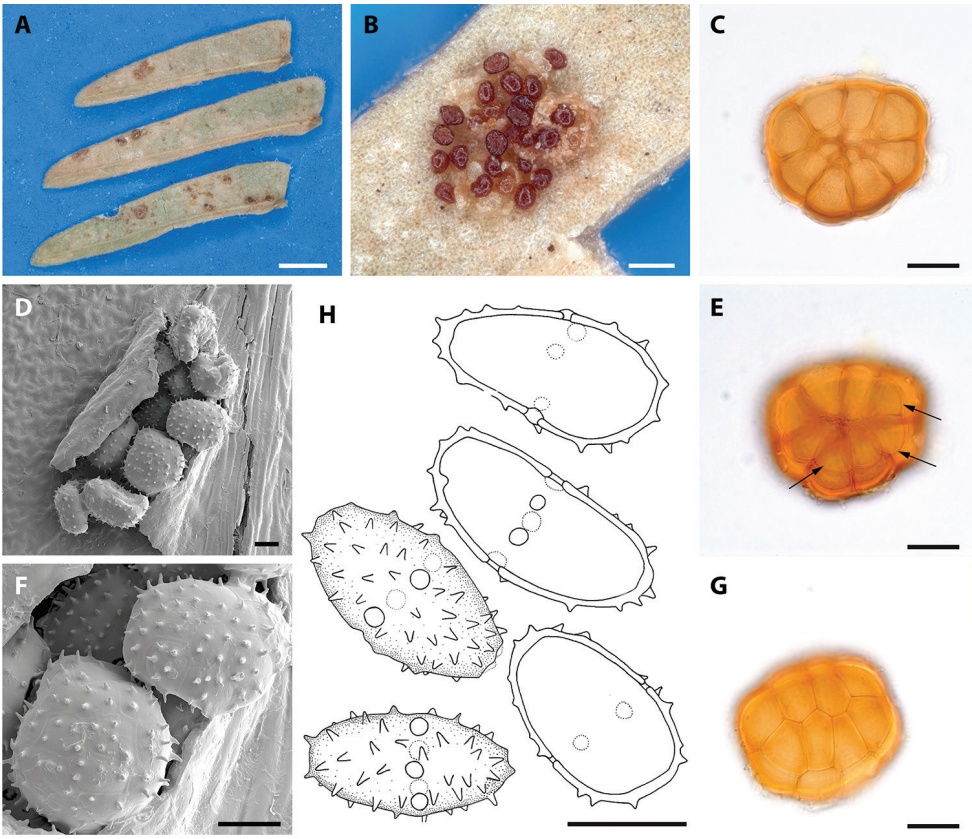

Figure 3. *Ravenelia hernandezii*. **A** Infected leaflets of *S. tenuifolia* **B** Mixed sori containing urediniospores and teliospores **C** Teliospore seen in LM **D** telium seen by SEM **E** Adaxial view of a teliospore by LM, with arrows indicating the uniseriate cysts **F** SEM view of spinescent teliospores **G** LM view of the upper surface **H** drawing of a urediniospore. Scale Bars: 0.5 mm (**A**); 0.1 mm (**B**); 20 mm (**C–G**); 10 mm (**H**).

Table 2. Summary of morphological characteristics of *Ravenelia* species infecting *Senegalia* trees in the neotropics. All measurements are given in mm. Absent characters are indicated with dashes.

Species	Teliospore characters								Source
	Teliospore size	Probasidial cell size	Epispore	Ornamentation			Cells in Diameter	Arrangement of Cysts	
				Number per cell	length	shape			
R. cohniana	(39)45–73(74)	16–22 × 13–15	not stated	(2)3–5(8).	3–5	spinescent	(3)4–5(6)	uniseriate	Hernández and Hennen (2002)
R. escharoides	55–90	30–35 × 16–20	up to 6	4–9	1–2	verrucose	6–8	multiseriate	Doidge (1939)
R. halsei	80–112	25–30 × 10–15	5–6	–	–	smooth	9–11	uniseriate	Doidge (1939)
R. hernandezii	(59)67–75(96)	(19)22–25(39) × (11)17–22(28)	(2.5)3–4.5(6)	3–5	(1)3–4(6)	spinescent	5–6	uniseriate	This study
R. lata	53–64	(18)22–26 (width)	not stated	6–20	not stated	spinescent	4	multiseriate	Hennen et al. (2005)
R. monosticha	(50)53–55 × 65–70	16–19 × 13–15	not stated	4–8	not stated	verrucose	4–6	uniseriate	Spegazzini (1923)
R. pienaarii	80–120	25–30 × 10–15	up to 7	4–7	1–1.5(2)	verrucose	(6)7–10	multiseriate	Doidge (1939)
R. piepenbringiae	(44)58–73(78)	(19)22–26(31) × (11)17–22(28)	2–4(5)	7–11	(1)2–3(4.5)	spinescent	4–6	uniseriate	This study
R. pringlei	(55)70–95(105)	(12)14–18(20) (width)	not stated	not stated	not stated	verrucose	(5)6–8	uniseriate	Cummins (1975)
R. rata	(30)33–40(44)	14–20 × 12–17	1.5	not stated	2–3	verrucose	2–4	uniseriate	Hennen et al. (2005)
R. roemerianae	63–100	Not stated	not stated	3–10	2	verrucose	5–7	uniseriate	Long (1917)
R. scopulata	(55)65–100(110)	(13)16–19(21) (width)	not stated	not stated	not stated	smooth	5–8	multiseriate	Cummins and Baxter (1976)
R. stevensii	40–63	Not stated	not stated	1–3	6–19	verrucose	3–6	multiseriate	Arthur (1915)
R. transvaalensis	75–100	30–35 × 15–17.5	up to 6	–	–	smooth	5–6	multiseriate	Doidge (1939)
R. versatilis	85–105	10–16 (width)	not stated	–	–	smooth	7–9	not stated	Dietel (1894)

	Paraphyses		Urediniospore characters					Source
	Position	Shape	Size	Cell wall	Germ pores		Shape	
					Number	Position		
R. cohniana	–	–	(12)20–28(32) × (11)13–17(19)	1.5–2.5(3)	(3)4(6)	equatorial	oblong-ellipsoidal	Hernández and Hennen (2002)
R. escharoides	–	–	17–22×14–17	1.5	Not stated	not stated	obovoidal-ellipsoidal	Doidge (1939)
R. halsei	not stated	not stated	–	–	–	–	–	Doidge (1939)
R. hernandezii	–	–	(17)18–21(24) × (8)9–10(12)	(0.5)1–1.5	5–6	equatorial	obovoidal-ellipsoidal	This study
R. lata	peripheral	capitate	(22)25–32(36) × (12)14–17(18)	1.5–2	(4)5–6	equatorial	obovoidal-oblong	Hennen et al. (2005)
R. monosticha	peripheral	capitate	(23)26–30(33) × (8)12–14(15)	1.5–2	4–5(6)	equatorial	obovoidal-ellipsoidal	Spegazzini (1923)
R. pienaarii	–	–	20–25 × 15–19	1.5	6	equatorial	ellipsoidal-subglobose	Doidge (1939)
R. piepenbringiae	–	–	(18)21–25(29) × 12–15(20)	1–1.5	4–7	equatorial	obovoidal-limoniform	This study
R. pringlei	not stated	clavate - capitate	(10)11–15(17) × (20)26–33(35)	(1)1.5(2)	8	bizonate	oblong-ellipsoidal	Cummins (1975)
R. rata	–	–	–	–	–	–	–	Hennen et al. (2005)
R. roemerianae	intrasoral	clavate	10–14 × 27–38	1–1.5	8	bizonate	obovoidal-oblong	Long (1917)
R. scopulata	not stated	clavate	(17)19–24 × (11)12–14(15)	(1)1.5(2)	6–8	bizonate	oblong-ellipsoidal	Cummins and Baxter (1976)
R. stevensii	peripheral	clavate - capitate	8–13 × 25–30	<1	4	equatorial	oblong-obovoidal	Arthur (1915)
R. transvaalensis	–	–	–	–	–	–	–	Doidge (1939)
R. versatilis	intrasoral	clavate - capitate	13–18 × 26–32	Not stated	8	bizonate	obovoidal-oblong	Dietel (1894)

Etymology. Named after J.R. Hernández who collected the type specimen.

Spermogonia and aecia not seen. Uredinia hypophyllous, minute, single or in small and often loose groups, ochraceous to light brown, 0.1–0.3 mm in diameter, aparaphysate, subepidermal, erumpent and surrounded by torn epidermis; urediniospores obovoidal, ellipsoidal, often reniform or slightly curved, ochraceous brown, often with an attached fragment of the pedicel, (17)18–21(24) × (8)9–10(12) mm; spore wall thin, laterally (0.5)1–1.5 mm thick, apically and basally slightly thickened, distinctly echinulate; aculei approximately 1.0–1.5 mm high, germ pores 5–6, in equatorial position. Telia replacing uredinia, chestnut- to dark brown. Teliospores (59)67–75(96) mm, roundish or broadly ellipsoidal to oblong in planar view, hemispherical in lateral view, 5–6 probasidial cells across, single-layered, central cells often arranged in two rows of 3 or 4 cells, each cell (19)22–25(39) × (11)17–22(28) mm, cell wall thickened at the apex, (2.5)3.0–4.5(6.0) mm thick, often with a thin and hyaline outer layer, probasidial cells each with 3–5 rod-shaped straight spines (1)3–4(6) mm long; cysts on the abaxial side of the teliospores, uniseriate and in same position and number as the peripheral probasidial cells, globose, hyaline, swelling in water, slight swelling in lactophenol.

Discussion

A total of 10 species of *Ravenelia* have been described to date from the neotropics parasitising *Senegalia* trees: *R. cohniana* Hennings on *S. praecox* (Griseb.) Seigler & Ebinger, *R. idonea* Jackson & Holway, *R. lata* Hennen & Cummins on *S. glomerosa* (Benth.) Britton & Rose, *R. monosticha* Speg. on *S. bonariensis* (Gillies ex Hook. & Arn.) Seigler & Ebinger, *R. pringlei* Cummins on *S. greggii* (A. Gray) Britton & Rose, *R. rata* Jackson & Holway on *S. pedicellata* (Benth.) Seigler & Ebinger, *R. roemerianae* Long on *S. roemeriana* (Scheele) Britton & Rose, *R. scopulata* Cummins & Baxter on *S. greggii* (A. Gray) Britton & Rose, *R. stevensii* Arthur on *S. riparia* (Kunth) Britton & Rose ex Britton & Killip and *R. versatilis* (Peck) Dietel on *S. anisophylla* (Watson) Britton & Rose. No species of *Ravenelia* has been reported to affect *Senegalia hayesii* or *S. tenuifolia*. Most of these species known to parasitise *Senegalia* spp. are distinguished from species identified in this study by abundant paraphyses in the uredinia, except for *Ravenelia rata* which also lacks paraphyses in the uredinia. However, this species differs from *R. piepenbringiae* and *R. hernandezii* by abundant tuberculate teliospore ornamentations 2–3µm in length and by formation of only 2–4 cysts per teliospore. Both newly described species exhibit longer tuberculate spines and bear 6–8 cysts per teliospore. *Ravenelia cohniana* is the only species that resembles various teliospore and urediniospore characteristics of *R. piepenbringiae* and *R. hernandezii* (see Table 2). The teliospores of *R. hernandezii*, however, are larger in size than those of the latter two species (Table 2). In contrast to the teliospores, urediniospores of *R. hernandezii* tend to be smaller and more slender, while they mostly lack the characteristic acuminate apex present in urediniospores of *R. piepenbringiae* (Table 2; compare Figures 1H and 2H). Hernández and Hennen (2002) considered *R. concinna* Syd. on *S. riparia* (Kunth) Britton & Rose ex Britton & Killip

and *S. glomerosa*, *R. distans* Arthur & Holway on an unidentified mimosoid host and *R. lindquistii* Hennen & Cummins on *Senegalia praecox* as synonyms of *R. cohniana* due to a nearly identical morphology. However, given the likewise close morphological resemblance in *R. piepenbringiae*, *R. hernandezii* and *R. cohniana*, despite being phylogenetic entities, this assumption needs revision by molecular phylogenetic means.

The resemblance of teliospore characters in *R. cohniana* and the species identified in the present study suggests a close relationship which is supported by the phylogenetic reconstructions. These neotropical rusts on *Senegalia* further appear to have evolved independently from those *Senegalia* rusts that have a paleotropic origin (Fig. 1, Table 1). The phylogenetic distinction of both lineages is also mirrored by a morphological feature: the arrangement of teliosporic cysts is uniseriate in the analysed neotropic species but multiseriate in all investigated paleotropic *Senegalia* rusts (Table 2).

Key to species of Ravenelia infecting neotropical Senegalia trees

1 Teliospores ≤64 mm; urediniospores with equatorially arranged germ pores **2**
– Teliospores >64 mm; urediniospores with bizonate or equatorially arranged germ pores **4**
2 Paraphyses present in uredinia **3**
– Paraphyses absent in uredinia....***R. rata***
3 Teliospores with <6 verrucae per cell; on *S. riparia*....***R. stevensii***
– Teliospores with 6–20 spines per cell; on *S. glomerosa* ....***R. lata***
4 Urediniospores with 6–8 bizonate germ pores; teliospores verrucose or smooth **5**
– Urediniospores if present with equatorially arranged germ pores; teliosporesspinescent or verrucose; teliospore cysts uniseriate....**8**
5 Teliospores smooth **6**
– Teliospores verrucose **7**
6 On *S. anisophylla*; urediniospores 12–14 × 19–24 mm....***R. versatilis***
– On *S. greggii*; urediniospores 13–18 × 26–32 mm....***R. scopulata***
7 With intrasoral paraphyses; on *S. roemeriana* ....***R. roemerianae***
– On *S. greggii* ....***R. pringlei***
8 Paraphyses present; teliospores verrucose; on *S. bonariensis* ....***R. monosticha***
– Paraphyses absent; teliospores spinescent....**9**
9 Teliospores with 7–11 spines per cell; urediniospores often limoniform; on *S. hayesii* ....***R. piepenbringiae***
– Teliospores with 3–5 spines per cell; urediniospores obovoidal to ellipsoidal,sometimes limoniform **10**
10 Teliospores 59–96 mm in diameter; urediniospores <13mm in width; urediniospore wall laterally 1–1.5 mm; on *S. tenuifolia*....***R. hernandezii***
– Teliospores 39–75 mm in diameter; urediniospores 11–19 mm in width; urediniospore wall laterally 1.5–2.5 mm; on *S. praecox* .... ***R. cohniana***

Acknowledgements

We gratefully acknowledge Dr. Meike Piepenbring, the US National Fungus Collections (USDA-ARS) and the South African Mycology Collections (PREM) for providing herbarium specimens on loan. We also wish to thank Katharina Görges for providing drawings of the urediniospores of *R. piepenbringia* and *R. hernandezii*.

References

Aime C (2006) Toward resolving family-level relationships in rust fungi (Uredinales). Mycoscience 47: 112–122. https://doi.org/10.1007/S10267-006-0281-0

Berndt R (2004) A checklist of Costa Rican rust fungi. In: Agerer R, Piepenbring M, Blanz P (Eds) Frontiers in Basidiomycete Mycology. IHW Verlag, München, 185–236 .

Cummins GB, Hiratsuka Y (2003) Illustrated Genera of Rust Fungi (3rd edn). Phytopathological Society, St. Paul, MN, APS Press, St. Paul, MN.

Dianese JC, Medeiros RB, Santos LTP, Furlanetto C, Sanchez M, Dianese AC (1993) *Batistopsora* gen. nov. and new *Phakopsora*, *Ravenelia*, *Cerotellium*, and *Skierka* species from the Brazilian Cerrado. Fitopatologia Brasileira 18: 436–450.

Farr DF, Rossman AY (2015) Fungal Databases, Systematic Mycology and Microbiology Laboratory, ARS, USDA. http://nt.ars-grin.gov/fungaldatabases [Accessed 17 December 2015]

Hennen JF, Figueiredo MB, de Carvalho Jr AA, Hennnen PG (2005) Catalogue of the species of plant rust fungi (Uredinales) of Brazil. Instituto de Pesquisas, Jardim Botanico do Rio de Janeiro: Rio de Janeiro, Brazil.

Hennings P (1896) Beiträge zur Pilzflora Südamerikas I. Myxomycetes, Phycomycetes, Ustilagineae und Uredineae. Hedwigia 35: 246.

Hernández JR, Hennen JF (2002) The Genus *Ravenelia* in Argentina. Mycological Research 106: 954–974. https://doi.org/10.1017/S0953756202006226

Katoh K, Standley DM (2013) MAFFT multiple sequence alignment software version 7: improvements in performance and usability. Molecular Biology and Evolution 30: 772–780. https://doi.org/10.1093/molbev/mst010

Moncalvo JM, Wang HH, Hseu RS (1995) Phylogenetic relationships in Ganoderma inferred from the internal transcribed spacers and 25S ribosomal DNA sequences. Mycologia 87: 223–238. https://doi.org/10.1080/00275514.1995.12026524

Piepenbring M (2006) Checklist of fungi in Panama. Puente Biológico Volume 1: 1–190.

Rambaut A (2009) FigTree, a graphical viewer of phylogenetic trees. http://tree.bio.ed.ac.uk/software/figtree

Rezende DV, Dianese JC (2001) New *Ravenelia* species on leguminous hosts from the Brazilian Cerrado. Fitopatologia Brasileira 26: 627–634. https://doi.org/10.1590/S0100-41582001000300008

Rodriguez FJ, Oliver JL, Marín A, Medina JR (1990) The general stochastic model of nucleotide substitution. Journal of Theoretical Biology 142: 485–501. https://doi.org/10.1016/S0022-5193(05)80104-3

Scholler M, Aime C (2006) On some rust fungi (Uredinales) collected in an *Acacia koa–Metrosideros polymorpha* woodland, Mauna Loa Road, Big Island, Hawaii. MycoScience 47: 159–165. https://doi.org/10.1007/S10267-006-0286-8

Silvestro D, Michalakis I (2012) raxmlGUI: a graphical front-end for RAxML. Organisms Diversity and Evolution 12: 335–337. doi: 10.1007/s1127-011-0056-0

Spegazzini CL (1909) Mycetes Argentinenses. Anales del Museo Nacional de Buenos Aires. Series. 3, 12: 296.

Stamatakis A (2014) RAxML version 8: a tool for phylogenetic analysis and post-analysis of large phylogenies. Bioinformatics 30: 1312–1313. https://doi.org/10.1093/bioinformatics/btu033

Sydow H, Sydow P (1916) Fungi amazonici a cl. E. Ule lecti. Annales Mycologici 14: 65–97.

Tamura K, Stecher G, Peterson D, Filipski A, Kumar S (2013) MEGA6: Molecular Evolutionary Genetics Analysis version 6.0. Molecular Biology and Evolution 30: 2725–2729. https://doi.org/10.1093/molbev/mst197

Vilgalys R, Hester M. (1990) Rapid genetic identification and mapping of enzymatically amplified ribosomal DNA from several *Cryptococcus* species. Journal of Bacteriology 172: 4238–4246. https://doi.org/10.1128/jb.172.8.4238-4246.1990

White TJ, Bruns T, Lee S, Taylor JW (1990) Amplification and direct sequencing of fungal ribosomal RNA genes for phylogenetics. In: Innis MA, Gelfand DH, Sninsky JJ, White TJ (Eds) PCR Protocols: A Guide to Methods and Applications. Academic Press, Inc., New York, 315–324.

MycoKeys 41: 65–90 (2018)
doi: 10.3897/mycokeys.41.28987
http://mycokeys.pensoft.net

RESEARCH ARTICLE

A peer-reviewed open-access journal
MycoKeys
Launched to accelerate biodiversity research

Additions to the taxonomy of *Lagarobasidium* and *Xylodon* (Hymenochaetales, Basidiomycota)

Ilya Viner[1,2], Viacheslav Spirin[2,3], Lucie Zíbarová[4], Karl-Henrik Larsson[3]

1 *Lomonosov State University, Faculty of Biology, Leninskie Gory 1/12, 119234 Moscow, Russia* **2** *Botany Unit (Mycology), Finnish Museum of Natural History, P.O. Box 7, FI-00014 University of Helsinki, Finland* **3** *Natural History Museum, University of Oslo, P.O. Box 1172, Blindern, 0318 Oslo, Norway* **4** *Resslova 26, Ústí nad Labem, CZ-400 01, Czech Republic*

Corresponding authors: *Karl-Henrik Larsson* (k.h.larsson@nhm.uio.no)

Academic editor: *R. Henrik Nilsson* | Received 9 August 2018 | Accepted 26 September 2018 | Published 23 October 2018

Citation: Viner I, Spirin V, Zíbarová L, Larsson K-H (2018) Additions to the taxonomy of *Lagarobasidium* and *Xylodon* (Hymenochaetales, Basidiomycota). MycoKeys 41: 65–90. https://doi.org/10.3897/mycokeys.41.28987

Abstract

Lagarobasidium is a small genus of wood-decaying basidiomycetes in the order Hymenochaetales. Molecular phylogenetic analyses have either supported *Lagarobasidium* as a distinct taxon or indicated that it should be subsumed under *Xylodon*, a genus that covers the majority of species formerly placed in *Hyphodontia*. We used sequences from the ITS and nuclear LSU regions to infer the phylogenetic position of the type species *L. detriticum*. Analyses confirm *Lagarobasidium* as a synonym of *Xylodon*. Molecular and morphological information show that the traditional concept of *L. detriticum* covers at least two species, *Xylodon detriticus* from Europe and *X. pruinosus* with known distribution in Europe and North America. Three species currently placed in *Lagarobasidium* are transferred to *Xylodon*, viz. *X. magnificus*, *X. pumilius* and *X. rickii*. Three new *Xylodon* species are described and illustrated, *X. ussuriensis* and *X. crystalliger* from East Asia and *X. attenuatus* from the Pacific Northwest America. The identity of *X. nongravis*, described from Sri Lanka, is discussed.

Keywords

Agaricomycetes, *Hyphodontia*, ITS, LSU, phylogeny

Introduction

The genus *Lagarobasidium* was introduced by Jülich (1974) for three corticioid species, *L. cymosum* (D.P.Rogers & H.S.Jacks.) Jülich, *L. nikolajevae* (Parmasto) Jülich and *L. pruinosum* (Bres.) Jülich (the generic type). These species possess prominent, thin- or slightly thick-walled cystidia, suburniform tetrasporic basidia and thick-walled basidiospores. Eriksson and Ryvarden (1976) concluded that *L. pruinosum* is a later synonym of *Peniophora detritica* Bourdot (Bourdot 1910), which prompted Jülich (1979) to move *P. detritica* to *Lagarobasidium*. At present, *L. detriticum* is accepted in a wide sense, with *Hyphodontia magnacystidiata* Lindsey & Gilb., *H. nikolajevae* Parmasto and *Odontia pruinosa* Bres. as synonyms (http://www.mycobank.org [accessed 07 May 2018]).

Controversies over the taxonomic position of *Peniophora detritica* emerged during the last decades. In modern morphology-based systems, it was first attributed to *Hyphodontia* J. Erikss., mainly due to hyphal characters and the shape of basidia (Eriksson 1958, Langer 1994). A second solution was introduced by Eriksson and Ryvarden (1976) who stressed the shape of cystidia and the thick-walled cyanophilous basidiospores and placed the species in *Hypochnicium*. The third option and the one chosen by Jülich (1974), was to place *P. detritica* in a genus of its own (Jülich 1974, 1979, Hjortstam and Ryvarden 2009).

Larsson et al. (2006) used the nrLSU and 5.8S genes for a phylogenetic analysis of Hymenochaetales and recovered *Peniophora detritica* nested in a fairly well-supported clade that also included several species usually classified in *Hyphodontia*. This result supported the original opinion on relationships introduced by Eriksson (1958) but also showed that *Hyphodontia* sensu Eriksson was polyphyletic. The clade with *Peniophora detritica.* recovered by Larsson et al. (2006), was later identified as *Xylodon*, type species *X. quercinus*, a genus that now covers the majority of species earlier referred to *Hyphodontia* (Hjortstam and Ryvarden 2009). On the other hand, Dueñas et al. (2009) studied sequences from the ITS region and concluded that molecular information supported recognition of the separate genus *Lagarobasidium*. These same ITS sequences have been used by several subsequent researchers, who therefore maintained *Lagarobasidium* separate from *Hyphodontia* sensu lato (Yurchenko and Wu 2014, Riebesehl et al. 2015, Chen et al. 2016, Chen et al. 2017, Kan et al. 2017, Riebesehl and Langer 2017, Yurchenko et al. 2017, Chen et al. 2018).

In the present study, we revise the *Lagarobasidium detriticum* complex based on morphological and molecular methods. We propose to consider *Lagarobasidium* as a later synonym of *Xylodon* and to restore *Odontia pruinosa* as an independent species. In addition, we describe three new *Xylodon* species and make five new combinations.

Materials and methods

Morphological methods

Type material and specimens from herbaria H, S, O, GB, BPI, TAAM and BAFC were studied. Herbarium abbreviations are given according to Index Herbariorum (Thiers).

Microscopic methods are described in Miettinen et al. (2006). All measurements were made in Cotton Blue (CB, Merck 1275) with phase contrast illumination (1250×). The following abbreviations are used in microscopic descriptions: L – mean spore length; W – mean spore width; Q – mean L/W ratio; n – number of spores (hyphae, basidia) measured per number of specimens. We excluded 5% of measurements from each end of the range representing variation of basidiospores and cystidia. Excluded extreme values are given in parentheses when they differ substantially from the lower or higher 95% percentile.

DNA extraction and sequencing

For DNA extraction we used either the standard CTAB protocol (Griffith and Shaw 1998) or DNeasy Plant Mini kit (Qiagen, Hilden, Germany). Primers ITS1F (Gardes and Bruns 1993), ITS4 (White et al. 1990) and LR21 (Hopple and Vilgalys 1999) were used to amplify the internal transcribed spacers 1 and 2 and the 5.8S gene. LR0R, LR5 (Moncalvo et al. 2002) and LR7 (Hopple and Vilgalys 1999) were used to amplify 28S large ribosomal subunit. Polymerase chain reaction (PCR) products were purified with the Cleanup Standard kit (Evrogen Ltd, Moscow, Russia) or QIAquick PCR purification kit (Qiagen, Hilden, Germany). Sequencing reactions were performed either by the Evrogen company (Moscow, Russia) following the BigDye terminator protocol (ABI Prism) on an Applied Biosystems 3730 xl automatic sequencer (Applied Biosystems, CA, USA) with primers ITS1F and ITS4 or with an external service provided by Macrogen (South Korea) using primers ITS1, ITS4, CTB6 (http://plantbio.berkeley.edu/~bruns/), LR5 and LR3R (Hopple and Vilgalys 1999).

Phylogenetic analyses

DNA sequences were edited in Geneious (Biomatters Ltd, Auckland, New Zealand) or in Sequencher 5.2.4 (Gene Codes Co., Ann Arbor, MI, USA) and deposited in GenBank (Table 1). We compiled two sequence datasets. The first one contains full ITS sequences from 83 specimens. The second dataset includes ITS and nLSU sequences from 24 specimens and is a subset of the taxa in the ITS-only dataset. In both datasets, *Hastodontia hastata* (Litsch.) Hjortstam & Ryvarden (Hymenochaetales) was included as outgroup (Larsson et al. 2006). We generated 13 ITS and 6 nLSU sequences for this study; other sequences used in the analyses were downloaded from GenBank (Benson et al. 2018) or UNITE (Kõljalg et al. 2013) (Table 1). Alignments were calculated through MAFFT 7.407 online server (https://mafft.cbrc.jp/alignment/server/) using the L-INS-I strategy (Katoh et al. 2017) and then manually adjusted. The alignments are deposited in TreeBASE (http://purl.org/phylo/treebase/phylows/study/TB2:S23057).

We inferred phylogenetic trees with maximum likelihood (ML), maximum parsimony (MP) and Bayesian Inference (BI) but provide only the last one since all trees show congruity of the phylogenetic signal. Substitution models were determined with the aid of TOPALi 2.5 (Milne et al. 2008) based on Bayesian information criterion

Table 1. Specimens and GenBank and UNITE accession numbers for DNA sequences used in this study.

Species	Specimen voucher	GenBank or UNITE accession numbers for ITS	GenBank or UNITE accession numbers for LSU	Reference
Hastodontia hastata (Litsch.) Hjortstam & Ryvarden	Larsson 14646	MH638232	MH638232	this study
Lyomyces allantosporus Riebesehl, Yurchenko & E. Langer	FR-0249548, Holotype	KY800397	KY795963	Yurchenko et al. (2017)
Lyomyces crustosus (Pers.) P. Karst.	Larsson 11731	DQ873614	DQ873614	Larsson et al. (2006)
Lyomyces erastii (Saaren. & Kotir.) Hjortstam & Ryvarden	MA-Fungi 34,336	JX857800		Yurchenko et al. (2017)
Lyomyces griseliniae (G. Cunn.) Riebesehl & E. Langer	Larsson 12971	DQ873651		Larsson et al. (2006)
Lyomyces mascarensis Riebesehl, Yurchenko & E. Langer	KAS-GEL4833, Holotype	KY800399	KY795964	Yurchenko et al. (2017)
Lyomyces microfasciculatus (Yurchenko & Sheng H. Wu) Riebesehl & E. Langer	TNM F24757, Holotype	JN129976		Yurchenko and Wu (2014)
Lyomyces organensis Yurchenko & Riebesehl	MSK7247, Holotype	KY800403	KY795967	Yurchenko et al. (2017)
Lyomyces orientalis Riebesehl, Yurchenko & E. Langer	KAS-GEL3400	DQ340326	DQ340353	Yurchenko et al. (2017)
Lyomyces pruni (Lasch) Riebesehl & E. Langer	Ryberg 021018	DQ873624	DQ873625	Larsson et al. (2006)
Lyomyces sambuci (Pers.) P. Karst.	KAS-GEL2414	KY800398		Yurchenko et al. (2017)
	KAS-JR7	KY800402	KY795966	Yurchenko et al. (2017)
Lyomyces vietnamensis (Yurchenko & Sheng H. Wu) Riebesehl & E. Langer	TNM F973, Holotype	JX175044		Yurchenko and Wu (2014)
Palifer verecundus (G. Cunn.) Stalpers & P.K. Buchanan	Larsson 12261	DQ873642		Larsson et al. (2006)
Xylodon apacheriensis (Gilb. & Canf.) Hjortstam & Ryvarden	Canfield 180, Holotype	KY081800		Riebesehl and Langer (2017)
Xylodon asperus (Fr.) Hjortstam & Ryvarden	H6013167	UDB031926		Unpublished
	KG Nilsson s. n.	DQ873606	DQ873607	Larsson et al. (2006)
	UC2023169	KP814365		Riebesehl and Langer (2017)
Xylodon astrocystidiatus (Yurchenko & Sheng H. Wu) Riebesehl, Yurchenko & E. Langer	Wu 9211-71	JN129972	JN129973	Yurchenko and Wu (2014)
Xylodon attenuatus Spirin & Viner	Spirin 8775, Holotype	MH324476		this study
Xylodon borealis (Kotir. & Saaren.) Hjortstam & Ryvarden	Spirin 9416	MH317760	MH638259	this study
	TU115575	UDB016473		Unpublished
	UC2022850	KP814307		Riebesehl and Langer (2017)
	KUN2352	MH307753	MH638263	this study
	TU115495	UDB016350		Unpublished
	TU124171	UDB028164		Unpublished
Xylodon bubalinus (Min Wang, Yuan Y. Chen & B.K. Cui) C.C. Chen & Sheng H. Wu	Cui 12887	KY290982		Wang and Chen (2017)
Xylodon chinensis (C.C. Chen & Sheng H. Wu) C.C. Chen & Sheng H. Wu	Wu 1307-42	KX857802		Chen et al. (2017)
	Wu 1407-105, Holotype	KX857804		Chen et al. (2017)
Xylodon crystalliger Viner	KUN2312, Holotype	MH324477		this study
Xylodon detriticus (Bourdot) Viner & Spirin	Zíbarová 30.10.17	MH320793	MH651372	this study
	Zíbarová 26.05.17	MH320794	MH638264	this study
Xylodon flaviporus (Berk. & M.A. Curtis ex Cooke) Riebesehl & E. Langer	ICMP13836	AF145585		Paulus et al. (2000)
Xylodon hastifer (Hjortstam & Ryvarden) Hjortstam & Ryvarden	Ryvarden 19767, Holotype	KY081801		Riebesehl and Langer (2017)

Species	Specimen voucher	GenBank or UNITE accession numbers for ITS	GenBank or UNITE accession numbers for LSU	Reference
Xylodon heterocystidiatus (H.X. Xiong, Y.C. Dai & Sheng H. Wu) Riebesehl, Yurchenko & E. Langer	Wu 9209-27	JX175045		Yurchenko and Wu (2014)
Xylodon lenis Hjortstam & Ryvarden	Wu 0808-32	JX175043	KX857820	Yurchenko and Wu (2014)
	Wu 890714-3, Holotype	KY081802		Riebesehl and Langer (2017)
Xylodon mollissimus (L.W. Zhou) C.C. Chen & Sheng H. Wu	LWZ20160318-3, Holotype	KY007517		Kan et al. (2017)
Xylodon nespori (Bres.) Hjortstam & Ryvarden	B Nordén 030915	DQ873622		Larsson et al. (2006)
	GEL3158	DQ340310	DQ340346	Riebesehl and Langer (2017)
	GEL3290	DQ340309		Unpublished
	GEL3302	DQ340308		Unpublished
	GEL3309	DQ340307	DQ340345	Yurchenko and Wu (2014)
Xylodon niemelaei (Sheng H. Wu) Hjortstam & Ryvarden	GC 1508-146	KX857798		Chen et al. (2017)
	GEL4998	EU583422	DQ340348	Riebesehl and Langer (2017)
	Wu 1010-62	KX857799		Chen et al. (2017)
Xylodon nongravis (Lloyd) Spirin & Viner	CHWC1506-2	KX857800		Chen et al. (2017)
	Dai 11686	KT989968		Chen et al. (2017)
	GC1412-22	KX857801		Chen et al. (2017)
	Spirin 5763	MH324469	MH656724	this study
Xylodon nothofagi (G. Cunn.) Hjortstam & Ryvarden	PDD:91630	GQ411524		Fukami et al. (2010)
Xylodon ovisporus (Corner) Riebesehl & E. Langer	ICMP13837	AF145587		Paulus et al. (2000)
	KUC20130725-29	KJ668513	KJ668365	Jang et al. (2016)
	Wu 0809-76	KX857803		Chen et al. (2017)
Xylodon paradoxus (Schrad.) Chevall.	FCUG 1517	AF145572		Paulus et al. (2000)
	FCUG 2425	AF145571		Paulus et al. (2000)
	Miettinen 7978	FN907912	FN907912	Miettinen and Larsson (2011)
Xylodon pruinosus (Bres.) Spirin & Viner	Larsson 14653	UDB024816		Unpublished
	Spirin 2877	MH332700		this study
	UC2023108	KP814412		Rosenthal et al. (2017)
Xylodon pseudotropicus (C.L. Zhao, B.K. Cui & Y.C. Dai) Riebesehl, Yurchenko & E. Langer	Dai 10768, Holotype	KF917543		Zhao et al. (2014)
Xylodon quercinus (Pers.) Gray	Kotiranta 27060	MH320792		this study
	Larsson 11076	KT361633	AY586678	Ariyawansa et al. (2015)
	Miettinen 15050,1	KT361632		Ariyawansa et al. (2015)
	Spirin 8565	MH316007		this study
	Spirin 8840	MH320791		this study
Xylodon raduloides (Pers.) Riebesehl & E. Langer	Dai 12631	KT203307	KT203328	Moncalvo et al. (2002)
	ICMP13833	AF145580		Paulus et al. (2000)
Xylodon ramicida Spirin & Miettinen	Spirin 7664, Holotype	KT361634		Ariyawansa et al. (2015)
Xylodon reticulatus (C.C. Chen & Sheng H. Wu) C.C. Chen & Sheng H. Wu	GC 1512-1	KX857808		Chen et al. (2017)
	Wu 1109-178, Holotype	KX857805		Chen et al. (2017)
Xylodon rhizomorphus (C.L. Zhao, B.K. Cui & Y.C. Dai) Riebesehl, Yurchenko & E. Langer	Dai 12354	KF917544		Zhao et al. (2014)

Species	Specimen voucher	GenBank or UNITE accession numbers for ITS	GenBank or UNITE accession numbers for LSU	Reference
Xylodon rimosissimus (Peck) Hjortstam & Ryvarden	CFMR:DLL2011-081	KJ140600		Brazee et al. (2014)
	Ryberg 021031	DQ873627	DQ873628	Larsson et al. (2006)
	UC2022842	KP814311		Rosenthal et al. (2017)
	UC2023109	KP814414		Rosenthal et al. (2017)
	UC2023147	KP814193		Rosenthal et al. (2017)
	UC2023148	KP814194		Rosenthal et al. (2017)
Xylodon spathulatus (Schrad.) Kuntze	GEL2690	KY081803		Riebesehl and Langer (2017)
	Larsson 7085	KY081804		Riebesehl and Langer (2017)
Xylodon subtropicus (C.C. Chen & Sheng H. Wu) C.C. Chen & Sheng H. Wu	Wu 1508-2	KX857806		Chen et al. (2017)
	Wu 9806-105, Holotype	KX857807		Chen et al. (2017)
Xylodon ussuriensis Viner	KUN1989, Holotype	MH324468		this study

(BIC). GTR + G (nst = 6, rates = gamma) were the best-fit models for the whole ITS region in the ITS dataset as well as in the ITS + nrLSU dataset. SYM + G (nst = 6, rates = gamma, statefreqpr = fixed(equal)) was the best-fit model for the nrLSU region in the ITS + nrLSU dataset. The suggested models were implemented in the Bayesian phylogenetic analyses. We performed Bayesian inference with MrBayes 3.2 (Ronquist et al. 2012). In the analyses, three parallel runs with four chains each, temp = 0.2, were run for 3 million generations. All chains converged to <0.01 average standard deviation of split frequencies. A burn-in of 25% was used in the final analyses.

Maximum-likelihood (ML) analysis was performed in RAxML 7.2.8 (Stamatakis 2006) implemented in Geneious. Following models suggested by TOPALi 2.5, we preferred to use the GTR model with gamma correction (GTRGAMMA) in ML analysis for both datasets. The bootstrapping was performed using the 'Rapid bootstrapping' algorithm with the number of bootstrap replicates set as 1000.

Maximum parsimony (MP) analysis was performed using MEGA 7 (Kumar et al. 2016). We used the Subtree-Pruning-Regrafting (SPR) algorithm using all sites. The number of bootstrap replicates was set as 1000.

Specimens examined (sequenced specimens are marked by an asterisk)

Xylodon attenuatus. USA. Washington: Clallam Co., La Push, *Pseudotsuga menziesii*, 8 Oct 2014, Spirin 8286a (H), Sol Duc, *Tsuga heterophylla*, 6 Oct 2014, Spirin 8133 (H); Jefferson Co., Hoh River, *Acer macrophyllum*, 20 Oct 2014, Spirin 8775* (H, holotype), *Tsuga heterophylla*, 20 Oct 2014, Spirin 8779 (H); Pend Oreille Co., Gypsy Meadows, *Picea engelmannii*, 17 Oct 2014, Spirin 8694* (H). Canada. British Columbia: Fraser-Fort George Reg. Dist., Mt. Robson Provincial Park, *Picea sp*., 25 Jul 2015, Spirin 8900a (H).

X. borealis. Russia. Nizhny Novgorod Reg.: Lukoyanov Dist., Panzelka, *Quercus robur* (very rotten log), 17 Aug 2015, Spirin 9416* (H).

X. brevisetus. Russia. Moscow: Losiny Ostrov Nat. Park, log of *Pinus sylvestris*, 1 Oct 2016, A.Nechaev KUN2352* (H).

X. crystalliger. Russia. Primorie: Khasan Dist., Kedrovaya Pad Nat. Res., on angiosperm wood, 25 Jul 2016, I.Viner KUN 2312* (H, holotype); ibidem 29 Jul 2017, F.Bortnicov, KUN 3347 (H).

X. detriticus. Czech Republic. Karlovarský kraj: Sokolov, Antonín mine spoil, on *Phragmites australis*, 26 May 2017, L.Zíbarová (H*); Liberecký kraj: Liberec, Uhelná, on *Calamagrostis epigejos*, 30 Oct 2017, L.Zíbarová (H*). France. Auvergne: Allier, St. Priest, on fern, 1 Sep 1909, H.Bourdot 7226 (S F204453, lectotype of *Peniophora detritica*). Italy. Lazio: Circeo Nat. Park, on *Pinus pinea* bark, 23 Oct 1984, K.H.Larsson 5496 (GB); ibidem, on fallen leaves, 24 Oct 1984, K.H.Larsson 5622 (GB); ibidem, on ferns, 24 Oct 1984, K.H.Larsson 5627 (GB).

X. magnificus. Argentina. Tierra del Fuego: Ushuaia, Estancia Moat, on *Drimys winteri*, 21 Mar 1998, A.Greslebin 1387 (GB, paratype duplicate).

X. nongravis. Russia. Khabarovsk Reg.: Khabarovsk Dist., Ulun, on *Salix schwerinii*, 25 Aug 2012, V.Spirin 5615 (H); ibidem, on *Corylus mandshurica*, 28 Aug 2012, V.Spirin 5763* (H); Primorie Reg.: Krasnoarmeiskii Dist., Melnichnoe, on *Corylus mandshurica*, 21–23 Aug 2013, V.Spirin 6218, 6260, 6281 (H). Sri Lanka. Peradeniya, on rotten branch, T.Petch (BPI US0305211, holotype of *Polyporus nongravis*).

X. pruinosus. Estonia. Ida-Virumaa: Kohtla-Järve, Pärnassaare, on *Betula pubescens*, 1 Oct 1958, E.Parmasto (TAAM, holotype of *Hyphodontia nikolajevae*). Finland. Helsinki: Veräjämäki, on *Salix caprea*, 4 Sep 2011, O.Miettinen 14651.4 (H). Germany. Nordrhein-Westfalen, on *Betula* sp., W.Brinkmann (S F204462, isolectotype of *Odontia pruinosa*). Norway. Akershus: Frogn, decaying deciduous wood, 3 Oct 2010, K.H.Larsson 14653* (O). Russia. Nizhny Novgorod Reg.: Bogorodsk Dist., Krastelikha, on *Quercus robur*, 11 Aug 2009, V.Spirin 2877* (H); Lukoyanov Dist., Panzelka, on *Populus tremula*, 19 Aug 2015, V.Spirin 9581 (H); Razino, on *Quercus robur*, 16 Aug 2015, V.Spirin 9350 (H); Srednii, on *Tilia cordata*, 18 Aug 2006, V.Spirin 2601 (H); Pavlovo Dist., Chudinovo, on *Populus tremula*, 3 Oct 2015, V.Spirin 9994 (H); Sverdlovsk Reg.: Nizhnisereginskii Dist., Olenii Ruchii Nat. Park, on *Populus tremula*, 19–20 Aug 2002, H.Kotiranta 19684b, 19687, 19715a (H). USA. New York: Franklin County, Paul Smith's, on *Populus tremuloides*, 12 Sep 1965, R.L.Gilbertson 5481 (GB, isotype of *Hyphodontia magnacystidiata*).

X. pumilius. Argentina. Chubut: Río Senguer, Lago La Plata, on *Nothofagus pumilio*, 26–28 Mar 1996, A.Greslebin 701 (GB, paratype duplicate).

X. quercinus. Canada. Alberta: Yellowhead Co., William A. Switzer Prov. Park, on *Populus tremuloides*, 24 Jul 2015, V.Spirin 8840* (H). Finland. Uusimaa: Helsinki, Veräjänmäki, on angiosperm wood, 12 Apr 2008, O.Miettinen 12409* (H). Russia. Chukotka: Anadyr, on *Alnus fruticosa*, 19 Sep 2009, H.Kotiranta 27060* (H). USA. Washington: Pend Oreille Co., Slate Creek, on *Corylus cornuta*, 15 Oct 2014. V.Spirin 8565* (H).

X. rickii. Brazil. Rio Grande do Sul: S. Salvador, 5 Apr 1944, J.Rick 20847 (O, isotype of *Odontia polycystidifera*).

X. ussuriensis. Russia. Primorie: Khasan Dist., Kedrovaya Pad Nat. Res., angiosperm wood, 24 Jul 2016, I.Viner KUN 1989* (H, holotype of *Xylodon ussuriensis*), I.Viner KUN 2103, 2186.

Results

For both datasets, the Bayesian inference returned trees with two main clades (Figures 1, 2); the largest clade is well-supported and corresponds to *Xylodon* (pp 1.0), while the other clade is unsupported and includes *Lyomyces*, the *Hyphodontia crustosa* group, *H. pruni* and *Rogersella griseliniae* (pp 0.89). Basal relationships within *Xylodon* are not resolved. *Peniophora detritica* and its allied species are nested within *Xylodon* and form a well-supported subclade together with *X. borealis* and *X. brevisetus* (Figures 1, 2). Maximum likelihood and maximum parsimony returned similar topologies and relevant support values from these analyses are indicated on nodes in Figures 1, 2.

In the ITS-only tree, three terminal branches represent new species that are described below. *Xylodon attenuatus* occurs as a sister taxon to *X. rimosissimus*; *X. crystalliger* forms a subclade with *X. astrocystidiatus*, *X. paradoxus* and *X. heterocystidiatus*; and *X. ussuriensis* is the sister taxon to *X. detriticus* and *X. pruinosus* (Figure 1).

The results allow us to introduce new species and new combinations as follows.

Xylodon attenuatus Spirin & Viner, sp. nov.

Mycobank No: MB825367
Figure 3

Type. USA. Washington: Jefferson Co., Hoh River, on *Acer macrophyllum*, 20 Oct 2014, V.Spirin 8775 (H) – ITS sequence, GenBank MH324476.

Etymology. Attenuatus (lat., adj.) – exhausted, thin.

Description. Basidiocarp effused, up to 5 cm in widest dimension. Sterile margin white, up to 1 mm wide. Hymenial surface cream-coloured, grandinioid to odontoid; projections rather regularly arranged, from 80 µm to 200 µm high, 70–90 µm broad at base, 6–8(–9) per mm. Hyphal structure monomitic, hyphae clamped, cyanophilous. Subicular hyphae densely interwoven, thin-walled, (2–)2.4–4.6 µm in diam. (n=60/6), often short-celled, the outline of these hyphae often irregular. Tramal hyphae subparallel, thin-walled, in subhymenium densely arranged, sometimes short-celled, 2.4–3.6 µm in diam. (n=62/6). Large stellate crystals 10–13.3 µm in diam. present in subiculum and trama. Cystidia originating from subhymenium, of two types: a) subcapitate or capitate cystidia, (12–)13.5–25.1(–37)×(2.7–)3.3–5(–5.5) µm (n=80/6), b) hyphoid cystidia, (14–)16–38.3(–40.8)×2.8–4.5 (n=51/6), sometimes with crystalline cap on the top; some cystidia with granular contents in CB. Basidia suburniform, 4-spored, (12.2–)14–22(–25)×(3–)3.3–4.6(–5) µm (n=61/2), slightly thick-walled at the base. Basidiospores thin-walled, ellipsoid, (3.7–)4.1–5.5(–6)×(3–)3.4–4.5(–4.9) µm (n=180/6), L=4.85, W=3.98, Q=1.22, slightly cyanophilous.

Distribution and ecology. North-western USA (Washington), on angiosperm and gymnosperm wood (fallen decorticated logs).

Remarks. *Xylodon attenuatus* bears morphological similarity to *X. borealis*, although densely arranged hyphae, star-like crystals and a regular presence of cystidia with granular contents make it easily recognisable. The crystalline caps on hyphoid cystidia are other characteristics useful for the identification of *X. attenuatus*.

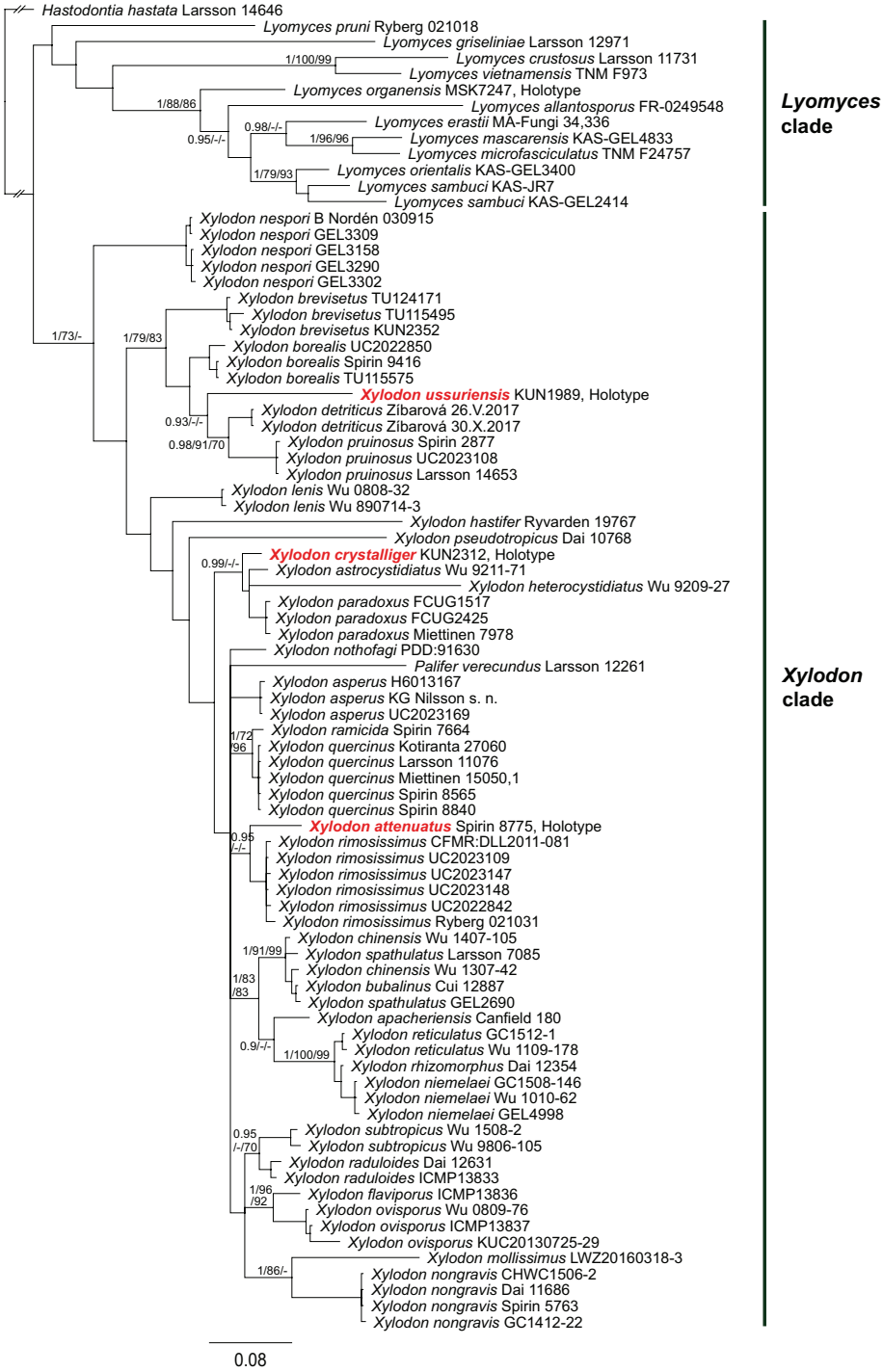

Figure 1. Phylogenetic relationships of *Xylodon* inferred from ITS sequences using Bayesian analysis. A 50% majority rule consensus phylogram. Bayesian posterior probabilities, ML bootstrap and MP bootstrap values are shown on nodes; branch lengths reflect estimated number of changes per site.

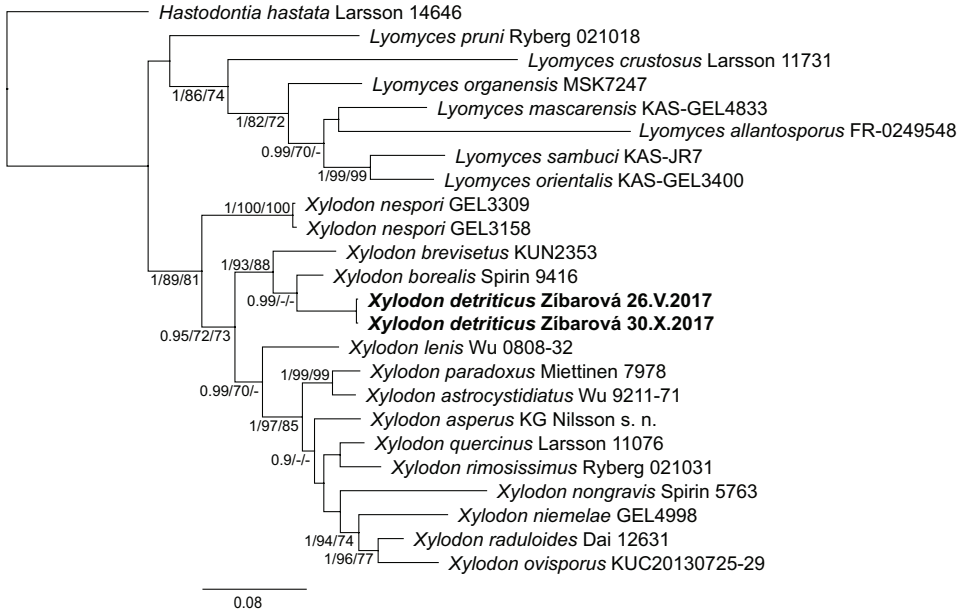

Figure 2. Phylogenetic relationships of *Xylodon* inferred from ITS and LSU sequences using Bayesian analysis. A 50% majority rule consensus phylogram. Bayesian posterior probabilities, ML bootstrap and MP bootstrap values are shown on nodes; branch lengths reflect estimated number of changes per site.

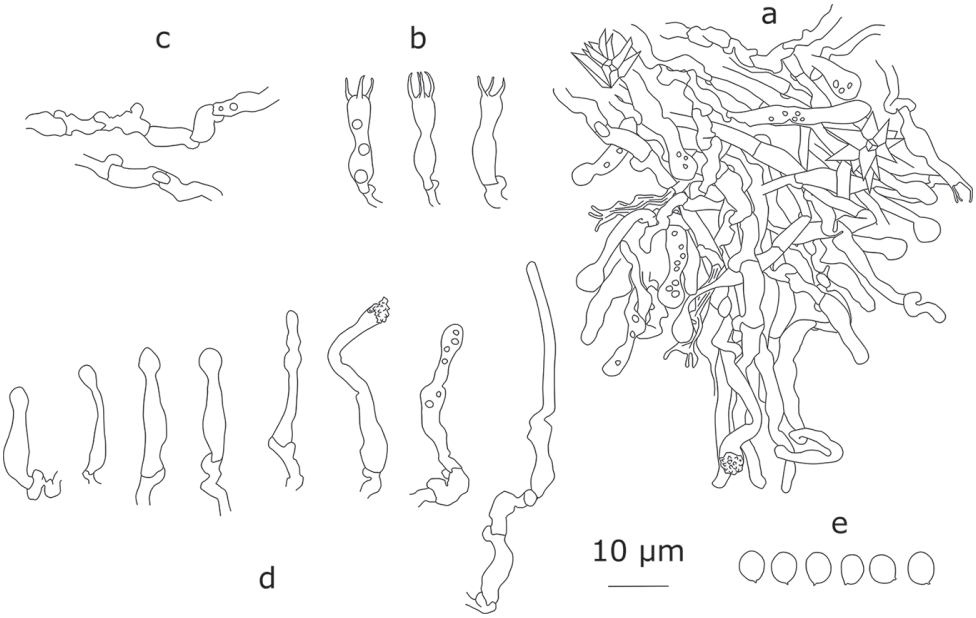

Figure 3. *Xylodon attenuatus* (holotype): **a** section through an aculeus **b** basidia **c** subhymenial short-celled hyphae **d** cystidia **e** basidiospores.

Xylodon crystalliger **Viner, sp. nov.**
Mycobank No: MB825368
Figure 4

Type. RUSSIA. Primorie: Khasan Dist., Kedrovaya Pad Nat. Res., on angiosperm wood, 25 Jul 2016, I.Viner KUN 2312 (H) – ITS sequence, GenBank MH324477.

Etymology. Crystalliger (lat., adj.) – bearing crystals.

Description. Basidiocarp effused, soft membranaceous, up to 6 cm in widest dimension. Sterile margin poorly defined, up to 0.3 mm wide. Hymenial surface white, minutely odontioid, i.e. covered by small peg-like hyphal projections up to 60–100 µm high, 60–75 µm broad at base, 10–15 per mm, with flattened

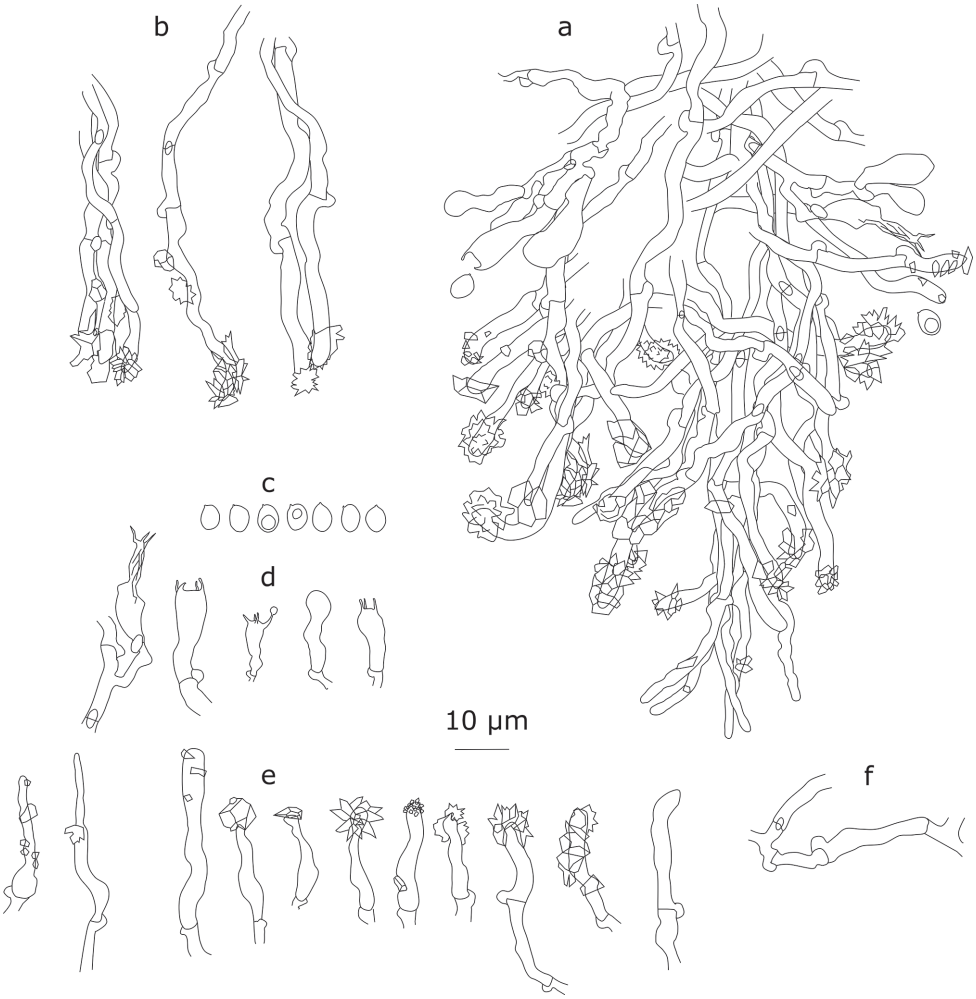

Figure 4. *Xylodon crystalliger* (holotype): **a** section through an aculeus **b** apically encrusted hyphae from aculeal tips **c** basidiospores **d** basidia **e** cystidia **f** subhymenial hyphae.

fimbriate apices. Surface between projections porulose-reticulate. Hyphal structure monomitic, hyphae clamped, faintly cyanophilous. Subicular hyphae densely interwoven, often with thickened walls, 3.2–4.4 µm in diam. (n=20/2), smooth or sparsely encrusted. Tramal hyphae subparallel, thin- to clearly thick-walled, sparsely encrusted, subhymenial hyphae densely arranged, sometimes short-celled, 2.5–3.2 µm in diam. (n=20/2), sparsely encrusted. Hyphal ends at the top of projections often strongly encrusted. Cystidia of two types: a) sparsely encrusted hyphoid cystidia at the top of projections, 21.0–29.0×2.9–4.1(–4.4) µm (n=40/2), b) subcapitate or cylindrical cystidia, of subhymenial origin, rather variable in shape and size, (11.8–)14.1–25.0(–28.0)×(2.6–)2.9–4.6(–4.8) µm (n=40/2), often heavily encrusted and rarely with a stellate crystalline cap 3.5–4.5 µm in diam. Basidia suburniform, 4-spored, 13.4–18.4(–19.0)×4.2–4.7 µm (n=20/2), slightly thick-walled at the base. Basidiospores thin-walled, elliptical, occasionally with an oil-drop, (3.1–)4.2–5.1(–5.9)×(2.4–)3.3–4.2 µm (n=60/2), L=4.66, W=3.71, Q=1.26, slightly cyanophilous.

Distribution and ecology. East Asia (Russian Far East), on decayed angiosperm logs.

Remarks. The peg-like hymenial projections and cystidia with stellate caps are characteristic for *X. crystalliger* and make it reminiscent of *Xylodon astrocystidiatus* (Yurchenko & Sheng H. Wu) Riebesehl, Yurchenko & Langer. The latter species is known from Taiwan and differs from *X. crystalliger* by having longer basidiospores and presence of constricted and bladder-like hymenial cystidia.

***Xylodon detriticus* (Bourdot) K.H. Larss., Viner & Spirin, comb. nov.**
Mycobank No: MB825366
Figures 5, 6c, 7

Basionym. *Peniophora detritica* Bourdot, Revue Scientifique du Bourbonnais et du Centre de la France 23: 13. 1910. ≡ *Lagarobasidium detriticum* (Bourdot) Jülich, Persoonia 10: 334. 1979. Type. France. Auvergne: Allier, St. Priest, fern, 1.IX.1909 Bourdot 7226 (lectotype S! [F204453], designated by Eriksson and Ryvarden 1976: 703).

Description. Basidiocarps effused, up to 5 cm in widest dimension. No differentiated margin. Hymenial surface white, smooth or warted, farinaceous. Hyphal structure monomitic, hyphae clamped, faintly cyanophilous, thin-walled. Subicular hyphae interwoven and frequently branched, (2.2–)3.0–5.9 µm in diam. (n=61/6). Tramal hyphae subparallel, subhymenial hyphae short-celled, (1.5–)1.9–3.5 µm in diam. (n=61/6). Large, rhomboid or stellate crystals abundant in trama and subiculum, 8–10.5 µm in diam. Cystidia of two types: a) large, thin-walled cystidia of subicular or tramal origin, cylindrical or clavate, rarely slightly thick-walled (wall not exceeding 1 µm thick), (30.0–)58.9–110.0(–115.0)×4.1–8.5(–9.6) µm (n=120/6), occasionally bearing 1–2 clamped septa, b) rare astrocystidia of subhymenial origin, with a stellate crystalline cap 10–23×2–3.1 µm, in some specimens difficult to find. Basidia suburniform, 4-spored,

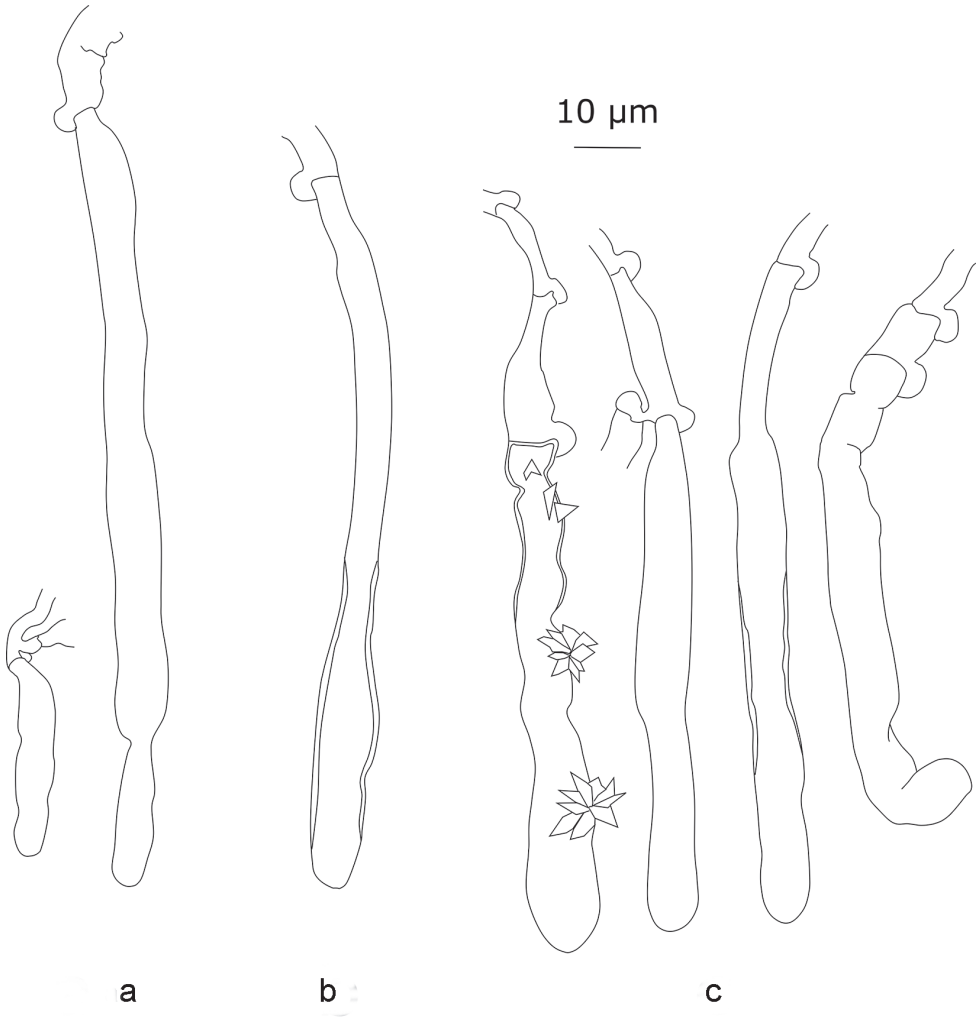

Figure 5. Cystidial elements of *Xylodon detriticus*: **a** Larsson 5496 **b** Zíbarová 26.V.2017 **c** Zíbarová 30.X.2017.

(12.2–)13.1–20.0×(3.1–)3.4–5.0 µm (n=61/6), thin-walled. Basidiospores clearly thick-walled, elliptical to broadly elliptical, usually with an oil-drop, (3.3–)4.3–5.7(–6.1)×3.2–4.1(–4.5) µm (n=190/6), L=4.92, W=3.69, Q=1.34, cyanophilous.

Distribution and ecology. Europe (Czech Republic, France, Italy), on herbaceous remnants, once collected from pine bark at the same spot where it was found on fern remains.

Remarks. Eriksson and Ryvarden (1976) selected Bourdot 7226 (in herb. S) as lectotype. They also treated *Hyphodontia nikolajevae* and *Odontia pruinosa* as synonyms. However, the type specimens of *H. nikolajevae* and *O. pruinosa* reveal small differences from the type material and other collections of *X. detriticus* studied by us. The main

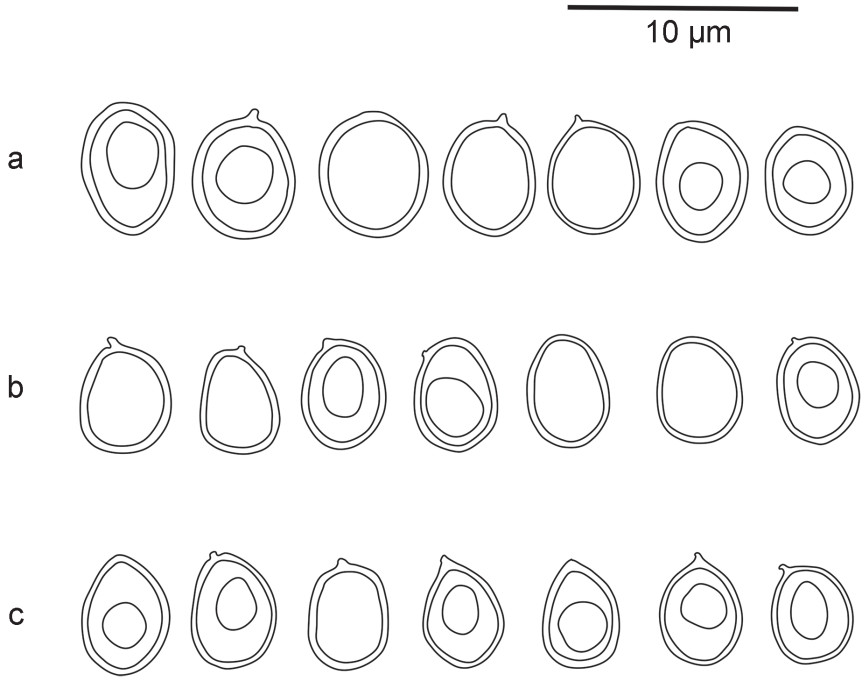

Figure 6. Basidiospores of two *Xylodon* species in CB: **a** *X. pruinosus* (Spirin 9994) **b** *X. pruinosus* (isotype of *Hyphodontia magnacystidiata*) **c** *X. detriticus* Zíbarová (26.V.2017).

Figure 7. Basidiocarp of *Xylodon detriticus* (Zíbarová 26.V.2017). Scale bar: 5 mm.

features of *X. detriticus* versus the two other taxa are narrower basidiospores (must be observed in cotton blue) and longer, narrower cystidia having no distinct intercalary inflation (Tables 2, 3, Figures 5, 6). Eriksson and Ryvarden (1976) attributed the differences in cystidia morphology between Bourdot's specimen and types of *H. nikolajevae* and *O. pruinosa* to different stages of basidiocarp development. Our investigation indicates that the differences are genetic and species specific. Differences in basidiospore size and shape are detectable in CB but not in KOH, which could explain why they have gone unnoticed in earlier studies.

Hjortstam and Ryvarden (2009) added *Hyphodontia magnacystidiata* to the synonymy of *X. detriticus*. This species is, as far as we know, only known from the type, collected on dead wood of *Populus* in New York, USA (Lindsey and Gilbertson 1977). It has an odontioid basidiocarp and its cystidia are similar to those of *X. pruinosus* (Table 3, Figures 6, 8). On the other hand, the basidiospore size is very close to *X. detriticus* (Table 2). In the absence of sequenced material, it is not possible to decide whether this is an independent species or not. Considering that the single specimen was growing on wood and that *X. detriticus* is not yet found in North America, we prefer to keep *H. magnacystidiata* as a synonym of *X. pruinosus* (see below).

Xylodon detriticus grows on ferns and grasses, developing thin farinaceous basidiocarps. The species evidently has a more southern distribution than *X. pruinosus*. Earlier reports of *X. detriticus* from woody substrates should be treated with caution and may represent *X. pruinosus* or as yet undescribed taxa.

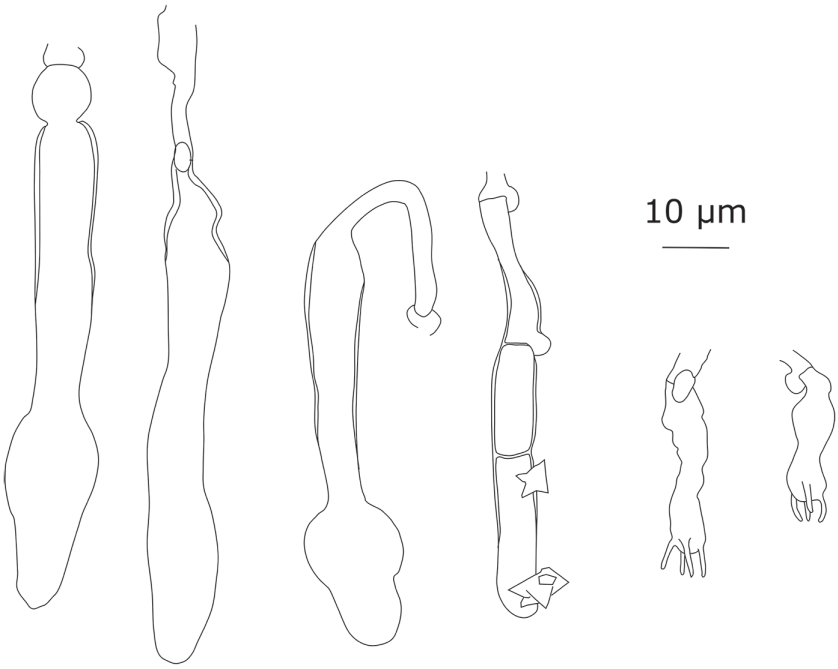

Figure 8. Cystidial elements and basidia of *Xylodon pruinosus* (isotype of *Hyphodontia magnacystidiata*).

Table 2. Spore measurements of five *Xylodon* species.

Species / specimen	L'	L	W'	W	Q'	Q	n
Xylodon attenuatus	(3.7) 4.1–5.5 (6)	4.85	(3) 3.4–4.5 (4.9)	3.98	(0.98) 1.06–1.38 (1.46)	1.22	180
Holotype	(4.3) 4.4–5.7 (5.8)	4.86	(3) 3.5–4.3 (4.7)	3.84	(1.1) 1.2–1.4 (1.5)	1.27	30
Spirin 8133	(4.4) 4.54–5.3 (5.5)	5.01	(3.2) 3.8–4.6 (4.7)	4.14	(1.06) 1.1–1.33 (1.38)	1.21	30
Spirin 8286	(4.1) 4.14–5.74 (6)	4.98	(3.1) 3.84–4.5 (4.5)	4.11	(1.02) 1.09–1.34 (1.36)	1.21	30
Spirin 8779	(4) 4–5.2 (5.4)	4.67	(3) 3.2–4.3 (4.4)	3.82	(0.98) 1.04–1.38 (1.43)	1.23	30
Spirin 8900a	(3.7) 3.95–5.25 (5.6)	4.56	(3.4) 3.4–4.35 (4.9)	3.94	(1.02) 1.02–1.29 (1.37)	1.16	30
Spirin 8964	(4.5) 4.6–5.6 (5.7)	5.02	(3.5) 3.6–4.3 (4.8)	4.04	(1.1) 1.1–1.4 (1.4)	1.25	30
Xylodon crystalliger	(3.1) 4.2–5.1 (5.9)	4.66	(2.4) 3.3–4.2 (4.3)	3.71	(1) 1.1–1.4 (1.6)	1.26	60
Holotype	(3.1) 4.2–5.1 (5.9)	4.63	(2.4) 3.1–3.8 (3.9)	3.5	(1.2) 1.2–1.5 (1.6)	1.32	30
Bortnicov KUN 3347	(4.2) 4.2–5.3 (5.5)	4.69	(3.3) 3.6–4.2 (4.3)	3.91	(1) 1.1–1.4 (1.4)	1.2	30
Xylodon detriticus	(3.3) 4.3–5.7 (6.1)	4.92	(3.1) 3.2–4.1 (4.5)	3.69	(0.7) 1.1–1.6 (1.8)	1.34	190
Lectotype	(4.2) 4.3–6 (6.1)	5.07	(3.1) 3.2–4 (4.1)	3.59	(1.2) 1.2–1.6 (1.7)	1.42	39
Larsson 5496	(3.3) 4.2–5.5 (6)	4.87	(3.1) 3.2–4.1 (4.5)	3.61	(0.7) 1.1–1.6 (1.8)	1.36	30
Larsson 5622	(4) 4.2–5.1 (5.5)	4.6	(3.3) 3.4–3.9 (4)	3.63	(1.1) 1.1–1.4 (1.5)	1.27	30
Larsson 5627	(4) 4.2–5 (5.6)	4.69	(3.3) 3.3–4.1 (4.2)	3.73	(1.1) 1.2–1.4 (1.4)	1.26	31
Zibarova 26.V.2017	(4.4) 4.7–5.8 (5.9)	5.26	(3.2) 3.3–4.2 (4.3)	3.83	(1.1) 1.2–1.6 (1.7)	1.38	30
Zibarova 30.X.2017	(4.2) 4.2–5.7 (5.9)	4.99	(3.2) 3.3–4.1 (4.2)	3.78	(1.1) 1.1–1.5 (1.7)	1.32	30
Xylodon pruinosus	(4) 4.5–5.9 (7)	5.09	(3.3) 3.7–4.8 (5.7)	4.12	(0.8) 1.1–1.4 (1.5)	1.24	192
Holotype of *Hyphodontia nikolajevae*	(4.6) 4.7–6 (7)	5.26	(3.5) 3.8–5 (5.3)	4.32	(1) 1.1–1.4 (1.4)	1.22	31
Holotype of *Odontia pruinosa*	(4) 4.1–5.7 (5.9)	4.95	(3.5) 3.6–4.5 (4.6)	4.03	(1.1) 1.1–1.4 (1.4)	1.23	40
Spirin 2877	(4.5) 4.7–6.1 (6.3)	5.28	(3.5) 3.8–5 (5.2)	4.21	(1) 1.1–1.4 (1.5)	1.26	30
Spirin 9350	(4.4) 4.7–5.7 (6.2)	5.21	(3.5) 3.8–4.8 (5.7)	4.17	(0.8) 1.1–1.4 (1.5)	1.26	31
Spirin 9581	(4.2) 4.2–5.8 (6.1)	4.99	(3.3) 3.6–4.4 (4.6)	3.98	(1) 1.1–1.4 (1.4)	1.25	30
Spirin 9994	(4.2) 4.6–5.1 (5.3)	4.89	(3.5) 3.6–4.5 (4.6)	4.04	(1.1) 1.1–1.3 (1.4)	1.21	30
Holotype of *Hyphodontia magnacystidiata*	(4) 4.3–5.5 (5.6)	4.92	(3.1) 3.1–4 (4.2)	3.68	(1.1) 1.1–1.6 (1.7)	1.35	30
Xylodon ussuriensis	(4.8) 5.1–6 (6.2)	5.48	(3.7) 3.8–4.6 (4.8)	4.21	(1.2) 1.2–1.4 (1.5)	1.3	92
Holotype	(4.9) 5.1–5.9 (6.2)	5.48	(3.7) 3.8–4.6 (4.8)	4.22	(1.2) 1.2–1.4 (1.4)	1.3	32
Viner KUN 2103	(4.8) 5–6.1 (6.2)	5.6	(3.8) 3.8–4.7 (4.7)	4.24	(1.2) 1.2–1.4 (1.5)	1.32	30
Viner KUN 2186	(5) 5–5.7 (5.8)	5.37	(3.8) 4–4.5 (4.6)	4.18	(1.2) 1.2–1.4 (1.5)	1.28	30

Xylodon magnificus (Gresl. & Rajchenb.) K.H. Larss., comb. nov.

Mycobank No: MB827074

Basionym. *Hyphodontia magnifica* Gresl. & Rajchenb., Mycologia 92: 1160. 2000.

Type. Argentina. Tierra del Fuego: Dpto. Ushuaia, Estancia Moat, on *Drimys winteri*, 21 Mar 1998, M. Rajchenberg 11370 (holotype: BAFC [50038], by original designation).

For a detailed description and illustration, see Greslebin and Rajchenberg (2000). The authors compared the new species with *Xylodon detriticus* (as *Hyphodontia detritica*) and *Hypochnicium rickii*. Our investigation of authentic material confirms the morphological similarity amongst these three species.

Table 3. Measurements of cystidial elements of *Xylodon detriticum* and *X. pruimosus*.

Species / specimen	L'	L	W'	W	n
Xylodon detriticus	(30) 58.9–110 (115)	85	(4) 4.1–8.5 (9.6)	6.3	120
Lectotype	(67) 69.9–96.7 (110)	83.8	(4) 4–9.1 (9.2)	6.5	20
Larsson 5496	(30) 45.2–108.2 (112)	81.2	(4.1) 4.3–7 (7.2)	5.7	20
Larsson 5622	(30) 45–103 (110)	82.7	(4.1) 4.3–7.5 (8.5)	5.7	20
Larsson 5627	(56) 58.7–104.6 (110)	79.1	(4.4) 4.8–8.9 (9.6)	6.4	20
Zibarova 26.V.2017	(80) 83.8–103.3 (110)	95.1	(4) 5.4–8.1 (8.5)	7.1	20
Zibarova 30.X.2017	(67) 73.7–112.2 (115)	87.7	(4) 5–7.4 (7.5)	6.3	20
Xylodon pruinosus	(35) 44–84 (107)	61.9	(4) 4.9–10.9 (12.4)	7.2	146
Holotype of *Hyphodontia nikolajevae*	(41) 43–95 (99)	64	(4) 5–12 (12)	7.7	21
Isolectotype of *Odontia pruinosa*	(43) 45.9–80.4 (107)	64	(4.6) 5.3–10.6 (12.4)	7.3	20
Spirin 2877	(35) 42.6–80 (80)	58.4	(4) 4.8–7.9 (8)	6.2	20
Spirin 9350	(41) 44.8–83.2 (86)	61.8	(4.6) 4.7–10 (10.7)	7.2	20
Spirin 9581	(49) 51.8–84.1 (86)	64.6	(4.9) 5–9 (11)	7.1	20
Spirin 9994	(45) 45.8–75.3 (81)	58.9	(5.3) 5.6–10.2 (10.8)	7.8	20
Isotype of *Hyphodontia magnacystidiata*	(48) 51–95 (104)	75.8	(4.1) 6–12 (14)	8.4	25

Xylodon nongravis (Lloyd) C.C. Chen & Sheng H. Wu, in Chen et al. 2018: 349
Figure 9

Basionym. *Polyporus nongravis* Lloyd, Mycol. Writings 6 (61): 891. 1919.
Type. Sri Lanka. Peradeniya, on rotten branch, T.Petch (holotype BPI [305211]).

Wu (2000) re-described and illustrated this poroid species as *Hyphodontia nongravis* (Lloyd) S.H. Wu. Our specimens collected in the Russian Far East fit well with his description. One of these collections (Spirin 5763) was sequenced and proved to

Figure 9. Basidiocarp of *Xylodon nongravis* (Spirin 5763). Scale bar: 5 mm.

be close to other sequences of *H. nongravis* available in GenBank. The species undoubtedly belongs to the core *Xylodon* clade (Figure 1) where it has been combined by Chen et al. (2018). However, the type specimen of *Polyporus nongravis* possesses small but clear morphological differences from our collections: in particular, wider pores (2–3 per mm in the type, 3–4 per mm in East Asian specimens) and broader tramal hyphae (4–6 µm vs. 3–4.5 µm in diam.), as well as broader, predominantly subglobose basidiospores, 3.9–4.7×3.6–4.2 µm (n=30/1), L=4.27, W=3.97, Q=1.08 (vs ovoid-ellipsoid, 4.0–5.2×3.0–4.1 µm (n=60/2), L=4.74, W=3.46, Q=1.38 in East Asian specimens). An epitype for *P. nongravis* from the *locus classicus* is needed to reintroduce this species based on modern methods and to clarify the taxonomic status of *X. nongravis* sensu East Asia.

Xylodon pruinosus **(Bres.) Spirin & Viner, comb. nov.**
Mycobank No: MB825369
Figures 6 a,b, 8, 10, 11

Basionym. *Odontia pruinosa* Bres., Annales Mycologici 18 (1–3): 43. 1920. ≡ *Lagarobasidium pruinosum* (Bres.) Jülich, Persoonia 8: 84. 1974.
Type. Germany. Nordrhein-Westfalen, Lengerich, W.Brinkmann (lectotype L [L 0053271], designated by Jülich 1974: 84).

= *Hyphodontia nikolajevae* Parmasto, Conspectus Systematis Corticiacearum: 213. 1968. Type: Estonia. Ida-Virumaa, Kohtla-Järve, Pärnassaare, on *Betula pubescens*, 1 Oct 1958, E.Parmasto (holotype: TAAM [9683], by original designation).
= *Hyphodontia magnacystidiata* Lindsey & Gilb., Mycotaxon 5: 315. 1977. Type: USA. New York, Franklin County, Paul Smith's, on *Populus tremuloides*, 12 Sep 1965, R.L.Gilbertson 5481 (holotype: BPI [266395], by original designation).

Description. Basidiocarps annual, resupinate, up to 5 cm in widest dimension. Margin poorly differentiated, pruinose. Hymenial surface greyish-white or pale cream-coloured, grandinioid to odontoid; projections rather regularly arranged, from 100 µm to 250 µm high, 80–100 µm broad at base, 6–8 per mm. Hyphal structure monomitic, hyphae clamped, faintly cyanophilous, thin-walled. Subicular hyphae interwoven and frequently branched, 2.2–4.7(–6.1) µm in diam. (n=60/6). Tramal hyphae subparallel, subhymenial hyphae short-celled, 2.0–3.5(–3.9) µm in diam. (n=60/6). Stellate crystals abundant in trama, subiculum and subhymenium, 4.4–8.3 µm in diam. Cystidia large, thin-walled, of subicular, tramal or subhymenial origin, clavate to spathuliform, often with an intercalary inflation, sometimes slightly thick-walled (wall not exceeding 1 µm thick), rarely forked, (35.0–)44.0–84.0(–107.0)×(4.0–)4.9–10.9(–12.4) µm (n=121/6), occasionally bearing 1–2 clamped septa. Basidia suburniform, 4-spored, (12.0–)14.0–20.8(–24.0)×3.4–4.2(–5.5) µm (n=60/6), thin-walled. Basidiospores clearly thick-walled, ellipsoid to broadly ellipsoid, usually with an oil-drop, (4.0–)4.5–5.9(–7.0)×(3.3–)3.7–4.8(–5.7) µm (n=192/6), L=5.09, W=4.12, Q=1.24, cyanophilous.

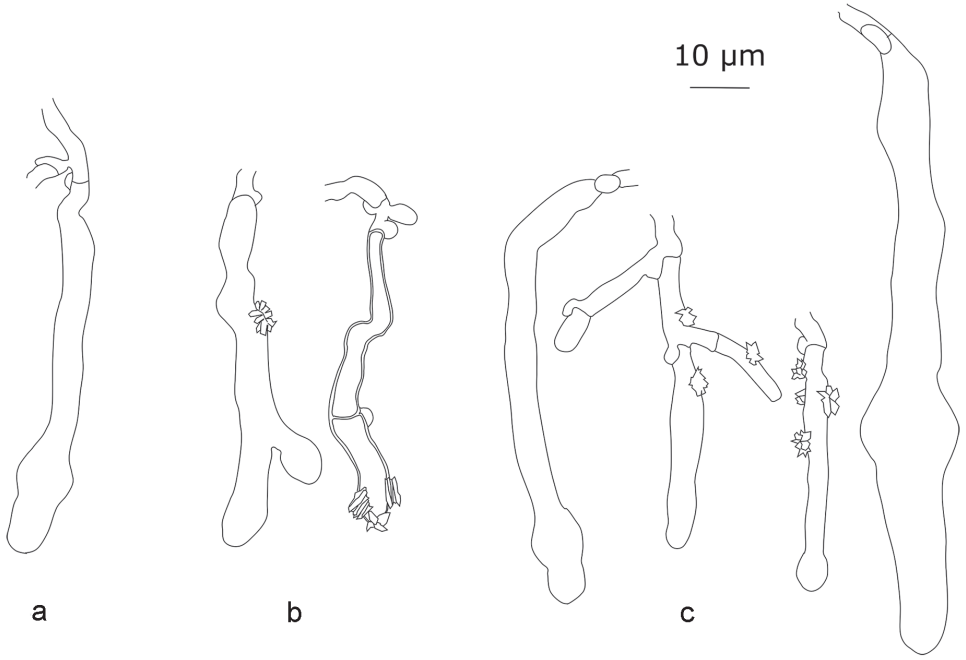

Figure 10. Cystidial elements of *Xylodon pruinosus*: **a** Spirin 9581 **b** Spirin 2877 **c** holotype of *Hyphodontia nikolajevae*.

Figure 11. Basidiocarp of *Xylodon pruinosus* (Spirin 2877). Scale bar: 5 mm.

Distribution and ecology. Europe (Estonia, Finland, Germany, Norway, Russia – up to Ural Mts.), North America, on medium-decayed wood of angiosperms.

Remarks. The type specimen of *Hyphodontia nikolajevae* Parmasto reveals no essential differences from the type and other collections of *X. pruinosus* studied by us. On average, *Xylodon pruinosus* has wider basidiospores than *X. detriticus* (Table 2).

***Xylodon pumilius* (Gresl. & Rajchenb.) K.H. Larss., comb. nov.**
Mycobank No: MB827075

Basionym. *Hyphodontia pumilia* Gresl. & Rajchenb., Mycologia 92: 1162. 2000.

Type. Argentina. Chubut. Dpto Languiñeo, Lago Engaño, on *Nothofagus pumilio*, 19 Apr 1996, A.Greslebin 650 (holotype BAFC [50031], by original designation).

For a detailed description and illustration, see Greslebin and Rajchenberg (2000). The presence of both hymenial, capitate cystidia and enclosed, tubular to moniliform cystidia with homogenous contents strongly stained by cotton blue, make this species morphologically reminiscent of *Xylodon brevisetus* and *X. tuberculatus*. *X. pumilius* differs from both by a smooth hymenium and thick-walled basidiospores.

***Xylodon rickii* (Hjortstam & Ryvarden) K.H. Larss., comb. nov.**
Mycobank No: MB827076
Figure 1

Basionym. *Hypochnicium rickii* Hjortstam & Ryvarden, Mycotaxon 15: 271. 1982. ≡ *Odontia polycystidifera* Rick, Iheringia, Sér. Bot. 5: 163. 1959. Nom. inval. (Code Art. 40.1).

Type. Brazil. S. Salvador, 5 Apr 1944, Rick 20847 (holotype PACA, by original designation).

For a description, see Hjortstam and Ryvarden (1982). Gorjón (2012) could not verify the presence of large capitate cystidia, similar to those present in *X. magnifica* and included in the original description by Hjortstam and Ryvarden (1982). We restudied the isotype in herbarium O and can confirm that these large cystidia do exist, which supports a possible position of this species close to *X. detriticus* and *X. pruinosus*.

***Xylodon ussuriensis* Viner, sp. nov.**
Mycobank No: MB825356
Figure 12

Type. RUSSIA. Primorie: Khasan Dist., Kedrovaya Pad Nat. Res., on angiosperm wood, 24 Jul 2016, I.Viner KUN 1989* (H) – ITS sequence, GenBank MH324468.

Etymology. Ussuriensis (lat., adj.) – from the river Ussuri in Russian Far East and adjacent China.

Description. Basidiocarps effused, up to 10 cm in longest dimension. Sterile margin white to pale ochraceous, floccose, up to 1 mm wide. Hymenial surface pale ochraceous, grandinioid to odontoid; projections rather regularly arranged, from 100 µm to 250 µm high, 90–110 µm broad at base, 6–8(–9) per mm. Hyphal structure monomitic, hyphae clamped, faintly cyanophilous, thin-walled. Subicular hyphae interwoven, (3.0–)3.4–6.2 µm in diam. (n=30/3). Tramal hyphae subparallel, sub-

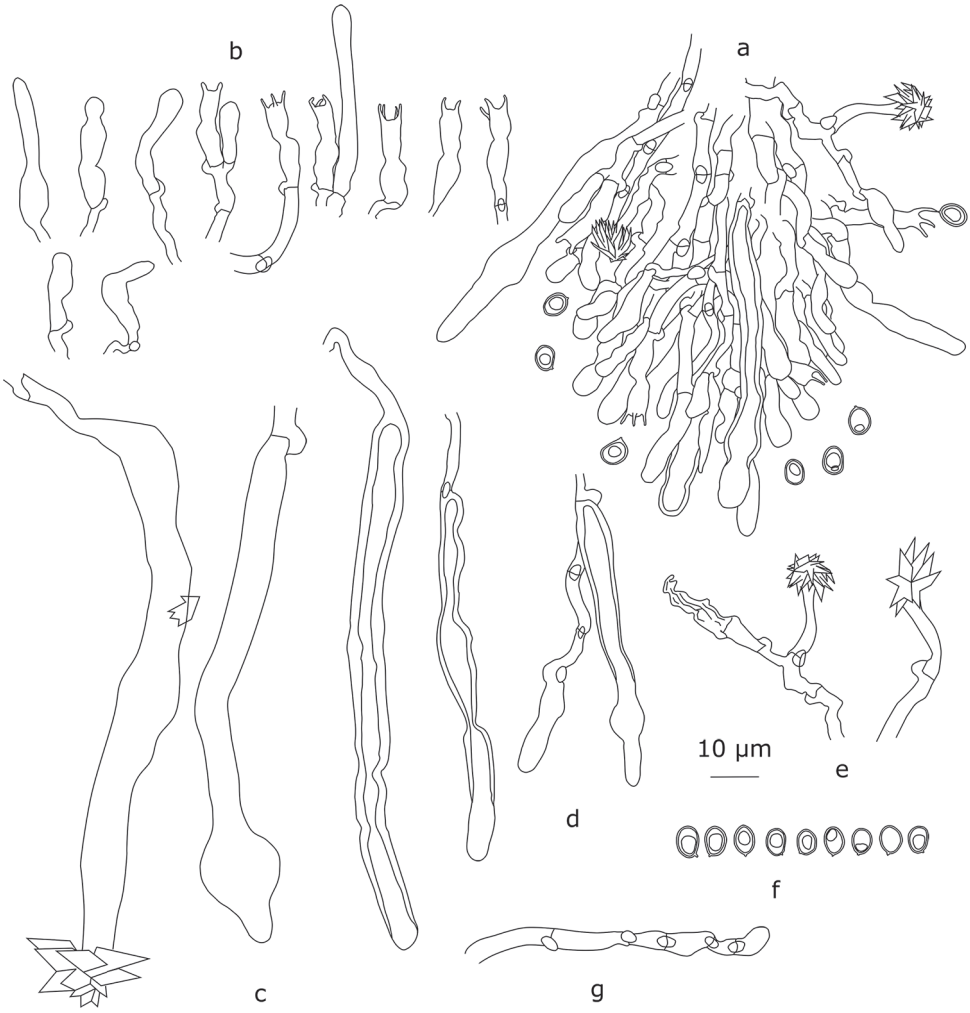

Figure 12. *Xylodon ussuriensis* (holotype): **a** section through an aculeus **b** basidia, basidioles and hymenial cystidia **c** thick- and thin-wall tramal cystidia **d** thick- and thin-wall subhymenial cystidia **e** astrocystidia **f** basidiospores **h** short-celled hyphae from aculei.

hymenial hyphae short-celled, 1.9–3.9 µm in diam. (n=30/3). Large rhomboid or stellate crystals rarely present in trama and subiculum, 10–19 µm in diam. Cystidia of three types: a) large, thin- or fairly thick-walled (wall up to 2.8 µm thick) cystidia of subicular, tramal or subhymenial origin, cylindrical, spathuliform, almost capitate or with one intercalary inflation at the upper part, (64.0–)71.0–188.9(–220.0)×(5.0–)5.7–9.4(–11.9) µm (n=30/3), often apically encrusted by large rhomboid crystals, b) astrocystidia of subhymenial origin, bearing a stellate crystalline cap 15–17×4.5–4.8 µm, sometimes rare, c) cystidia of subhymenial origin, thin-walled, varying from fusoid to cylindrical or submoniliform, rarely forked, 40.0–84.0(–92.0)×5.0–9.0(–11.4) µm (n=30/3). Basidia suburniform, 4-spored, 14.7–22.8(–24.0)×3.4–4.9 µm (n=30/3),

thin-walled. Basidiospores clearly thick-walled, ellipsoid to broadly ellipsoid, usually with an oil-drop, (4.8–)5.1–6.0×3.8–4.6 µm (n=92/3), L=5.48, W=4.21, Q=1.30, cyanophilous.

Distribution and ecology. East Asia (Russian Far East – Primorie), on decayed angiosperm wood; seemingly not rare in secondary oak-dominated forest.

Remarks. The distinctly thick-walled tubular cystidia of *X. ussuriensis* make it different from other *Lagarobasidium*-like species treated here. Subhymenial astrocystidia found in *X. ussuriensis* are also present in some specimens of *X. detriticus* although they are apparently rare in the latter species.

Discussion

Our study confirms the results from Larsson et al. (2006) and Larsson (2007) that *Peniophora detritica* clusters with *Xylodon quercinus*, the type species of *Xylodon*. Here we also show that *Peniophora pruinosa*, the type of *Lagarobasidium*, belongs in *Xylodon* and is a sister species to *X. detriticus*. This contradicts the results published by Dueñas et al. (2009) who came to the conclusion that *Lagarobasidium* was a genus separate from *Hyphodontia* sensu lato. As support for that result, they published ITS sequences of *L. detriticum* and the new species *L. calongei* (GenBank FM876211 and FM876212, respectively). However, at least the sequence of *L. detriticum* (FM876211) seems to be based on a misidentification or contamination during the laboratory process. This sequence is 100% identical to several sequences of *Hyphoderma roseocremeum*, a species belonging in Polyporales (e.g. UNITE database UDB031922).

Blasting FM876212 against public sequence databases does not return any reliable results, which, if the sequence is correct, suggests that the species does not belong in *Xylodon*. Remaining species referred to *Lagarobasidium* and not already discussed include *L. cymosum* (D.P. Rogers & H.S. Jacks.) Jülich and *L. subdetriticum* (S.S. Rattan) J. Kaur & Dhingra. The former has been placed in *Hypochnicium* because of the thick-walled basidiospores but numerous subulate cystidia makes it a deviating element in that genus. Only access to sequence information can disclose its relationships. *Lagarobasidium subdetriticum* was originally described in *Hyphodontia* and should be retained in that genus also when the genus is taken in a restricted sense (Hjortstam and Ryvarden 2009).

For the phylogenetic analyses of *Hyphodontia* sensu lato, only nuclear ribosomal genes have so far been applied. All published results confirm that *Hyphodontia* sensu lato is polyphyletic and that most species can be referred to one of three clusters, viz *Hyphodontia* sensu stricto, the *Kneiffiella* cluster and the *Xylodon* cluster (including *Lyomyces*). Within these clusters the relationships are not well resolved when the ribosomal genes are the sole source for genetic information. On such detailed level, analyses become highly sensitive to sampling and outgroup choice. It is clear that both a wider sampling and more markers must be included in analyses in order to establish a stable genus level classification for all species that have been referred to *Hyphodontia* in a wide sense.

Acknowledgements

Curators of herbaria S, GB, BPI, TAAM and BAFC sent us types and other herbarium specimens used in the present study. The first author is grateful to the Kedrovaya Pad Nature Reserve staff, in particular, to Gleb Sedash and Dina Matyukhina. We also thank Eugeny Antonov and Fedor Bortnicov (Moscow) for their assistance during fieldwork and providing valuable fungal collections.

References

Ariyawansa HA, Hyde KD, Jayasiri SC et al. (2015) Fungal diversity notes 111–252—taxonomic and phylogenetic contributions to fungal taxa. Fungal Diversity 75(1): 27–274. https://doi.org/10.1007/s13225-015-0346-5

Benson DA, Cavanaugh M, Clark K, Karsch-Mizrachi I, Ostell J, Pruitt KD, Sayers EW (2018) GenBank. Nucleic Acids Research 46(D1): D41–D47. https://doi.org/10.1093/nar/gkx1094

Bourdot H (1910) Corticiés nouveaux de la flore mycologique de France III. Revue Scientifique du Bourbonnais et du Centre de la France 23: 1–15.

Brazee NJ, Lindner DL, D'Amato AW, Fraver S, Forrester JA, Mladenoff DJ (2014) Disturbance and diversity of wood-inhabiting fungi: effects of canopy gaps and downed woody debris. Biodiversity and Conservation 23: 2155–2172. https://doi.org/10.1007/s10531-014-0710-x

Chen CC, Wu SH, Chen CY (2017) Three new species of *Hyphodontia* s.l. (Basidiomycota) with poroid or raduloid hymenophore. Mycological Progress 16: 553–564. https://doi.org/10.1007/s11557-017-1286-0

Chen CC, Wu SH, Chen CY (2018) *Xylodon subflaviporus* sp. nov. (Hymenochaetales, Basidiomycota) from East Asia. Mycoscience 59: 343–352. https://doi.org/10.1016/j.myc.2017.12.004

Chen JJ, Zhou LW, Ji XH, Zhao CL (2016) *Hyphodontia dimitica* and *H. subefibulata* spp. nov. (Schizoporaceae, Hymenochaetales) from southern China based on morphological and molecular characters. Phytotaxa 269(1): 1–13. https://doi.org/10.11646/phytotaxa.269.1.1

Dueñas M, Telleria MT, Melo I, Martín MP (2009) *Lagarobasidium calongei* (Aphyllophorales, Basidiomycota), a new species of corticioid fungi from Azores Islands. Anales del Jardín Botánico de Madrid 66(S1): 41–46. https://doi.org/10.3989/ajbm.2230

Eriksson J (1958) Studies in the Heterobasidiomycetes and Homobasidiomycetes — Aphyllophorales of Muddus National Park in North Sweden. Symbolae Botanicae Upsalienses. 16(1): 1–172.

Eriksson J, Ryvarden L (1976) The Corticiaceae of North Europe volume 4, *Hyphodermella–Mycoacia*. Fungiflora, Oslo, 1–338.

Fukami T, Dickie IA, Paula Wilkie J et al. (2010) Assembly history dictates ecosystem functioning: evidence from wood decomposer communities. Ecology Letters 13(6): 675–684. https://doi.org/10.1111/j.1461-0248.2010.01465.x

Gardes M, Bruns TD (1993) ITS primers with enhanced specificity for basidiomycetes – application to the identification of mycorrhizae and rusts. Molecular Ecology 2(2): 113–118. https://doi.org/10.1111/j.1365-294X.1993.tb00005.x

Gorjón SP (2012) Some species of *Hyphodontia* s.l. with encrusted cystidial elements. Mycosphere 3(4): 464–474. https://doi.org/10.5943/mycosphere/3/4/10

Greslebin AG, Rajchenberg M (2000) The genus *Hyphodontia* in the Patagonian Andes forests of Argentina. Mycologia 92: 1155–1165. https://doi.org/10.2307/3761483

Griffith GW, Shaw DS (1998) Polymorphisms in *Phytophthora infestans*: Four mitochondrial haplotypes are detected after PCR amplification of DNA from pure cultures or from host lesions. Applied and Environmental Microbiology 64(10): 4007–4014.

Hjortstam K, Ryvarden L (1982) Studies in tropical Corticiaceae (Basidiomycetes) IV. Type studies of taxa described by J. Rick. Mycotaxon 15: 261–276.

Hjortstam K, Ryvarden L (2009) A checklist of names in *Hyphodontia* sensu stricto-sensu lato and *Schizopora* with new combinations in *Lagarobasidium*, *Lyomyces*, *Kneiffiella*, *Schizopora*, and *Xylodon*. Synopsis Fungorum 26: 33–55.

Hopple JS Jr, Vilgalys R (1999) Phylogenetic relationships in the mushroom genus *Coprinus* and dark-spored allies based on sequence data from the nuclear gene coding for the large ribosomal subunit RNA: divergent domains, outgroups, and monophyly. Molecular Phylogenetics and Evolution 13: 1–19. https://doi.org/10.1006/mpev.1999.0634

Jang Y, Jang S, Lee J, Lee H, Lim YW, Kim C, Kim JJ (2016) Diversity of wood-inhabiting polyporoid and corticioid fungi in Odaesan National Park, Korea. Mycobiology 44(4): 217–236. https://doi.org/10.5941/MYCO.2016.44.4.217

Jülich W (1974) The genera of the Hyphodermoideae (Corticiaceae). Persoonia 8(1): 59–97

Jülich W (1979) Studies in resupinate basidiomycetes VI. On some new taxa. Persoonia 10(3): 325–336.

Kan YH, Qin WM, Zhou LW (2017) *Hyphodontia mollissima* sp. nov. (Schizoporaceae, Hymenochaetales) from Hainan, southern China. Mycoscience 58(4): 297–301. https://doi.org/10.1016/j.myc.2017.04.003

Katoh K, Rozewicki J, Yamada KD (2017) MAFFT online service: multiple sequence alignment, interactive sequence choice and visualization. Briefings in Bioinformatics: bbx108. https://doi.org/10.1093/bib/bbx108

Kõljalg U, Nilsson RH, Abarenkov K, Tedersoo L, Taylor AF, Bahram M, Bates ST, Bruns TD, Bengtsson-Palme J, Callaghan TM, Douglas B, Drenkhan T, Eberhardt U, Dueñas M, Grebenc T, Griffith GW, Hartmann M, Kirk PM, Kohout P, Larsson E, Lindahl BD, Lücking R, Martín MP, Matheny PB, Nguyen NH, Niskanen T, Oja J, Peay KG, Peintner U, Peterson M, Põldmaa K, Saag L, Saar I, Schüßler A, Scott JA, Senés C, Smith ME, Suija A, Taylor DL, Telleria MT, Weiss M, Larsson KH (2013) Towards a unified paradigm for sequence-based identification of fungi. Molecular Ecology 22: 5271–5277. https://doi.org/10.1111/mec.12481

Kumar S, Stecher G, Tamura K (2016) MEGA7: Molecular Evolutionary Genetics Analysis Version 7.0 for Bigger Datasets. Molecular Biology and Evolution 33(7): 1870–1874. https://doi.org/10.1093/molbev/msw054

Langer E (1994) Die Gattung *Hyphodontia* John Eriksson. Bibliotheca Mycologica 154: 1–298

Larsson KH (2007) Re-thinking the classification of corticioid fungi. Mycological Research 111: 1040–1063. https://doi.org/10.1016/j.mycres.2007.08.001

Larsson KH, Parmasto E, Fischer M, Langer E, Nakasone KK, Redhead SA (2006) Hymenochaetales: a molecular phylogeny for the hymenochaetoid clade. Mycologia 98(6): 926–936. https://doi.org/10.1080/15572536.2006.11832622

Lindsey JP, Gilbertson RL (1977) New species of corticioid fungi on quaking aspen. Mycotaxon 5: 311–319.

Miettinen O, Larsson KH (2011) *Sidera*, a new genus in Hymenochaetales with poroid and hydnoid species. Mycological Progress 10(2): 131–141. https://doi.org/10.1007/s11557-010-0682-5

Miettinen O, Niemelä T, Spirin W (2006) Northern *Antrodiella* species: the identity of *A. semisupina* and type studies of related taxa. Mycotaxon 96: 211–239.

Milne I, Lindner D, Bayer M, Husmeier D, McGuire G, Marshall DF, Wright F (2008) TOPALi v2: a rich graphical interface for evolutionary analyses of multiple alignments on HPC clusters and multi-core desktops. Bioinformatics 25(1): 126–127. https://doi.org/10.1093/bioinformatics/btn575

Moncalvo JM, Vilgalys R, Redhead SA, Johnson JE, James TY, Aime MC, Hofstetter V, Verduin SJ, Larsson E, Baroni TJ (2002) One hundred and seventeen clades of euagarics. Molecular Phylogenetics and Evolution 23: 357–400. https://doi.org/10.1016/S1055-7903(02)00027-1

Paulus B, Hallenberg N, Buchanan PK, Chambers GK (2000) A phylogenetic study of the genus *Schizopora* (Basidiomycota) based on ITS DNA sequences. Mycological Research 104(10): 1155–1163. https://doi.org/10.1017/S0953756200002720

Riebesehl J, Langer E (2017) *Hyphodontia* s.l. (Hymenochaetales, Basidiomycota): 35 new combinations and new keys to all 120 current species. Mycological Progress 16(6): 637–666. https://doi.org/10.1007/s11557-017-1299-8

Riebesehl J, Langer EJ, Ordynets A, Striegel MM, Witzany C (2015) *Hyphodontia borbonica*, a new species from La Réunion. Mycological Progress 14: 104. https://doi.org/10.1007/s11557-015-1126-z

Ronquist F, Teslenko M, Van Der Mark P, Ayres DL, Darling A, Höhna S, Larget B, Liu L, Suchard M, Huelsenbeck JP (2012) MrBayes 3.2: Efficient Bayesian Phylogenetic Inference and Model Choice Across a Large Model Space. Systematic Biology 61: 539–542. https://doi.org/10.1093/sysbio/sys029

Rosenthal LM, Larsson KH, Branco S, Chung JA, Glassman SI, Liao HL, Peay KG, Smith DP, Talbot JM, Taylor JW, Vellinga EC, Vilgalys R, Bruns TD (2017) Survey of corticioid fungi in North American pinaceous forests reveals hyperdiversity, underpopulated sequence databases, and species that are potentially ectomycorrhizal. Mycologia 109: 115–127. https://doi.org/10.1080/00275514.2017.1281677

Stamatakis A (2006) Raxml-vi-hpc: maximum likelihood-based phylogenetic analyses with thousands of taxa and mixed models. Bioinformatics 22: 2688–2690. https://doi.org/10.1093/bioinformatics/btl446

Thiers B (continuously updated) Index Herbariorum: a global directory of public herbaria and associated staff. New York Botanical Garden's Virtual herbarium. http://sweetgum.nybg.org/ih [accessed 29 March 2018]

Wang M, Chen YY (2017) Phylogeny and taxonomy of the genus *Hyphodontia* (Hymenochaetales, Basidiomycota) in China. Phytotaxa 309(1): 45–54. https://doi.org/10.11646/phytotaxa.309.1.4

White TJ, Bruns TD, Lee SB, Taylor JW (1990) Amplification and direct sequencing of fungal ribosomal RNA genes for phylogenetics. In: Innis MA, Gelfand DH, Sninsky JJ, White TJ (Eds) PCR protocols: a guide to methods and applications. Academic Press, New York, 315–322. https://doi.org/10.1016/B978-0-12-372180-8.50042-1

Wu SH (2000) Studies on *Schizopora flavipora* s. l., with special emphasis on specimens from Taiwan. Mycotaxon 76: 51–66.

Yurchenko E, Riebesehl J, Langer E (2017) Clarification of *Lyomyces sambuci* complex with the descriptions of four new species. Mycological Progress 16(9): 865–876. https://doi.org/10.1007/s11557-017-1321-1

Yurchenko E, Wu SH (2014) Three new species of *Hyphodontia* with peg-like hyphal aggregations. Mycological Progress 13(3): 533–545.https://doi.org/10.1007/s11557-013-0935-1

Zhao CL, Cui BK, Dai YC (2014) Morphological and molecular identification of two new species of *Hyphodontia* (Schizoporaceae, Hymenochaetales) from southern China. Cryptogamie Mycologie 35(1): 87–97. https://doi.org/10.7872/crym.v35.iss1.2014.87

MycoKeys 41: 91–106 (2018)
doi: 10.3897/mycokeys.41.29070
http://mycokeys.pensoft.net

RESEARCH ARTICLE

A peer-reviewed open-access journal
MycoKeys
Launched to accelerate biodiversity research

Three new species of *Phanerochaete* (Polyporales, Basidiomycota)

Sheng-Hua Wu[1,2], Che-Chih Chen[2], Chia-Ling Wei[1]

1 *Department of Biology, National Museum of Natural Science, Taichung 40419, Taiwan* **2** *Department of Plant Pathology, National Chung Hsing University, Taichung 40227, Taiwan*

Corresponding author: *Sheng-Hua Wu* (shwu@mail.nmns.edu.tw)

Academic editor: *Bao-Kai Cui* | Received 14 August 2018 | Accepted 1 October 2018 | Published 26 October 2018

Citation: Wu S-H, Chen C-C, Wei C-L (2018) Three new species of *Phanerochaete* (Polyporales, Basidiomycota). MycoKeys 41: 91–106. https://doi.org/10.3897/mycokeys.41.29070

Abstract

Phanerochaete canobrunnea, *P. cystidiata* and *P. fusca* are presented as new species, supported by morphological studies and two sets of phylogenetic analyses. The 5.8S+nuc 28S+*rpb1* dataset shows the generic placement of the three species within the phlebioid clade of Polyporales. The ITS+nuc 28S dataset displays relationships for the new taxa within *Phanerochaete* s.s. *Phanerochaete canobrunnea* grew on angiosperm branches in subtropical Taiwan and is characterised by greyish brown hymenial surface, brown generative hyphae and skeletal hyphae and absence of cystidia. *Phanerochaete cystidiata* grew on angiosperm branches above 1000 m in montane Taiwan and SW Yunnan Province of China and is characterised by cream to yellowish hymenial surface and more or less encrusted leptocystidia. *Phanerochaete fusca* grew on angiosperm branches at 1700 m in Hubei Province of China and is characterised by dark brown hymenial surface, leptocystidia, brown subicular hyphae and colourless to brownish basidiospores.

Keywords

China, corticioid fungi, multi-marker phylogeny, Phanerochaetaceae, Taiwan

Introduction

The genus *Phanerochaete* P. Karst., typified by *P. alnea* (Fr.) P. Karst., belongs to the Polyporales of the Basidiomycota and encompasses, when taken in a broad sense (Eriksson et al. 1978; Burdsall 1985; Wu 1990), over 150 names (Index Fungorum 2018). *Phanerochaete* spp. are typically recognised by its membranaceous, effuse, smooth hymenial surface (some are tuberculate, odontioid-hydnoid or merulioid-poroid), mostly mono-

mitic hyphal system, simple-septate generative hyphae or with rare clamp connections in the subiculum, clavate basidia and ellipsoid to cylindrical, thin-walled and smooth basidiospores, which are inamyloid and non-dextrinoid. *Phanerochaete* is widely distributed and occurs on twigs, branches or trunks of angiosperms or gymnosperms, causing white rot in wood.

Phanerochaete recently has been shown to be a polyphyletic group, containing members placed throughout the phlebioid clade of Polyporales (Binder et al. 2005; Wu et al. 2010; Floudas and Hibbett 2015; Miettinen et al. 2016; Justo et al. 2017). *Phanerochaete* s.l. comprises some segregate genera: *Efibula* Sheng H. Wu, *Hydnophlebia* Parmasto, *Phaeophlebiopsis* Floudas & Hibbett, *Phlebiopsis* Jülich, *Rhizochaete* Gresl., Nakasone & Rajchenb. and *Scopuloides* (Massee) Höhn. & Litsch. (Burdsall 1985; Wu 1990; Greslebin et al. 2004; Wu et al. 2010; Floudas and Hibbett 2015).

The field survey of the corticioid fungi from Taiwan and mainland China conducted in 2014, 2015 and 2017, have revealed three new species of *Phanerochaete* s.s. presented herein, based on morphological and phylogenetic evidence.

Materials and methods

Morphological studies

Voucher specimens are deposited at the herbarium of National Museum of Natural Science of ROC (TNM). We used three mounting media for microscopic studies: 5% potassium hydroxide (KOH) with 1% phloxine was used for observation and measurements; Melzer's reagent (IKI) was utilised to determine amyloidity and dextrinoidity and Cotton blue (CB) was utilised to check cyanophily. A standard method of measurement for microscopic characters follows Wu (1990). Below abbreviations were used when presenting statistic measurements of basidiospores: L = mean basidiospore length, W = mean basidiospore width, Q = variation in L/W ratio, n = number of measured spores. The terminology of microscopic characters followed Wu (1990).

DNA extraction and sequencing

Dried specimens or mycelia were first ground into a fine powder using liquid nitrogen and a TissueLyser II (Qiagen, Hilden, Germany). DNA was then extracted using the Plant Genomic DNA Extraction Miniprep System (Viogene-Biotek Corp., New Taipei, Taiwan) according to the manufacturer's instructions. The rDNA ITS1-5.8S-ITS2 (ITS) was amplified using primer pairs ITS1/ITS4 (White et al. 1990). The D1-D2 domain of nuc 28S rDNA (nuc 28S) was amplified using primer pair LR0R/LR5 (http://www2.clarku.edu/faculty/dhibbett/Protocols_Folder/Primers/Primers.pdf).

RNA polymerase II largest subunit (*rpb1*) was amplified using the primer pair RPB1-Af/RPB1-Cr (Stiller and Hall 1997; Matheny et al. 2002). Both RPB1-2.1f and RPB1-2.2f were used as alternative primers to pair with RPB1-Cr (Frøslev et al. 2005). The PCR protocols for ITS, nuc 28S and *rpb1* followed Wu et al. (2018). PCR products were directly purified and sequenced by the MB Mission Biotech Company (Taipei, Taiwan). We determined the identity and accuracy of newly obtained sequences by comparing them to sequences in GenBank and assembled them using BioEdit (Hall 1999). Newly obtained sequences were then submitted to GenBank (https://www.ncbi.nlm.nih.gov/genbank/; Table 1).

Phylogenetic analyses

We included two datasets for phylogenetic analyses. The 5.8S+nuc 28S+*rpb1* was compiled for inferring generic classification of target species within the phlebioid clade of Polyporales. The ITS+nuc 28S was compiled for getting better resolutions on species level within *Phanerochaete* s.s. The selection of strains and species consulted Wu et al. (2010), Floudas and Hibbett (2015), Volobuev et al. (2015), Liu and He (2016), Miettinen et al. (2016) and Wu et al. (2018). MAFFT v. 7 was used to align sequences of each marker with default settings (Katoh and Standley 2013). The resulting alignments were manually adjusted in MEGA 7 (Kumar et al. 2016). *Hyphoderma litschaueri* (Burt) J. Erikss. & Å. Strid and *H. mutatum* (Peck) Donk, were chosen as the outgroup in the 3-marker dataset. *Phlebiopsis gigantea* (Fr.) Jülich was chosen as the outgroup in the 2-marker dataset. Final datasets were deposited at TreeBASE (submission ID 23083).

For both datasets, Maximum Likelihood (ML) and Bayesian Inference (BI) analyses were performed, respectively, using RAxML BlackBox (Stamatakis et al. 2014) and MrBayes v. 3.2.6 (Ronquist et al. 2012) at the CIPRES Science Gateway (Miller et al. 2010; http://www.phylo.org/). For BI analysis, jModeltest 2.1.10 (Darriba et al. 2012) was first carried out to determine the best-fit substitution model for each marker based on Akaike Information Criterion (AIC). The GTR+I+G was used as the substitution model for the entire alignment of the 3-marker dataset, while, for the 2-marker dataset, the HKY+I+G and the GTR+I+G were used for the alignments of ITS and nuc 28S, respectively. The parameters for BI analyses were as follows: ngen = 10000000, samplefreq = 100, nchains = 4, nst = 6 for GTR, nst = 2 for HKY, rates = invgamma, burn-in = 25000. Fifty percent majority-rule consensus phylograms with posterior probability values (PP) were obtained when the average standard deviation of split frequencies was below 0.001. For ML analysis, the best-scoring tree with values of bootstrap (BS) was constructed using the GTR model with one hundred rapid bootstrap inferences. Gaps were regarded as missing data. Phylograms were visualised and edited by TreeGraph 2 (Stöver and Müller 2010) and Adobe Illustrator (Adobe Systems, Inc).

Table 1. Species and sequences used in the phylogenetic analyses. Newly generated sequences are shown in bold.

Taxon	Strain/Specimen	ITS (contains 5.8S)	nuc 28S	*rpb1*
Bjerkandera adusta	HHB-12826-Sp	KP134983	KP135198	KP134784
Byssomerulius corium	FP-102382	KP135007	KP135230	KP134802
Candelabrochaete africana	FP-102987-Sp	KP135294	KP135199	KP134872
Ceraceomyces serpens	HHB-15692-Sp	KP135031	KP135200	KP134785
Ceriporia alachuana	FP-103881-Sp	KP135341	KP135201	KP134845
Ceriporia purpurea	KKN-223-Sp	KP135044	KP135203	KP134788
Efibula americana	FP-102165	KP135016	AY684165	AY864873
Emmia lacerata	FP-55521-T	KP135024	KP135202	KP134805
Gloeoporus pannocinctus	L-15726-Sp	KP135060	KP135214	KP134867
Hydnophlebia chrysorhiza	FD-282	KP135338	KP135217	KP134848
Hyphoderma litschaueri	FP-101740-Sp	KP135295	KP135219	KP134868
Hyphoderma mutatum	HHB-15479-Sp	KP135296	KP135221	KP134870
Hyphodermella rosae	FP-150552	KP134978	KP135223	KP134823
Meruliopsis alnbostramineus	HHB-10729	KP135051	KP135229	KP134787
Phaeophlebiopsis peniophoroides	FP-150577	KP135417	KP135273	KP134813
Phanerochaete aculeata	Wu 880701-2	–	GQ470636	–
Phanerochaete affinis	KHL11839	EU118652	EU118652	–
Phanerochaete alnea	OM8110	KP135171	–	–
Phanerochaete arizonica	RLG-10248-Sp	KP135170	KP135239	KP134830
Phanerochaete australis	HHB-7105-Sp	KP135081	KP135240	KP134840
Phanerochaete bambusicola	Wu 0707-2	MF399404	MF399395	LC314324
Phanerochaete brunnea	He1873	KX212220	KX212224	–
Phanerochaete burtii	HHB-4618	KP135117	KP135241	KP134829
Phanerochaete calotricha	Vanhanen-382	KP135107	–	KP134826
Phanerochaete canobrunnea	**CHWC 1506-17**	**LC412093**	**LC412102**	–
	CHWC 1506-39	**LC412094**	**LC412103**	–
	CHWC 1506-66	**LC412095**	**LC412104**	–
Phanerochaete carnosa	HHB-9195-Sp	KP135129	KP135242	KP134831
Phanerochaete chrysosporium	HHB-6251-Sp	KP135094	KP135246	KP134842
Phanerochaete citrinosanguinea	FP-105385	KP135100	KP135234	KP134824
Phanerochaete concrescens	LE < RUS>:287,008	KP994375	–	–
Phanerochaete cumulodentata	H:6,033,465	LN833868	–	–
	VL212	JF440574	–	–
Phanerochaete cystidiata	**GC 1708-358**	**LC412096**	**LC412101**	**LC412107**
	Wu 1708-326	**LC412097**	**LC412100**	**LC412108**
Phanerochaete ericina	HHB-2288	KP135167	KP135247	KP134834
Phanerochaete exilis	HHB-6988	KP135001	KP135236	KP134799
Phanerochaete fusca	**Wu 1409-161**	**LC412098**	**LC412105**	**LC412109**
	Wu 1409-163	**LC412099**	**LC412106**	**LC412110**
Phanerochaete incarnata	WEI 16-078	MF399407	MF399398	LC314327
Phanerochaete krikophora	HHB-5796-Sp	KP135164	KP135268	KP134837
Phanerochaete laevis	HHB-15519-Sp	KP135149	KP135249	KP134836
Phanerochaete livescens	FD-106	KP135070	KP135253	KP134841
Phanerochaete magnoliae	HHB-9829-Sp	KP135089	KP135237	KP134838
Phanerochaete odontoidea	Wu 9310-8	MF399408	MF399399	LC314328

Taxon	Strain/Specimen	ITS (contains 5.8S)	nuc 28S	*rpb1*
Phanerochaete porostereoides	He1902	KX212217	KX212221	–
	He1908	KX212218	KX212222	–
Phanerochaete pseudomagnoliae	PP-25	KP135091	KP135250	KP134839
Phanerochaete pseudosanguinea	FD-244	KP135098	KP135251	KP134827
Phanerochaete rhodella	FD-18	KP135187	KP135258	KP134832
Phanerochaete robusta	Wu 1109-69	MF399409	MF399400	LC314329
Phanerochaete sacchari	Wu 880313-6	–	GQ470654	–
Phanerochaete sanguinea	HHB-7524	KP135101	KP135244	KP134825
Phanerochaete sanguineocarnosa	FD-359	KP135122	KP135245	KP134828
Phanerochaete sordida	FD-241	KP135136	KP135252	KP134833
Phanerochaete stereoides	VPCI207312	KF291012	–	–
	Wu 9708-118	–	GQ470661	–
Phanerochaete subceracea	FP-105974-R	KP135162	KP135255	KP134835
Phanerochaete subodontoidea	Wu 0106-35	MF399411	MF399402	LC314331
Phanerochaete taiwaniana	Wu 0112-13	MF399412	MF399403	LC314332
Phanerochaete thailandica	2015_07	MF467737	–	–
Phanerochaete velutina	Kotiranta21402	KP135179	–	–
Phlebia centrifuga	HHB-9239-Sp	KP135380	KP135262	KP134844
Phlebia chrysocreas	HHB-6333-Sp	KP135358	KP135263	KP134861
Phlebia fuscoatra	HHB-10782-Sp	KP135365	KP135265	KP134857
Phlebia radiata	AFTOL-484	AY854087	AF287885	AY864881
Phlebia uda	FP-101544-Sp	KP135361	KP135232	KP134859
Phlebiopsis gigantea	FP-70857-Sp	KP135390	KP135272	KP134821
Pirex concentricus	OSC-41587	KP134984	KP135275	KP134843
Rhizochaete radicata	FD-123	KP135407	KP135279	KP134816
Scopuloides rimosa	HHB-7042	KP135350	KP135282	KP134853
Terana caerulea	FP-104073	KP134980	KP135276	KP134865

Results

Phylogenetic analyses

The 5.8S+nuc 28S+*rpb1* dataset consisted of 58 sequences of 2481 characters including gaps, of which 931 sites were parsimony informative. The ITS+nuc 28S dataset consisted of 45 sequences of 2199 characters including gaps, of which 220 sites were parsimony informative. Topologies of phylogenetic trees of each dataset inferred from BI and ML methods were similar and, thus, only ML trees were shown (Figs 1, 2). In the 3-marker analyses (Fig. 1), three main subclades of the phlebioid clade of Polyporales, annotated as three families, Irpicaceae, Meruliaceae and Phanerochaetaceae, could be recognised in the ingroup (BS = 75–97%, PP = 1). Sequences of three new species were nested within the lineage of *Phanerochaete* s.s. of Phanerochaetaceae (BS = 100%, PP = 1). In the 2-marker analyses (Fig. 2), sequences of each of three new species formed well-supported monophyletic group (BS = 97–100%, PP = 1). *Phanerochaete canobrunnea, P. cystidiata* and *P. fusca* were allied to *P. thailandica* Kout & Sádlíková, *P. ericina* (Bourdot) J. Erikss. & Ryvarden and *P. porostereoides* S.L. Liu & S.H. He, respectively, based on available sequences.

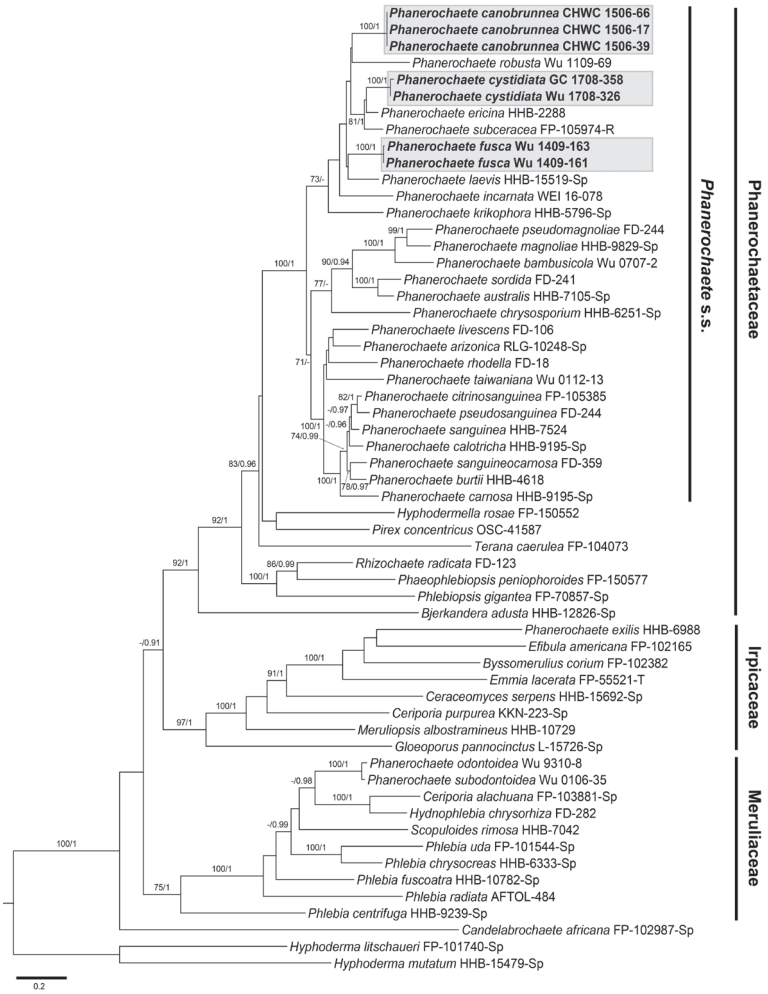

Figure 1. Phylogram inferred from Maximum likelihood analysis of the concatenated 5.8S+nuc 28S+*rpb1* dataset of representative taxa in the phlebioid clade of Polyporales. Branches are labelled with Maximum likelihood bootstrap values ≥70% and Bayesian posterior probabilities ≥0.9. Studied taxa are shaded with greyish boxes. Scale bar = substitutions per site.

Taxonomy

Phanerochaete canobrunnea **Sheng H. Wu, C.C. Chen & C.L. Wei, sp. nov.**
MycoBank No: 827411
Figs 3A, 4

Diagnosis. *Phanerochaete canobrunnea* is recognised by brown generative hyphae and brown skeletal hyphae, in combination with absence of cystidia.

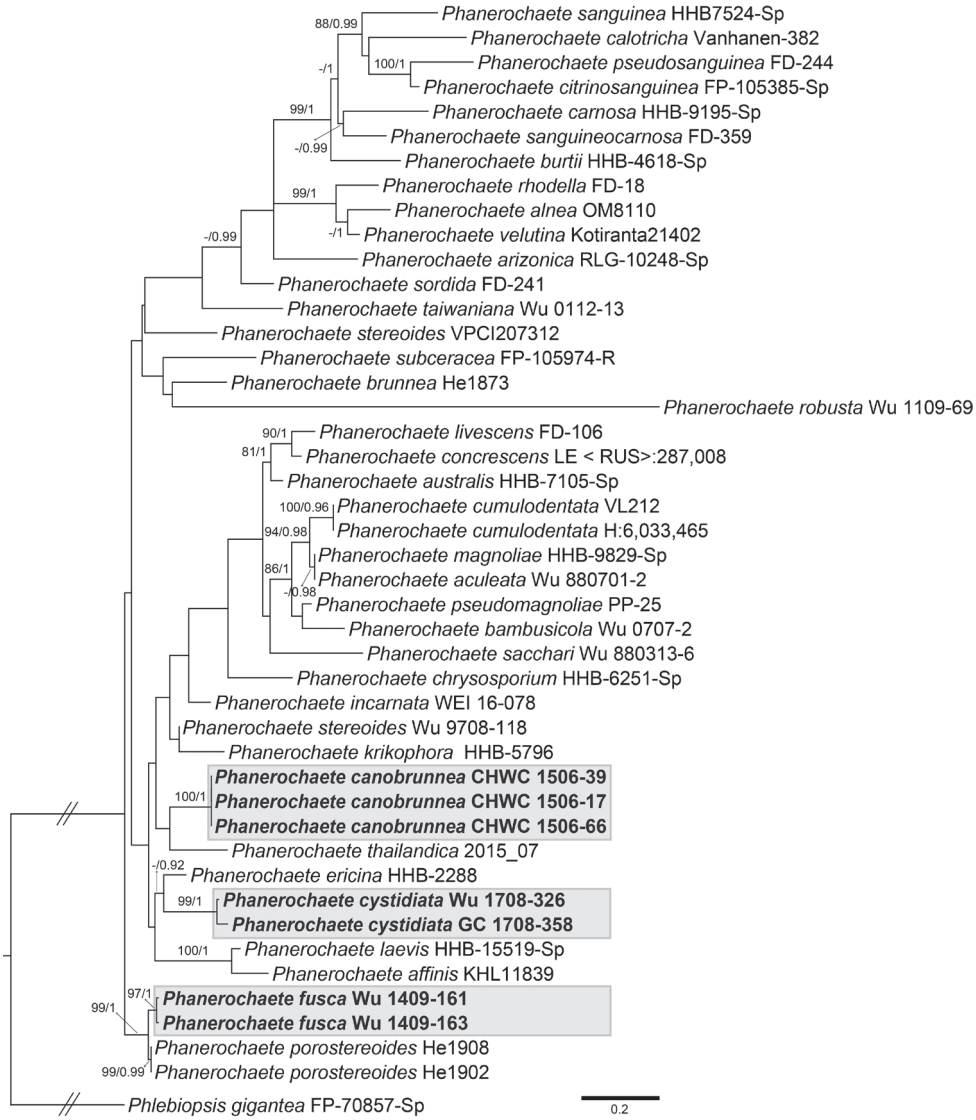

Figure 2. Phylogram inferred from Maximum likelihood analysis of the concatenated ITS+nuc 28S dataset of taxa in *Phanerochaete* s.s. Nodes are labelled with Maximum likelihood bootstrap values ≥70% and Bayesian Posterior probabilities ≥0.9. Studied taxa studied are shaded with greyish boxes. Scale bar = substitutions per site.

Holotype. TAIWAN. Nantou County: Yuchih Township, Lienhuachih, 23°55'N, 120°53'E, 715 m alt., on angiosperm branch, coll. W.C. Chen, C.C. Chen & C.L. Wei, 23 Jun 2015, *CHWC 1506-17* (TNM F0029207).

Etymology. From canus+brunneus (= greyish-brown), referring to the colour of the hymenial surface.

Figure 3. Basidiomes. **A** *Phanerochaete canobrunnea* (holotype, *CHWC 1506-17*) **B** *P. cystidiata* (holotype, *GC 1708-358*) **C** *P. fusca* (holotype, *Wu 1409-161*). Scale bar:1cm.

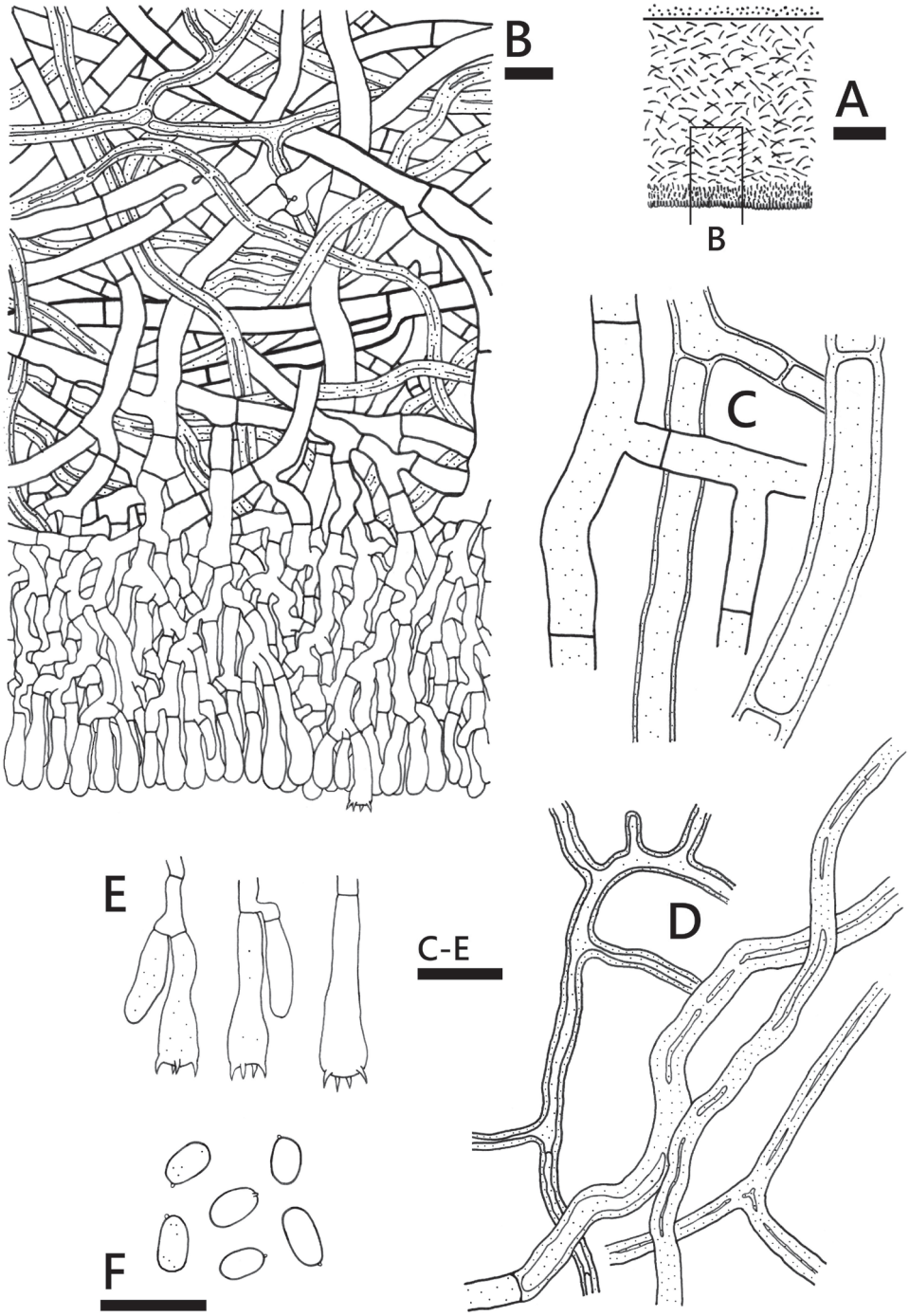

Figure 4. *Phanerochaete canobrunnea* (holotype, *CHWC 1506-17*) **A** profile of basidiome section **B** lower part of basidiome section **C** generative hyphae **D** skeletal hyphae **E** basidia **F** basidiospores. Scale bars: 100 µm (**A**); 10 µm (**B–F**).

Description. Basidiome resupinate, effuse, loosely adnate, membranaceous, 250–500 µm thick in section. Hymenial surface pale greyish-brown, slightly darkening in KOH, smooth, sometimes cracked; margin concolorous or brownish, slightly fibrillose or determinate.

Hyphal system dimitic; generative hyphae mostly simple-septate, single or double clamp connections occasionally present in subiculum. Subiculum fairly uniform, with fairly loose texture, 200–400 µm thick; generative hyphae interwoven, brown, more or less straight, moderately ramified, rarely encrusted, 4–9 (–11) µm diam., thin- to thick-walled, walls up to 1.5 µm thick, anastomoses occasional; skeletal hyphae interwoven, brown, more or less straight, un-ramified or ramified, 2–5 µm diam., usually subsolid or thick-walled, walls up to 1.5 µm, adventitious septa occasionally present. Hymenial layer thickening, with dense texture, 50–100 µm thick; hyphae more or less vertical, brownish to subcolourless, 3–6 µm diam., thin-walled. Cystidia lacking. Basidia subclavate to clavate, 15–25 × 5–6 µm, 4-sterigmate. Basidiospores ellipsoid to narrowly ellipsoid, adaxially flattened, smooth, thin-walled, IKI –, CB –, mostly 4.2–5.8 × 2.5–3 µm. [(4–) 4.5–5.8 (–6) × (2.5–) 2.7–3 (–3.2) µm, L = 5.10±0.54 µm, W = 2.86±0.18 µm, Q = 1.78 (n = 30) (*CHWC 1506-17*); (4–) 4.2–5 (–5.8) × (2.3–) 2.5–2.8 (–3) µm, L = 4.63±0.42 µm, W = 2.66±0.17 µm, Q = 1.75 (n = 30) (*CHWC 1506-39*)].

Additional specimens examined (paratypes). TAIWAN. Nantou County: Yuchih Township, Lienhuachih, 23°55'N, 120°53'E, 715 m alt., on angiosperm branch, coll. W.C. Chen, C.C. Chen & C.L. Wei, 23 Jun 2015, *CHWC 1506-39* (TNM F0029217); *CHWC 1506-66* (TNM F0029236).

Distribution. Known from subtropical Taiwan.

Remarks. Amongst the few species in *Phanerochaete* having brown subicular hyphae, only *P. canobrunnea* and *P. thailandica* possess skeletal hyphae [described as "quasi-binding hyphae" in the protologue of *P. thailandica*, Sadlikova and Kout (2017)]. These two species are also closely related according to the phylogenetic analyses (Fig. 2). However, *P. thailandica* bears leptocystidia and has larger basidiospores (7–8 × 4–4.5 µm) (Sadlikova and Kout 2017). *Phanerochaete brunnea* Sheng H. Wu resembles *P. canobrunnea* in lacking cystidia and having similar basidiospores, but its hyphal system is monomitic (Wu 1990). These two species are phylogenetically not closely related (Fig. 2).

Phanerochaete cystidiata **Sheng H. Wu, C.C. Chen & C.L. Wei, sp. nov.**

MycoBank No: 827412
Figs 3B, 5

Diagnosis. *Phanerochaete cystidiata* is characterised by having a fibrillose margin of the basidiome and apically narrow or tapering leptocystidia that are more or less encrusted. Additionally, crystal masses are present in the hymenial layer.

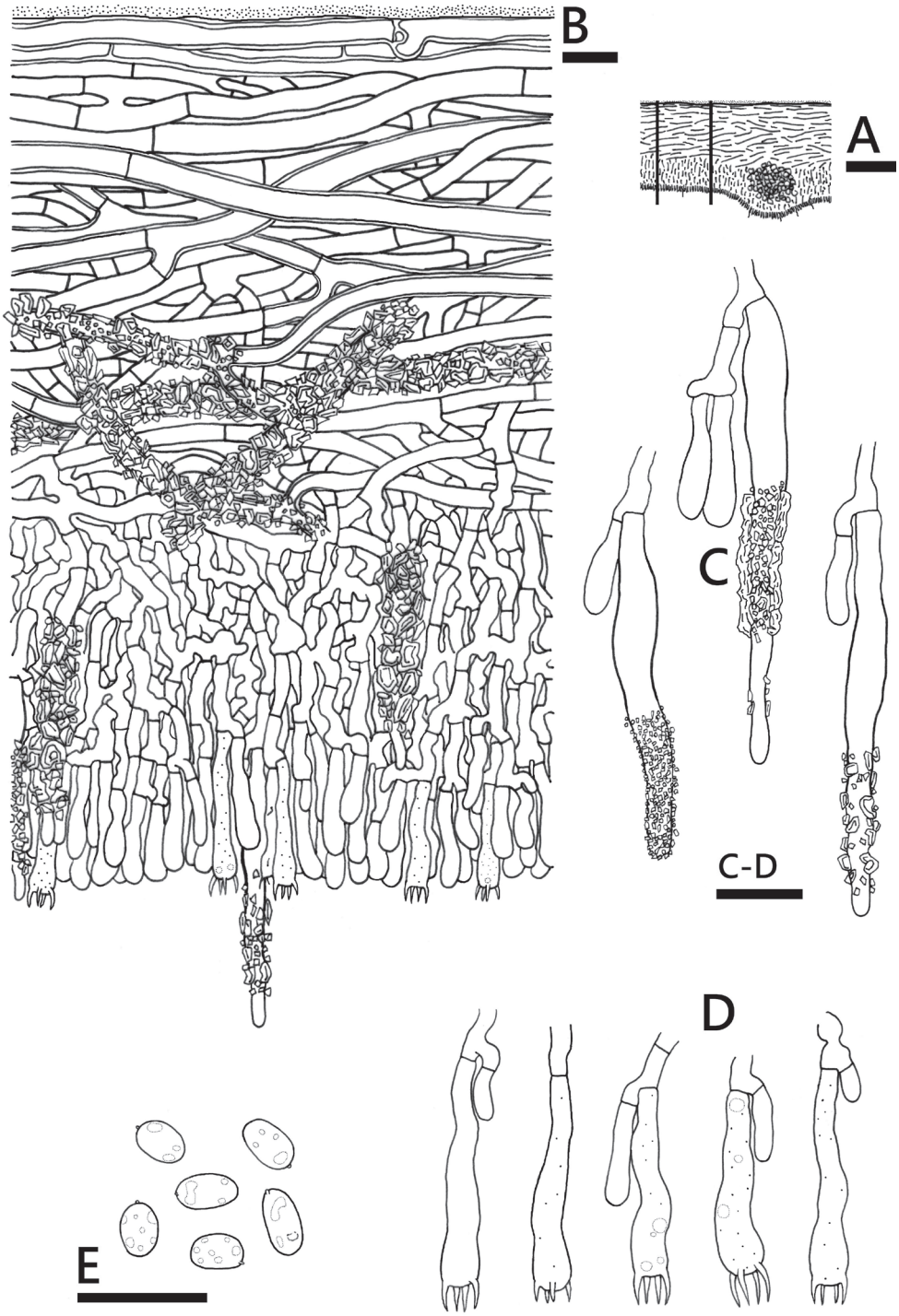

Figure 5. *Phanerochaete cystidiata* (holotype, *GC 1708-358*) **A** profile of basidiome section **B** basidiome section **C** leptocystidia **D** basidia **E** basidiospores. Scale bars: 100 µm (**A**); 10 µm(**B–E**).

Holotype. TAIWAN. Nantou County: Aowanta, 23°57'N, 121°10'E, 1200 m alt., on angiosperm branch, coll. C.C. Chen, 28 Aug 2017, *GC 1708-358* (TNM F0031801).

Etymology. From cystidiatus, referring to the presence of cystidia of this species.

Description. Basidiome resupinate, effuse, adnate, membranaceous, 120–250 (–330) µm thick in section. Hymenial surface creamish-yellow, brownish in KOH, smooth to occasionally slightly tuberculate (due to crystal masses in hymenial layer), sometimes cracked; margin whitish or concolorous, fibrillous to fimbriate, occasionally determinate.

Hyphal system monomitic; hyphae simple-septate, clamp connections rarely present in subiculum. Subiculum fairly uniform, with somewhat loose to fairly dense texture, usually very dense near the substrate, 70–150 µm thick; hyphae more or less horizontal, colourless, fairly straight, moderately ramified, occasionally strongly encrusted with crystals, 3–6 (–7) µm diam., with 0.8–1.5 µm thick walls, anastomoses occasional. Hymenial layer thickening, with fairly dense texture, 50–100 (–180) µm thick, occasionally stratified; hyphae more or less vertical, colourless, 2.5–5 µm diam., thin-walled. Crystal masses occasionally abundant in hymenial layer. Leptocystidia numerous, immersed or emergent, cylindrical, median part usually slightly swollen and slightly thick-walled, with narrow or tapering apices, sparsely to heavily encrusted, (35–) 40–60 × 4–5.5 µm. Basidia subclavate to narrowly clavate, usually guttulate when mature, 20–30 × 4.5–5.5 µm, 4-sterigmate. Basidiospores ellipsoid to narrowly ellipsoid, adaxially flattened, smooth, thin-walled, guttulate, IKI–, CB–, mostly 4–5.3 × 2.5–3 µm. [4–5 (–5.5) × (2.5–) 2.7–3 (–3.3) µm, L = 4.59±0.43 µm, W = 2.86±0.18 µm, Q = 1.61 (n = 30) (*GC 1708-358*); (4–) 4.2–5 (–5.5) × 2.5–3 (–3.2) µm, L = 4.72±0.40 µm, W = 2.79±0.20 µm, Q = 1.70 (n = 30) (*Wu 1708-326*)].

Additional specimens examined (paratypes). CHINA. Yunnan Province: Wenshan Zhuang and Miao Autonomous Prefecture, Maguan County, Dalishu Township, Lake, 23°07'04"N, 104°08'17"E, 1800 m alt., on angiosperm branch, coll. C.C. Chen, 7 Aug 2017, *GC 1708-76* (TNM F0031803). TAIWAN. Nantou County: Aowanta, 23°57'N, 121°10'E, 1200 m alt., on angiosperm branch, coll. S.H. Wu, 28 Aug 2017, *Wu 1708-326* (TNM F0031802).

Distribution. Known from China (Yunnan Province) and Taiwan (type locality).

Remarks. *Phanerochaete ericina* is the most closely related species (Figs 1, 2), but differs in having brownish hymenophore, frequently branched narrow hyphae (quasi-binding hyphae) and cystidia that are not encrusted (Wu 1990). *Phanerochaete burtii* (Romell) Parmasto, *P. carnosa* (Burt) Parmasto, *P. calotricha* (P. Karst.) J. Erikss. & Ryvarden, *P. citrinosanguinea* Floudas & Hibbett, *P. pseudosanguinea* Floudas & Hibbett, *P. sanguinea* (Fr.) Pouzar and *P. sanguineocarnosa* Floudas & Hibbett also have a more or less fimbriate margin of the basidiomes, apically narrow or tapering cystidia and similar-sized basidiospores; however, their cystidia are not or only rarely encrusted. These species form a strongly supported monophyletic group, while *P. cystidiata* is phylogenetically distantly related to this group (Figs 1, 2).

Phanerochaete fusca **Sheng H. Wu, C.C. Chen & C.L. Wei, sp. nov.**
MycoBank No: 827413
Figs 3C, 6

Diagnosis. *Phanerochaete fusca* is characterised by smooth to tuberculate dark brown hymenial surface, monomitic hyphal system with brown subicular hyphae and leptocystidia with narrow or tapering apices. Additional diagnostic features: hyphae and cystidia usually with adventitious septa, subicular hyphae sometimes swollen at hyphal ends and basidia becoming thick-walled and brownish when old.

Holotype. CHINA, Hubei Province: Shennongjia Forest Area, Wenshui Forest Farm, 31°44'N, 110°20'E, 1700 m alt., on angiosperm branch, coll. S.H. Wu, 19 Sep 2014, *Wu 1409-161* (TNM F0029722).

Etymology. From fuscus (= dark brown), referring to the colour of the hymenial surface.

Description. Basidiome resupinate, effuse, adnate, membranaceous, 250–580 µm thick in section. Hymenial surface dark brown, slightly darkening in KOH, smooth to tuberculate, not cracked; margin concolorous, more or less separable, determinate.

Hyphal system monomitic; hyphae simple-septate, clamp connections rarely present in subiculum. Subiculum fairly uniform, with dense texture, 200–480 µm thick; hyphae more or less horizontal, brown, fairly straight, moderately ramified, usually swollen at hyphal ends, usually encrusted near subhymenium, (2.5–) 3–7 (–7.5) µm diam., with slightly thick to up to 2 µm thick walls, with small oily drops, usually with adventitious septa. Hymenial layer thickening, with dense texture, 50–100 µm thick; hyphae more or less vertical, brownish to subcolourless, 2.5–4 µm diam., slightly thick-walled. Leptocystidia numerous, originating from hymenial layer, projecting, cylindrical with narrow or tapering apices, sometimes encrusted, subcolourless to brownish, usually with 1 or 2 adventitious septa, 50–70 × 3.5–5.5 (–6) µm, with thin to up to 1 µm thick walls. Basidia clavate or occasionally narrowly clavate, subcolourless to brownish, sometimes with an adventitious septum, 22–50 × 5–6 µm, with thin to up to 1 µm thick walls, 4-sterigmate. Basidiospores narrowly ellipsoid to subcylindrical, adaxially slightly concave, smooth, thin- to slightly thick-walled, colourless to sometimes brownish, IKI –, CB –, mostly 5.7–7.3 × 3–3.5 µm. [(5.3–) 5.7–7.3 (–7.8) × (2.8–) 3–3.5 (–3.7) µm, L = 6.63±0.64 µm, W = 3.24±0.28 µm, Q = 2.05 (n = 30) (*Wu 1409-161*)].

Additional specimen examined (paratype). CHINA. Hubei Province: Shennongjia Forest Area, Wenshui Forest Farm, 31°44'N, 110°20'E, 1700 m alt., on angiosperm branch, coll. S.H. Wu, 19 Sep 2014, *Wu 1409-163* (TNM F0029723).

Distribution. Known from China (Hubei Province).

Remarks. *Phanerochaete stereoides* Sheng H. Wu resembles *P. fusca* in having brown subicular hyphae and leptocystidia. However, hymenial surface of the former is pale greyish-brown, while the latter is dark brown. Moreover, cystidia of *P. stereoides* are uniformly thin-walled and colourless, not with 1 or 2 adventitious septa. These two species are not closely related according to the phylogenetic analyses (Fig. 2). *Phanerochaete porostereoides*

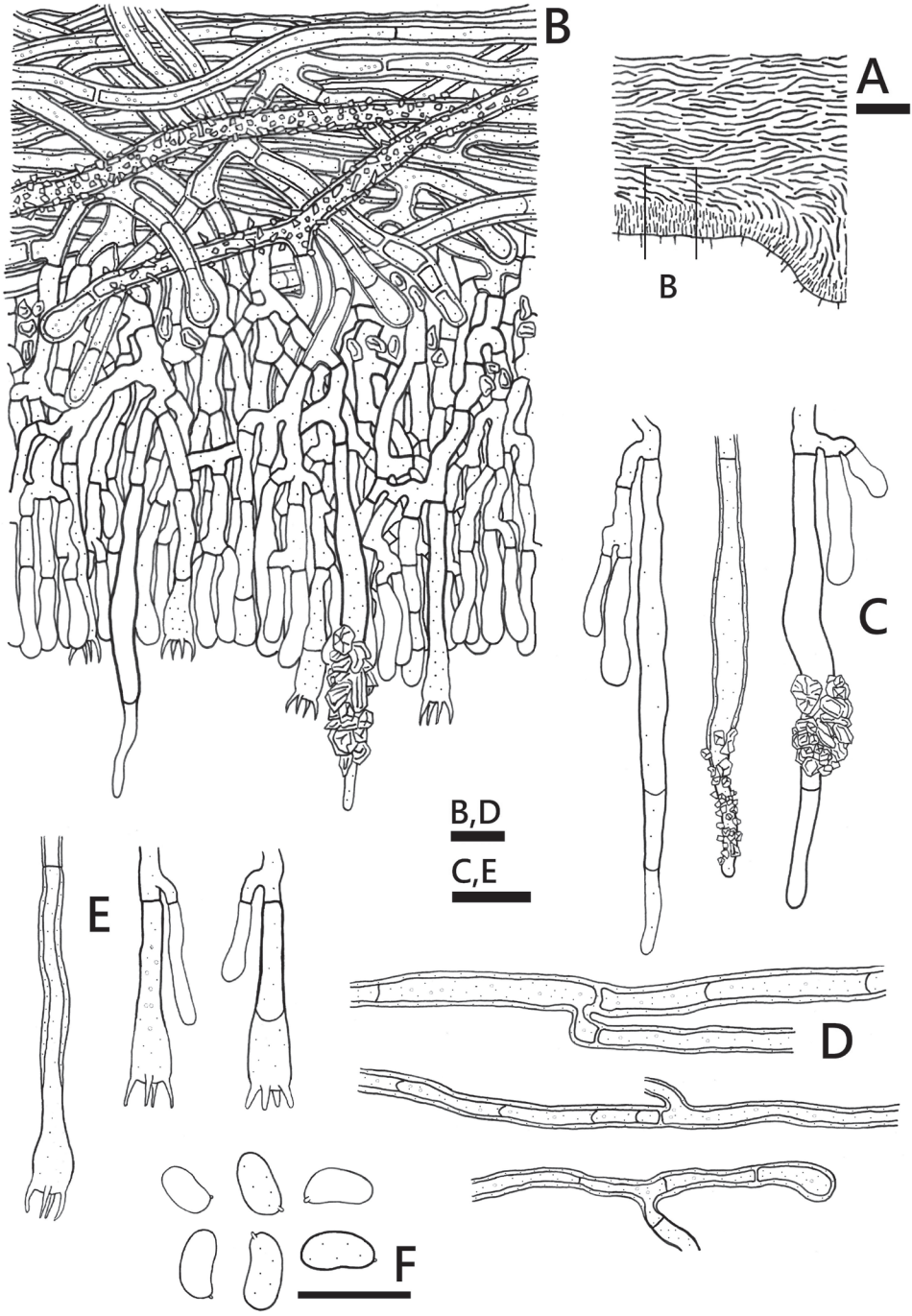

Figure 6. *Phanerochaete fusca* (holotype, *Wu 1409-161*) **A** profile of basiome section **B** basidiome section **C** leptocystidia **D** subicular hyphae, usually swollen at hyphal ends **E** basidia **F** basidiospores. Scale bars: 100 μm (A); 10 μm (**B–F**).

is the most closely related species (Fig. 2). Like *P. fusca*, it has brown subicular hyphae, but differs by lacking cystidia and by smaller basidiospores [(4.5–) 4.7–5.3 (–5.5) × (2.3–) 2.5–3.1 (–3.3) µm], according to Liu and He (2016).

Acknowledgments

This study was financed by Ministry of Science and Technology of Taiwan (ROC) (Grant no 107-2621-B-178-002-MY3). The authors thank Dr. Xiang-Hua Wang (Kunming Institute of Botany, China) for providing help in the field trips in SW Yunnan Province, China. We are also grateful to Ms. Siou-Zhen Chen (TNM) for managing studied specimens and to Shin-Yi Ke (TNM) for the help in DNA sequencing work.

References

Binder M, Hibbett DS, Larsson KH, Larsson E, Langer E, Langer G (2005) The phylogenetic distribution of resupinate forms across the major clades of mushroom-forming fungi (Homobasidiomycetes). Systematics and Biodiversity 3: 113–157. https://doi.org/10.1017/S1477200005001623

Burdsall HH (1985) A contribution to the taxonomy of the genus *Phanerochaete* (Corticiaceae, Aphyllophorales). Mycologia Memoir 10: 11–65.

Darriba D, Taboada GL, Doallo R, Posada D (2012) jModelTest 2: more models, new heuristics and parallel computing. Nature Methods 9: 772–772. https:// doi.org/10.1038/nmeth.2109

Eriksson J, Hjortstam K, Ryvarden L (1978) The Corticiaceae of North Europe 5. *Mycoaciella-Phanerochaete*. Fungiflora, Oslo.

Floudas D, Hibbett DS (2015) Revisiting the taxonomy of *Phanerochaete* (Polyporales, Basidiomycota) using a four gene dataset and extensive ITS sampling. Fungal Biology 119: 679–719. https://doi.org/10.1016/j.funbio.2015.04.003

Frøslev T, Matheny P, Hibbett D (2005) Lower level relationships in the mushroom genus *Cortinarius* (Basidiomycota, Agaricales): a comparison of RPB1, RPB2, and ITS phylogenies. Molecular Phylogenetics and Evolution 37: 602–618. https://doi.org/10.1016/j.ympev.2005.06.016

Greslebin A, Nakasone KK, Rajchenberg M (2004) *Rhizochaete*, a new genus of phanerochaetoid fungi. Mycologia 96: 260–271. https://doi.org/10.1080/15572536.2005.11832976

Hall TA (1999) BioEdit: a user-friendly biological sequence alignment editor and analysis program for Windows 95/98/NT. Nucleic Acids Symposium Series 41: 95–98.

Index Fungorum (2018) http://indexfungorum.org. Accessed 13 August 2018.

Justo A, Miettinen O, Floudas D, Ortiz-Santana B, et al. (2017) A revised family-level classification of the Polyporales (Basidiomycota). Fungal Biology 121: 798–824. https://doi.org/10.1016/j.funbio.2017.05.010

Katoh K, Standley DM (2013) MAFFT Multiple Sequence Alignment Software Version 7: Improvements in performance and usability. Molecular Biology and Evolution 30: 772–780. https://doi.org/10.1093/molbev/mst010

Kumar S, Stecher G, Tamura K (2016) MEGA7: Molecular Evolutionary Genetics Analysis version 7.0 for bigger datasets. Molecular Biology and Evolution 33: 1870–1874. https://doi.org/10.1093/molbev/msw054

Liu SL, He SH (2016) *Phanerochaete porostereoides*, a new species in the core clade with brown generative hyphae from China. Mycosphere 7: 648–655. https://doi.org/10.5943/mycosphere/7/5/10

Matheny PB, Liu YJ, Ammirati JF, Hall BD (2002) Using RPB1 sequences to improve phylogenetic inference among mushrooms (*Inocybe*, Agaricales). American Journal of Botany 89: 688–698. https:// doi.org/10.3732/ajb.89.4.688

Miettinen O, Spirin V, Vlasák J, Rivoire B, Stenroos S, Hibbett D (2016) Polypores and genus concepts in Phanerochaetaceae (Polyporales, Basidiomycota). MycoKeys 17: 1–46. https://doi.org/10.3897/mycokeys.17.10153

Miller MA, Pfeiffer W, Schwartz T (2010) Creating the CIPRES Science Gateway for inference of large phylogenetic trees. Proceedings of the Gateway Computing Environments Workshop (GCE), 14 Nov 2010, New Orleans, 1–8. https://doi.org/10.1109/GCE.2010.5676129

Ronquist F, Teslenko M, Van Der Mark P, Ayres DL, Darling A, Höhna S, Larget B, Liu L, Suchard MA, Huelsenbeck JP (2012) MrBayes 3.2: Efficient Bayesian phylogenetic inference and model choice across a large model space. Systematic Biology 61: 539–542. https://doi.org/10.1093/sysbio/sys029

Sadlikova M, Kout J (2017) A new *Phanerochaete* (Polyporales, Basidiomycota) with brown subicular hyphae from Thailand. Mycosphere 8: 1124–1030. http://doi.org/10.5943/mycosphere/8/6/4

Stamatakis A (2014) RAxML version 8: a tool for phylogenetic analysis and post-analysis of large phylogenies. Bioinformatics 30: 1312–1313. https://doi.org/10.1093/bioinformatics/btu033

Stiller JW, Hall BD (1997) The origin of red algae: implications for plastid evolution. Proceedings of the National Academy of Sciences 94: 4520–4525. https://doi.org/10.1073/pnas.94.9.4520

Stöver BC, Müller KF (2010) TreeGraph 2: Combining and visualizing evidence from different phylogenetic analyses. BMC Bioinformatics 11: 1–9. https://doi:10.1186/1471-2105-11-7

White TJ, Bruns T, Lee S, Taylor J (1990) Amplification and direct sequencing of fungal ribosomal RNA genes for phylogenetics. In: Innis MA, Gelfand DH, Sninsky JJ, White TJ (Eds) PCR Protocols: A Guide to Methods and Applications. Academic Press, San Diego, 315–322. https://doi.org/10.1016/b978-0-12-372180-8.50042-1.

Wu SH (1990) The Corticiaceae (Basidiomycetes) subfamilies Phlebioideae, Phanerochaetoideae and Hyphodermoideae in Taiwan. Acta Botanica Fennica 142: 1–12

Wu SH, Chen YP, Wei CL, Floudas D, Dai YC (2018) Two new species of *Phanerochaete* (Basidiomycota) and redescription of *P. robusta*. Mycological Progress 17: 425–435. https://doi.org/10.1007/s11557-017-1368-z

Wu SH, Nilsson HR, Chen CT, Yu SY, Hallenberg N (2010) The white-rotting genus *Phanerochaete* is polyphyletic and distributed throughout the phlebioid clade of the Polyporales (Basidiomycota). Fungal Diversity 42: 107–118. https://doi.org/10.1007/s13225-010-0031-7

Volobuev S, Okun M, Ordynets A, Spirin V (2015) The *Phanerochaete sordida* group (Polyporales, Basidiomycota) in temperate Eurasia, with a note on *Phanerochaete pallida*. Mycological Progress 14: 80. https://doi.org/10.1007/s11557-015-1097-0

MycoKeys 41: 107–118 (2018)
doi: 10.3897/mycokeys.41.28168
http://mycokeys.pensoft.net

RESEARCH ARTICLE

A peer-reviewed open-access journal
MycoKeys
Launched to accelerate biodiversity research

A new species of the lichenised genus *Anamylopsora* (Baeomycetaceae, Baeomycetales) from Tengger Desert of China

Ya-Bo Zuo[1,2], Da-Le Liu[1,2], Cui-Xin Li[1], Yu-Hui Chen[1], Xin-Li Wei[2,3]

1 *College of Life Sciences, Southwest Forestry University, Kunming, Yunnan 650224, China* **2** *State Key Laboratory of Mycology, Institute of Microbiology, Chinese Academy of Sciences, Beijing 100101, China* **3** *University of Chinese Academy of Sciences, Beijing 100049, China*

Corresponding authors: *Yu-Hui Chen* (cyh196107@126.com); *Xin-Li Wei* (weixl@im.ac.cn)

Academic editor: *T. Lumbsch* | Received 4 July 2018 | Accepted 20 September 2018 | Published 5 November 2018

Citation: Zuo Y-B, Liu D-L, Li C-X, Chen Y-H, Wei X-L (2018) A new species of the lichenised genus *Anamylopsora* (Baeomycetaceae, Baeomycetales) from Tengger Desert of China. MycoKeys 41: 107–118. https://doi.org/10.3897/mycokeys.110.28168

Abstract

The monotypic lichenised genus *Anamylopsora* (Baeomycetaceae, Baeomycetales), with its single species *A. pulcherrima*, is distributed in the arid areas of the Northern Hemisphere, including China. In this paper, we introduce another species new to science, *Anamylopsora pruinosa*. The new species is characterised by a densely pruinose upper surface, abundantly thick and strong rhizines and terricolous habitat. It is also strongly supported by the phylogenetic and species delimitation analyses based on nrDNA ITS sequences, in which *A. pruinosa* forms well-supported clade separated from *A. pulcherrima*.

Keywords

Lichen, morphology, phylogeny, taxonomy, Tengger Desert

Introduction

The monotypic genus *Anamylopsora* Timdal was established in 1991 (Timdal 1991), based on the species *Anamylopsora pulcherrima* (Vain.) Timdal. The species was previously excluded from *Psora* Hoffm., as *Psora pulcherrima* (Vain.) Elenkin, due to having, for example, a non-amyloid tholus and hymenial gelatine and is temporarily placed in

the collective genus *Lecidea* Ach. (Timdal 1984). Together with *Lecidea*, the genus *Anamylopsora* was included in the family Lecideaceae Chevall., although it was observed to be more similar to Trapeliaceae M. Choisy ex Hertel in the ascus structure (Timdal 1991). Lumbsch et al. (1995) established a monotypic family Anamylopsoraceae in the Agyriineae (Lecanorales) based on the ascus structure, chemistry, pycnidial structure and ascoma ontogeny, comparing with all the morphologically similar or related families, such as Agyriaceae Corda, Baeomycetaceae Dumort., Icmadophilaceae Triebel, Lecideaceae and Psoraceae Zahlbr.

Later, the family Anamylopsoraceae was synonymised with the Baeomycetaceae based on multigene phylogenetic analysis and the genus *Anamylopsora* is currently included under Baeomycetaceae (Baeomycetales) (Resl et al. 2015), together with *Ainoa* Lumbsch & I. Schmitt, *Baeomyces* Pers. and *Phyllobaeis* Kalb & Gierl (Jaklitsch et al. 2016). The family is distant from *Psora* (Lecanorales) and *Lecidea* (Lecideales) (Resl et al. 2015). Hence, *Anamylopsora pulcherrima* belongs to a monotypic genus, but not monotypic family.

Anamylopsora pulcherrima is saxicolous, common in the arid areas of the Northern Hemisphere, including Asia (China, Iran, Kirgizstan, Mongolia, Nepal, Japan), Russia and U.S.A. (Davydov 2014; Inoue 2010; Moniri and Sipman 2009; Timdal 1991; Zhurbenko 2010). During our field survey in the arid region of the Northwest China, a new species of *Anamylopsora* was found in Tengger Desert with the characters of terricolous habitat, dense pruina and abundant rhizines. The purpose of this study is to describe the new member of the previously monotypic genus. Phylogenetic and species delimitation analyses based on nrDNA ITS sequences are also provided.

Materials and methods

Phenotypic analysis

All the six specimens of the new species of *Anamylopsora* were collected from one locality in the Ningxia Hui Autonomous Region of China, close to the Inner Mongolia Autonomous Region and are preserved in the Lichen Section of Herbarium Mycologicum Academiae Sinicae (HMAS-L). A dissecting microscope (Zeiss Stemi SV11) and compound microscope (Zeiss Axioskop 2+) were used for the study of morphology and anatomy. Standardized thin-layer chromatography (TLC, solvent system C) was used for the identification of secondary metabolites (Culberson 1972; Culberson and Kristinsson 1970; Orange et al. 2001).

DNA extraction, amplification and sequencing

DNA was extracted from six fresh specimens of *Anamylopsora* (Table 1) following the modified CTAB method (Rogers and Bendich 1988). The internal transcribed spacer of

Table 1. Specimens of *Anamylopsora* from China and taxa used in the phylogenetic analysis in this study.

Taxon	Voucher specimens	GenBank No.
Anamylopsora pruinosa	XL2017133 (HMAS-L-141383)	MH558055*
A. pruinosa	ZW2018064 (HMAS-L-141384)	MH558056*
A. pruinosa	ZW2018099 (HMAS-L-141386)	MH558057*
A. pruinosa	ZW2018100 (HMAS-L-141385)	MH558058*
A. pruinosa	ZW2018101 (HMAS-L-141388)	MH558059*
A. pruinosa	ZW2018102 (HMAS-L-141387)	MH558060*
A. pulcherrima	Russia, Yakutia, 1992, Zhurbenko (ESS)	AF274089
A. pulcherrima	Zhurbenko 023, 2002(GZU)	KR017064
Ainoa mooreana	Nordin 7455 (UPS)	KJ462262
Ainoa mooreana	Thor 28340 (UPS)	KJ462263
Anzina carneonivea	Austria, Tyrol, 1996, Guderley & Heibel (ESS)	AF274077
Baeomyces placophyllus	XZ12147 (SDNU)	KT601493
B. rufus	yn138 (SDNU)	KT601494
Phyllobaeis imbricata	852	HQ650635
Psora crenata	Rui & Timdal SA11/02 (O)	MG677191
Tephromela armeniaca	u267	AY541278
Trapelia coarctata	Orange 23617 (NMW)	KY797787

* = sequences newly generated for this study by the authors

nuclear ribosome DNA (nrDNA ITS) was chosen as the genetic marker. Primers LR1 (Vilgalys and Hester 1990) and ITS1 (White et al. 1990) were used. Reactions were carried out in 50 µl reaction volume and the components used were 3 µl total DNA, 1 µl each primer (10 µM), 25 µl 2×Taq MasterMix and 20 µl ddH_2O. PCR amplifications were carried out in a Biometra T-Gradient thermal cycler, following conditions: initial heating step for 5 min at 95 °C, followed by 35 cycles of 30 s at 94 °C, 30 s at 56 °C, and 1 min 30 s at 72 °C; a final extension step of 8 min at 72 °C was added, after which the samples were kept at 4 °C. Negative controls were prepared for each amplification series. PCR products were purified using a gel purification kit (Shanghai Huashun Bioengineering Corporation, China) following the manufacturer's instructions.

Sequence alignment and phylogenetic analysis

PCR products were sequenced using the ABI 3730 XL Sequencer by Shanghai BioSune Corporation of China. Except sequences of the new species, the sequences of another species in *Anamylopsora*, *A. pulcherrima* and eight species in seven genera related as outgroups, i.e. *Ainoa mooreana*, *Anzina carneonivea*, *Baeomyces placophyllus*, *B. rufus*, *Phyllobaeis imbricata*, *Psora crenata*, *Trapelia coarctata* and *Tephromela armeniaca*, were downloaded from GenBank. The sequences were aligned using ClustalW Multiple Alignment (Thompson et al. 1994) in BioEdit 7.2.5 (Hall 1999). The programme Gblocks v0.91b (Castresana 2000; Talavera and Castresana 2007) was used to delimit and remove regions of alignment uncertainty, using options for a "less stringent" se-

lection on the Gblocks web server (http://molevol.cmima.csic.es/castresana/Gblocks_server.html). The alignment was subjected to a maximum likelihood (RAxML) analysis and nodal support was assessed using 1000 bootstrapping pseudo-replicates with RAxML-HPC v. 8.2.6 (Stamatakis 2014) and MrBayes v.3.2.6 (Huelsenbeck and Ronquist 2001; Ronquist and Huelsenbeck 2003) on the Cipres Science Gateway (http://www.phylo.org). In the ML and Bayesian analyses, substitution models for ITS were estimated using jModelTest-2.1.9 (Darriba et al. 2012; Guindon and Gascuel 2003). Based on these results, we used the TrN+I+G model with 1000 pseudoreplicates in the ML analysis and the TrN+G model in the Bayesian analysis. Two parallel Markov chain Monte Carlo (MCMC) runs were performed in MrBayes, each using 8 million generations and sampling every 1000 steps. A 50% majority-rule consensus tree was generated from the combined sampled trees of both runs after discarding the first 25% as burn-in. Tree files were visualised with FigTree v.1.4.2 (http://tree.bio.ed.ac.uk/software/figtree/). The intraspecific and interspecific genetic distances of the *Anamylopsora* species were also calculated and compared.

Species delimitation analyses

Two species delimitation methods were used to circumscribe species boundaries within the genus *Anamylopsora* – "Automatic Barcode Gap Discovery" (ABGD) (Puillandre et al. 2012) and a Bayesian implementation of the Poisson tree process model (bPTP) (Zhang et al. 2013). For ABGD we used default parameters except for using a Pmax at 0.01 and a relative gap width of 1.5, with the model Jukes-Cantor (JC69). The bPTP model is intended for delimiting species in these single-locus molecular phylogenies, and provides an objective approach for delimiting putative species boundaries that are consistent with the phylogenetic species criteria. We used the bPTP web server (http://species.h-its.org, Zhang et al. 2013) to delimit putative species groups using the ITS topology as the input tree and implementing default settings.

Results

Phylogenetic analysis

The aligned matrix contained 431 unambiguous nucleotide position characters for ITS. The phylogenetic tree included 10 taxa representing five families from ca. four different orders and is illustrated in Fig. 1. *Anamylopsora* formed a well-supported (BS=100, PP=1.00) monophyletic clade, within which the new species obviously separated from *A. pulcherrima*. The genetic distances (Table 2), based on nrDNA ITS sequences within *Anamylopsora*, showed that the intraspecific distance range was 0.00–0.01, while the interspecific distance range was 0.04–0.05, also indicating they are two different species.

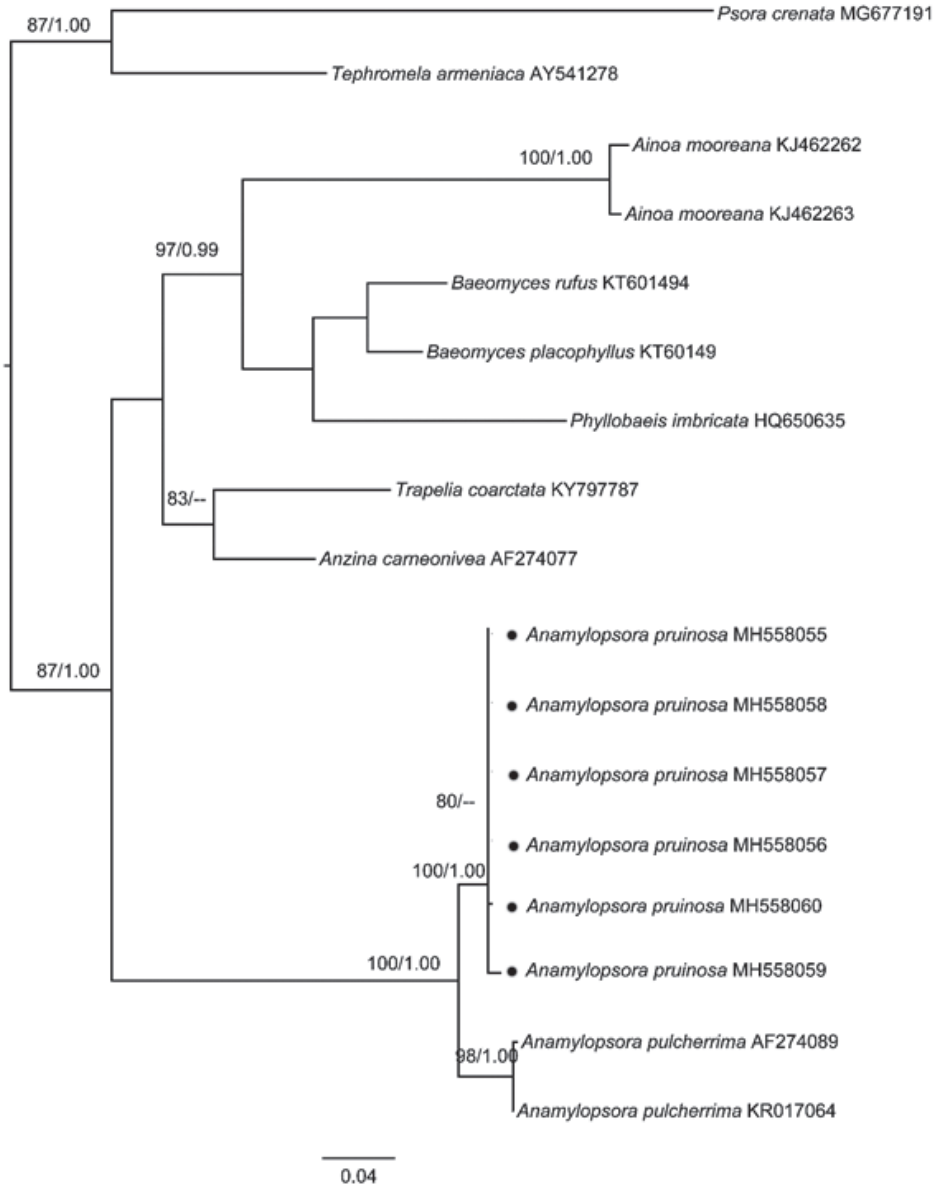

Figure 1. The maximum likelihood tree of *Anamylopsora* species based on the ITS sequences. The numbers in each node represent bootstrap support (BS) and posterior probability (PP) values. Bootstrap values ≥ 75 and posterior probability values ≥ 0.95 were plotted on the branches of the RAxML tree. Except for the new species *Anamylopsora pruinosa*, marked by the solid circle '●', all the other sequences were downloaded from GenBank. Scale bar: 0.04 substitution per site.

Table 2. Intraspecific and interspecific genetic distances range of the species in this study.

Taxon	1	2	3	4	5	6	7	8	9	10	11	12	13	14	15	16
1 *Anzina carneonivea* AF274077																
2 *Baeomyces placophyllus* KT601493	0.15															
3 *B. rufus* KT601494	0.14	0.06														
4 *Trapelia coarctata* KY797787	0.10	0.16	0.15													
5 *Diploschistes diacapsis* KX545503	0.30	0.32	0.33	0.31												
6 *D. muscorum* KX545481	0.29	0.33	0.32	0.30	0.02											
7 *Tephromela armeniaca* AY541278	0.18	0.20	0.20	0.21	0.36	0.35										
8 *Psora crenata* MG677191	0.26	0.27	0.30	0.32	0.46	0.46	0.23									
9 *Romjularia lurida* KF683091	0.16	0.19	0.20	0.19	0.37	0.37	0.21	0.27								
10 *Anamylopsora pulcherrima* KR017064	0.17	0.16	0.19	0.22	0.30	0.30	0.23	0.32	0.24							
11 *A. pulcherrima* AF274089	0.17	0.16	0.19	0.22	0.30	0.30	0.23	0.32	0.24	0.00						
12 *A. pruinosa* MH558055	0.18	0.17	0.19	0.23	0.31	0.31	0.21	0.32	0.25	0.04	0.04					
13 *A. pruinosa* MH558056	0.18	0.17	0.19	0.23	0.31	0.31	0.21	0.32	0.25	0.04	0.04	0.00				
14 *A. pruinosa* MH558057	0.18	0.17	0.19	0.23	0.31	0.31	0.21	0.31	0.25	0.04	0.04	0.00	0.00			
15 *A. pruinosa* MH558058	0.18	0.17	0.19	0.23	0.31	0.31	0.21	0.31	0.25	0.04	0.04	0.00	0.00	0.00		
16 *A. pruinosa* MH558059	0.19	0.18	0.20	0.24	0.33	0.33	0.22	0.32	0.25	0.05	0.05	0.01	0.01	0.01	0.01	
17 *A. pruinosa* MH558060	0.19	0.18	0.20	0.23	0.32	0.32	0.21	0.32	0.26	0.04	0.04	0.00	0.00	0.00	0.00	0.01

Species delimitation analyses

The ABGD analysis based on nrDNA ITS, provided evidence supporting *A. pruinosa* and *A. pulcherrima* as two different species (P = 0.001-0.01). The tree-based bPTP analysis also suggested two species (tree not shown) and within *A. pruinosa* group, the individuals coll. nos ZW2018102 and ZW2018101 clustered outermost, separating from other four samples, i.e. coll. nos. XL2017133, ZW2018064, ZW2018099 and ZW2018100.

Taxonomy

***Anamylopsora pruinosa* D.L. Liu & X.L. Wei, sp. nov.**
Fungal Names: FN570573
Figures 2a–i

Diagnosis. The species is characterised by densely pruinose upper surface, abundantly thick and strong rhizines and terricolous habitat.

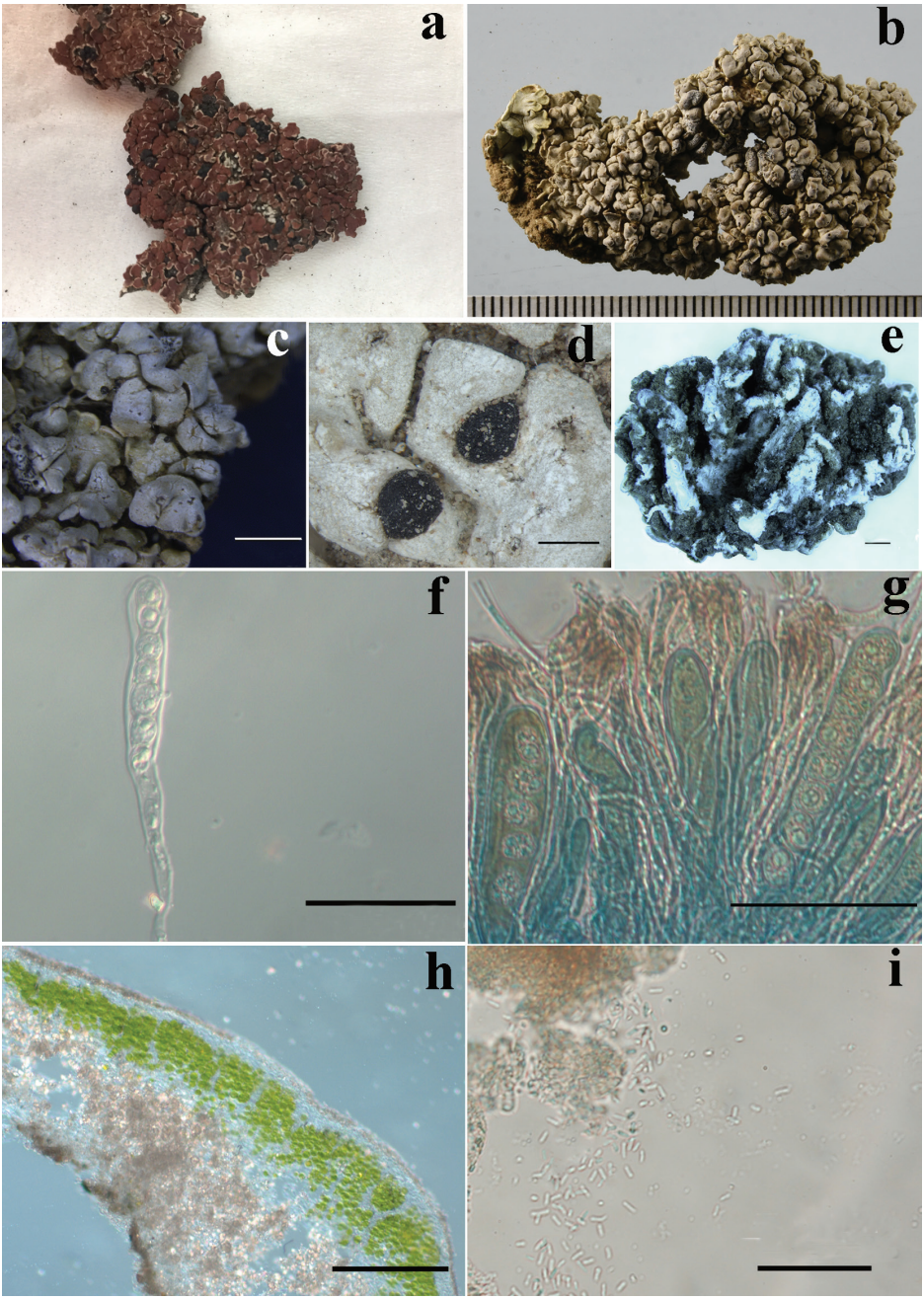

Figure 2. The new species *Anamylopsora pruinosa* (holotype, HMAS–L–141383). **a** Lichen thallus habit of *Anamylopsora pulcherrima* (C0090112F, F) **b** Lichen thallus habit of *Anamylopsora pruinosa* (holotype, HMAS–L–141383), scale in mm **c** Pruinose upper surface of the new species **d** The marginal apothecia of the new species **e** The abundant and thick and strong rhizines (white) at the lower surface **f** The asci with ascospores of the new species **g** The asci in iodine, showing the amyloid sheet **h** The thallus anatomical structure of the new species **i** The shortly bacilliform conidia of the new species. Scale bars: 0.2 mm (**c**); 0.5 mm (**d**); 0.95 mm (**e**); 50 µm (**f, g**); 200 µm (**h**); 50 µm (**i**).

Type material. CHINA. Ningxia: Zhongwei City, Ciu Liu Gou. 37°24'34.92"N, 104°35'8.66"E, 1577 m alt., on sandy soil, 15 July 2017, D.L. Liu & R. D. Liu XL2017133 (HMAS–L–141383– holotype).

Description. Thallus squamulose, 2–6 cm diam., terricolous, tightly adnate to the substrate. Squamules 2–3 mm diam., more or less imbricate, with areolate crust-like centre and slightly ascending and crenate margin. Upper surface densely pruinose, occasionally naked part khaki, dull to slightly shiny. Lower surface pale brown near the margin, mostly absence of well-developed cortex. Rhizines abundant, ecorticate, simple to branched, 4–6.5 mm long, 0.5–0.8 mm thick. Outer layer of upper cortex pale brown, ca. 50 µm high; inner layer of cortex colourless, 125–150 µm high. Photobiont layer continuous, 50–150 µm high; algal cells green, unicellular. Medulla 112.5–250 µm high, containing pale brown crystals. Lower cortex brownish, 15–17.5 µm high. Apothecia lecideine, marginal, 0.5–2 mm diam., dark brown to black, occasionally cracked, dull, epruinose. Epithecium dark brown, ca. 12.5 µm high. Hymenium colourless, 75–100 µm high, hemi-amyloid; asci clavate, 50–125 × 7.5–12.5 µm, surrounded by an amyloid sheet; tholus more or less well developed, non-amyloid. 4–8 ascospores per asci, i.e. 4, 5, 6, 8; ascospores simple, subglobose, colourless, 7.5–10 µm diam.; paraphyses weakly conglutinated, simple, with slightly thickened and brown pigmented apical cells. Pycnidia marginal, subglobose, dark brown to black, 275–425 × 275–375 µm; conidia shortly bacilliform, colourless, 3.75–5 × 1.25–2.5 µm.

Chemistry. Alectorialic and barbatolic acids.

Habitat and distribution. On the surface of sand soil in the arid region of Northwest China, Tengger Desert, where the annual precipitation is under 200 mm.

Etymology. Name refers the whole upper surface being densely pruinose.

Additional material examined. CHINA. Ningxia: Zhongwei City, Ciu Liu Gou. 37°24'34.92"N, 104°35'8.66"E, 1577 m alt., on sandy soil, 1 June 2018, D.L. Liu et al. ZW2018064 (HMAS–L–141384), ZW2018099 (HMAS–L–141386), ZW2018100 (HMAS–L–141385), ZW2018101 (HMAS–L–141388), ZW2018102 (HMAS–L–141387).

Notes. As known, *Anamylopsora pulcherrima* is saxicolous, growing on calciferous and non-calciferous rocks; upper surface epruinose or more rarely pruinose with more or less white pruinose margin (Timdal 1991). While the new species, *A. pruinosa*, is terricolous, growing directly on the surface of sandy soil, with thick and strong rhizines penetrating into the sand. On the other hand, the upper surface of *A. pruinosa* is densely white pruinose, occasionally very little part naked. Phylogenetic and species delimitation analyses based on ITS sequences (Fig.1) also well supported that they are two different species.

Discussion

Except for the diagnostic characters of the new species *Anamylopsora pruinosa*, most characters are accordant with the genus *Anamylopsora*, such as the habit of thallus (squamulose), type and location of apothecia (lecideine, marginal), weakly amyloid hymenium, asci with amyloid sheet, non-amyloid tholus, ascospores and conidia, and

chemistry, etc. (Lumbsch et al. 1995; Timdal 1991). In addition, the phylogenetic analysis showed *Anamylopsora*, including the two species, to be monophyletic. The species delimitation analyses, including ABGD and bPTP, also supported *A. pruinosa* and *A. pulcherrima* as two separate species. Therefore, both the phenotypic observations and ITS sequences well supported the new species.

As the genus *Anamylopsora* was known to be monotypic before this study and only the species *A. pulcherrima* is accepted, there are, however, three synonyms, i.e. *Lecidea pulcherrima* (Basionym), *Lecidea hedinii* and *Lecidea undulata* (Timdal 1991). Based on the original description of *L. hedinii* and *L. undulata* (Magnusson 1940; 1944), the morphological characters of *L. undulata* was suspected to be most similar to the new species *A. pruinosa* in greyish-white lobes, densely pruinose and terricolous habitat, but *L. undulata* has much smaller conidia (2.5–3.5 × 0.8 µm), and 'very large, reddish-brown apothecia' (Magnusson 1940), which is much different from the new species, *A. pruinosa*, with larger conidia (3.75–5 × 1.25–2.5 µm) and not large (0.5–2 mm diam.) and black apothecia. Especially, we could not find any fresh materials of *L. undulata* and the corresponding DNA sequences were unavailable. Therefore, we could not judge whether the new species *A. pruinosa* is exactly the synonymized *L. undulata* with the knowledge we have. Fresh materials corresponding to *L. undulata*, are needed and then it may be possible to answer this question.

In the phylogenetic analysis, we included the other three genera, i.e. *Ainoa*, *Baeomyces* and *Phyllobaeis*, within Baeomycetaceae (Jaklitsch et al. 2016) and some related taxa previously mentioned, i.e. *Anzina carneonivea* (Thelenellaceae, Incertae sedis order), *Psora crenata* (Psoraceae, Lecanorales), *Trapelia coarctata* (Agyriaceae, Baeomycetales) and *Tephromela armeniaca* (Lecanoraceae, Lecanorales) (Lumbsch et al. 2001a; b). The analyses well supported the monophyly of *Anamylopsora*. While obviously separating from the outgroup *Psora crenata* and *Tephromela armeniaca* (Lecanorales), the relationship amongst other orders, i.e. Baeomycetales, Trapeliales and Incertae sedis (Thelenellaceae), were not clearly shown. More species and gene loci are needed to clarify the above-mentioned relationships.

In China, *Anamylopsora pulcherrima* has been found and reported in some arid regions, such as Inner Mongolia and Gansu (Magnusson 1940; 1944; Schneider 1979), and also in Tibet (Obermayer 2004), but all these known species grow on calciferous stone, meaning that it is saxicolous. We did not find the corresponding description about whether rhizines were present in this species and we also did not find obvious rhizines through observation of the specimen deposited in F (C0090112F). However, the terricolous new species, *A. pruinosa*, directly grows on the surface of sandy soil, tightly adnate to the substrate by the abundant, thick and strong rhizines, forming an important type of lichen crust in the desert area, possibly contributing to sand-fixation. Previously, we generally focused on the predominant genus *Endocarpon* (Verrucariaceae, Verrucariales) in the Tengger Desert (Yang and Wei 2008; Zhang et al. 2017) due to their sand-fixation ability by rhizines. Comparing to *Endocarpon* spp., *Anamylopsora pruinosa* may, however, have more and greater advantages in their type of rhizines. Therefore, it is necessary to pay more attention to some other advantageous species like *Anamylopsora pruinosa* and try to apply them in the sand control engineering (Wei 2005) in the near future.

Acknowledgements

We sincerely thank Dr. H. Thorsten Lumbsch and Dr. Jen-Pan Huang helping to borrow specimens and take photos of *Anamylopsora pulcherrima* deposited in F. Special thanks to Dr. Einar Timdal and another anonymous reviewer for giving constructive comments and suggestions. This research was funded by one of National Key Research and Development Program of China (2016YFE0203400) and the National Natural Science Foundation of China (31770022, 31470149).

References

Castresana J (2000) Selection of conserved blocks from multiple alignments for their use in phylogenetic analysis. Molecular Biology and Evolution 17: 540–552. https://doi.org/10.1093/oxfordjournals.molbev.a026334

Culberson C (1972) Improved conditions and new data for identification of lichen products by standardized thin-layer chromatographic method. Journal of Chromatography 72: 113–125. https://doi.org/10.1016/0021-9673(72)80013-X

Culberson C, Kristinsson H (1970) A strandard method for the identfication of lichen products. Journal of Chromatography 46: 85–93. https://doi.org/10.1016/S0021-9673(00)83967-9

Darriba D, Taboada GL, Doallo R, Posada D (2012) jModelTest 2: more models, new heuristics and parallel computing. Nature Methods 9: 772. https://doi.org/10.1038/nmeth.2109

Davydov E (2014) The first checklist of lichens, lichenicolous and allied fungi of Altaisky krai (Siberia, Russia). Mycotaxon 129: 1–67.

Guindon S, Gascuel O (2003) A simple, fast, and accurate algorithm to estimate large phylogenies by maximum likelihood. Systematic Biology 52: 696–704. https://doi.org/10.1080/10635150390235520

Hall TA (1999) BioEdit: a user-friendly biological sequence alignment editor and analysis program for Windows 95/98/NT. Nucleic Acids Symposium Serie 41: 95–98.

Huelsenbeck JP, Ronquist F (2001) MRBAYES: Bayesian inference of phylogenetic trees. Bioinformatics 17: 754–755. https://doi.org/10.1093/bioinformatics/17.8.754

Inoue M (2010) Notes on four Lecideoid lichens new to Japan. Memoirs of the Faculty of Education & Human Studies Akita University (Natural Science) 65: 17–21.

Jaklitsch WM, Baral HO, Lücking R, Lumbsch HT (2016). Ascomycota. In: Frey W (Ed.) Syllabus of Plant Families –Adolf Engler's Syllabus der Pflanzenfamilien. Borntraeger, Stuttgart, 1–288.

Lumbsch HT, Lunke T, Feige GB, Huneck S (1995) Anamylopsoraceae — a new family of lichenized ascomycetes with stipitate apothecia (Lecanorales Agyriineae). Plant Systematics and Evolution 198: 275–286. https://doi.org/10.1007/BF00984742

Lumbsch HT, Schmitt I, Döring H, Wedin M (2001a) ITS sequence data suggest variability of ascus types and support ontogenetic characters as phylogenetic discriminators in the

Agyriales (Ascomycota). Mycological Research 105: 265–274. https://doi.org/10.1017/s0953756201003483

Lumbsch HT, Schmitt I, Döring H, Wedin M (2001b) Molecular systematics supports the recognition of an additional order of Ascomycota: the Agyriales. Mycological Research 105: 16–23. https://doi.org/10.1017/s095375620000321x

Magnusson AH (1940) Lichens from Central Asia I. Rep. Sci. Exped. N.W.China S.Hedin – The Sino-Swedish expedition – (Publ.13). XI.BoT., 1–168.

Magnusson AH (1944) Lichens from Central Asia II. Rep. Sci. Exped. N.W.China S.Hedin – The Sino-Swedish expedition – (Publ.13). XI.BoT., 1–168.

Moniri MH, Sipman HJM (2009) Lichens of two nature reserves in NE Iran. Willdenowia 39: 199–202. https://doi.org/10.3372/wi.39.39121

Obermayer W (2004) Additions to the lichen flora of the Tibetan region. Bibliotheca Lichenologica 88: 479–526.

Orange A, James PW, White F (2001) Microchemical Methods for the Identification of Lichens. British Lichen Society, 101 pp.

Puillandre N, Lambert A, Brouillet S, Achaz G (2012) ABGD, Automatic Barcode Gap Discovery for primaryspecies delimitation. Molecular Ecology 21: 1864–1877. https://doi.org/10.1111/j.1365-294X.2011.05239.x

Resl P, Schneider K, Westberg M, Printzen C, Palice Z, Thor G, Fryday A, Mayrhofer H, Spribille T(2015) Diagnostics for a troubled backbone: testing topological hypotheses of trapelioid lichenized fungi in a large-scale phylogeny of Ostropomycetidae (Lecanoromycetes). Fungal Diversity 73: 239–258. https://doi.org/10.1007/s13225-015-0332-y

Rogers S, Bendich A (1988) Extraction of DNA from Plant Tissues. Kluwer Academic Publishers, Boston, 1–10. https://doi.org/10.1007/978-94-017-5294-7_6

Ronquist F, Huelsenbeck JP (2003) MrBayes 3: Bayesian phylogenetic inference under mixed models. Bioinformatics 19: 1572–1574. https://doi.org/10.1093/bioinformatics/btg180

Schneider G (1979) Die Flechtengattung Psora sensu A.Zahlbruckner. Bibliotheca Lichenologica 13: 194.

Stamatakis A (2014) RAxML Version 8: A tool for phylogenetic analysis and post-analysis of large phylogenies. Bioinformatics 30: 1312–1313. https://doi.org/10.1093/bioinformatics/btu033

Talavera G, Castresana J (2007) Improvement of phylogenies after removing divergent and ambiguously aligned blocks from protein sequence alignments. Systematic Biology 56: 564–577. https://doi.org/10.1080/10635150701472164

Thompson J, Higgins D, Gibson T (1994) CLUSTAL W: improving the sensitivity of progressive multiple sequence alignment through sequence weighting, position-specific gap penalties and weight matrix choice. Nucleic Acids Research 22: 4673–4680. https://doi.org/10.1093/nar/22.22.4673

Timdal E (1984) The delimitation of *Psora* (Lecideaceae) and related genera, with notes on some species. Nordic Journal of Botany 4: 525–540. https://doi.org/10.1111/j.1756-1051.1984.tb02059.x

Timdal E (1991) *Anamylopsora*, a new genus in the Lecideaceae. Mycotaxon 42: 249–254.

Vilgalys R, Hester M (1990) Rapid genetic identifi cation and mapping of enzymatically amplifi ed ribosomal DNA from several *Cryptococcus* species. Journal of Bacteriology 172: 4238–4246. https://doi.org/10.1128/jb.172.8.4238-4246.1990

Wei JC (2005) Biocarpet engineering using microbiotic crust for controlling sand. Arid Zone Research 22: 287–288. [In Chinese]

White T, Bruns T, Lee S, Taylor J (1990) Amplification and Direct Sequencing of Fungal Ribosomal RNA Genes for Phylogenetics. Academic Press, San Diego, 315–322. https://doi.org/10.1016/B978-0-12-372180-8.50042-1

Yang J, Wei JC (2008) The new lichen species *Endocarpon crystallinum* from semiarid deserts in China. Mycotaxon 106: 445–448.

Zhang JJ, Kapli P, Pavlidis P, Stamatakis A (2013) A general species delimitation method with applications to phylogenetic placements. Bioinformatics 29: 2869–2876. https://doi.org/10.1093/bioinformatics/btt499

Zhang T, Liu M, Wang YY, Wang ZJ, Wei XL, Wei JC (2017) Two new species of *Endocarpon* (Verrucariaceae, Ascomycota) from China. Scientific Reports 7: 7193. https://doi.org/10.1038/s41598-017-07778-5

Zhurbenko M (2010) New and interesting lichenicolous fungi from Eurasia. II. Mycosphere 1: 213–222.

MycoKeys 41: 119–120 (2018)
doi: 10.3897/mycokeys.41.30558
http://mycokeys.pensoft.net

CORRIGENDA

A peer-reviewed open-access journal
MycoKeys
Launched to accelerate biodiversity research

Corrigendum for: "Oomycete-specific ITS primers for identification and metabarcoding" published in MycoKeys, doi: 10.3897/mycokeys.14.9244

Taavi Riit[1], Leho Tedersoo[1], Rein Drenkhan[2], Eve Runno-Paurson[3], Harri Kokko[4], Sten Anslan[1]

1 *Institute of Ecology and Earth Sciences, University of Tartu, Ravila 14a, 50411 Tartu, Estonia* **2** *Institute of Forestry and Rural Engineering, Estonian University of Life Sciences, Kreutzwaldi 5, 51014 Tartu, Estonia* **3** *Institute of Agricultural and Environmental Sciences, Estonian University of Life Sciences, Kreutzwaldi 5, 51014 Tartu, Estonia* **4** *Department of Environmental and Biological Sciences, University of Eastern Finland, P.O. Box 1627, FI-70211 Kuopio, Finland*

Corresponding author: *Taavi Riit* (taaviriit@hotmail.com)

Academic editor: *Thorsten Lumbsch* | Received 15 October 2018 | Accepted 15 October 2018 | Published 5 November 2018

Citation: Riit T, Tedersoo L, Drenkhan R, Runno-Paurson E, Kokko H, Anslan S (2018) Corrigendum for: "Oomycete-specific ITS primers for identification and metabarcoding" published in MycoKeys, doi: 10.3897/mycokeys.14.9244. MycoKeys 41: 119–120. https://doi.org/10.3897/mycokeys.41.30558

The oomycete-specific ITS primers published by Riit et al. (2016) have been put to use in the scientific community working with oomycetes. Recently, however, it has been brought to our attention that the sequences of the primers ITS1oo and ITS3oo shown in the first Figure of the published manuscript are incomplete, when compared to the sequences of the same primers as listed on the UNITE website. This discrepancy is derived from re-checking primer sequences from tube labels that are restricted to the first 18 bases.

Closer examination revealed that the sequence of primer ITS1oo in Figure 1 is missing one nucleotide from the 3' end and the primer ITS3oo is missing two nucleotides from the 3' end. These errors are expected to reduce relative primer specificity to Oomycetes, which probably results in a lower proportion of this group in metabarcoding studies. We hereby provide the updated figure (Figure 1) with correct information. We apologise to all users of these erroneous primers for their suboptimal performance. We are grateful to Dr. Diana Marčiulynienė and Dr. Sannakajsa Velmala for identifying these problems.

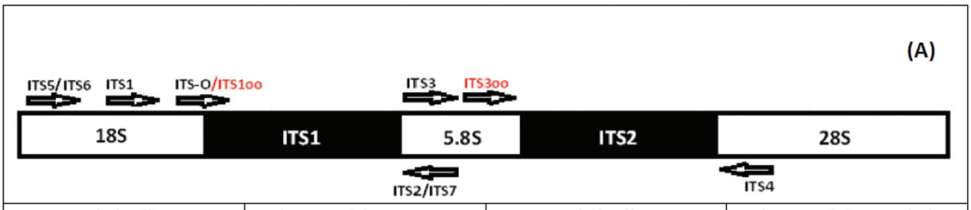

ITS1oo (5'-3') ITS-O (Bachofer 2004)	Mismatching taxon (% accessions)	ITS3oo (5'-3')	Mismatching (B) taxon (% accessions)
-GGAAGGATCATTACCACAC		AGTATGYYTGTATCAGTGTC	
CGGAAGGATCATTACCAC--			
-	-	*********M**********	*Hyaloperonospora* (100%)
-	-	G**********G*******T	*Perofascia* (100%)
WD*****RNNNNNN	*Fungi*	R*C*Y***Y**TYG**Y**N	*Fungi*
**********RNNNNNA	*Plantae*	G*C*C*****CC*GG*Y**Y	*Plantae*
**********Y*RH**	Other *Stramenopiles*	**C********CKG*****Y	Other *Stramenopiles*
ITS6 (Cooke et al. 2000)		**ITS7 (Cooke et al. 2000)**	
GAAGGTGAAGTCGTAACAAGG		AGCGTTCTTCATCGATGTGC	
-	-	**********G*****	*Saprolegnia* (90%)
-	-	Y*Y*S**********	*Aphanomyces* (40%)
-	-	*****C**********	*Halophytophthora* (85%)
****TAA**********	*Fungi*	T**********CSA	*Fungi*
*****A**********	*Plantae*	TR**********CNA	*Plantae*
**********	Other *Stramenopiles*	T**********T****G	Other *Stramenopiles*

Figure 1. A Map of universal and oomycete-specific ITS region primers **B** Taxa with mismatches in the binding sites of primers ITS1oo and ITS3oo. Only taxa with 10% or more mismatching accessions are shown.

References

Bachofer M (2004) Molekularbiologische Populationsstudien an Plasmopara halstedii, dem Falschen Mehltau der Sonnenblume Dissertation, Universitat Hohenheim Germany, 1–140.

Cooke DEL, Drenth A, Duncan JM, Wagels G, Brasier CM (2000) A molecular phylogeny of Phytophthora and related oomycetes. Fungal Genetics and Biology 30: 17–32. https://doi.org/10.1006/fgbi.2000.1202

Riit T, Tedersoo L, Drenkhan R, Runno-Paurson E, Kokko H, Anslan S (2016) Oomycete- specific ITS primers for identification and metabarcoding. MycoKeys 14: 17–30. https://doi.org/10.3897/mycokeys.14.9244